

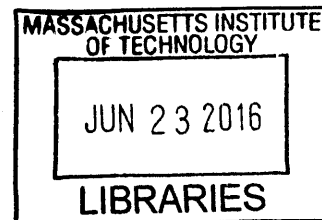
**Design, Synthesis, and Biological Evaluation of Diketopiperazine Based  
Ionizable Lipids for the In Vivo Delivery of Messenger RNA**

by

Owen Shea Fenton

B.A. Chemistry  
College of the Holy Cross, 2010

M.Sc. Organic Chemistry  
Massachusetts Institute of Technology, 2012



**ARCHIVES**

SUBMITTED TO THE DEPARTMENT OF CHEMISTRY IN PARTIAL  
FULFILLMENT OF THE REQUIREMENTS FOR THE DEGREE OF

DOCTOR OF PHILOSOPHY

AT THE  
MASSACHUSETTS INSTITUTE OF TECHNOLOGY

JUNE 2016

©2016 Massachusetts Institute of Technology.  
All Rights reserved.

Signature of Author: \_\_\_\_\_

Signature redacted

Department of Chemistry  
April 27, 2016

Certified by: \_\_\_\_\_

Signature redacted

Daniel G. Anderson

*Associate Professor of Chemical Engineering  
Thesis Supervisor*

Accepted by: \_\_\_\_\_

Signature redacted

Robert W. Field

*Haslam and Dewey Professor of Chemistry  
Chairman, Departmental Committee on Graduate Students*

This Doctoral Thesis has been examined by a committee of the Department of Chemistry as follows:

Signature redacted

---

Alexander M. Klibanov

*Firmenich Professor of Chemistry and Bioengineering*

*Thesis Committee Chair*

Signature redacted

---

Daniel G. Anderson

*Associate Professor of Chemical Engineering*

*Thesis Supervisor*

Signature redacted

---

John M. Essigmann

*William R. and Betsy P. Leitch Professor of Chemistry and Biological Engineering*

*Thesis Committee Member*

# Design, Synthesis, and Biological Evaluation of Diketopiperazine Based Ionizable Lipids for the In Vivo Delivery of Messenger RNA

By

Owen Shea Fenton

Submitted to the Department of Chemistry on April 20, 2016, in Partial Fulfillment of the Requirements for the Degree of Doctor of Philosophy in Chemistry

## Abstract

Thousands of human diseases could be treated by selectively increasing the intracellular concentration of specific proteins. The successful delivery of messenger RNA (mRNA) to target cells in the body could accomplish this goal, but serious limitations with its systemic delivery must still be overcome. Recently, lipid nanoparticles (LNPs) have shown promise for mRNA delivery *in vivo*, however, current leads are limited in terms of their efficacy, biodistribution, and toxicity. Here, we synthesize novel LNP delivery materials (i.e. ionizable lipids) that, when formulated into LNPs, both outperform current leads for mRNA delivery and elucidate key relationships between chemical structure and biological function.

Drawing inspiration from naturally occurring components of cellular membranes, we have designed and synthesized a new series of alkenyl amino alcohol (AAA) ionizable lipids for mRNA delivery to the liver. When formulated into LNPs, these AAA ionizable lipids induce high concentrations of human erythropoietin (EPO) protein at therapeutically relevant doses of mRNA. Notably, LNPs derived from our lead compound **OF-02** are the most potent mRNA delivery vehicle yet reported in the scientific literature.

While the liver is implicated in many diseases, targeting other tissues could drastically improve the clinical generality of mRNA based therapeutics. Towards this end, we have designed and synthesized ionizable lipid **OF-77**. Unlike other materials that afford more than 99% of total protein production in the liver, **OF-77** mRNA LNPs promote more than 85% of total protein production in the spleen. Notably, **OF-77** mRNA LNPs also demonstrate the first example of functional protein production within B lymphocytes, with current levels of protein production only limited by the administered dose.

Finally, we synthesize a novel series of ionizable lipids by varying three key structural parameters within **OF-77**; tail length, linker spacing, and total degrees of unsaturation. Both *in vitro* and *in vivo* experiments are explored to glean crucial information relating LNP structure to biological response. We also demonstrate that these compounds, including **OF-77**, are capable of both complexing and delivering siRNA to reduce specific intracellular protein concentrations.

Thesis Supervisor: Daniel G. Anderson

Title: Associate Professor of Chemical Engineering

## Acknowledgements

The completion of this Ph.D. would not have been possible without the tremendous support and guidance from countless individuals I have been fortunate enough to know in my life. While properly thanking everyone would require several more chapters, the hope of this section is to at least begin to express my gratitude to all of you who have made my growth as a scientist and individual possible over the last few years.

To begin, I would like to thank my advisor Professor Daniel G. Anderson. Thank you for providing me a perfect scientific environment to grow both creatively and as an experimentalist. You have truly helped to shape my approach to science, and have fostered such an incredible sense of collaboration, dedication, and passion here in the Koch Institute. Thank you for providing me unwavering support and help over the past few years, and for providing me the opportunity to work with so many incredible collaborators from nearly every scientific discipline. I cannot say enough good things about my time spent in our lab, and for that I will be forever grateful. In this same vein, I would also like to thank my committee members Professor Alexander Klibanov and Professor John Essigmann for their meticulous attention to detail and helpful scientific feedback. I would also like to thank Professor Mohammad Movassaghi for affording me the opportunity to synthesize complex alkaloid natural products during my early years at MIT – I have learned so much from you as a synthetic chemist, and for that I am eternally grateful.

I would also like to thank the many amazing collaborators and friends that I have met in our lab. Not only have you made my time here in the Anderson lab a truly exceptional educational experience, you have also helped to make it fun. Thank you to all of the following, and also to the many more that I have had the opportunity to interact with at some point over the last few years: Kevin Kauffman, Rebecca McClellan, Mark Tibbitt, Andrew Ayoob, Danny Zeng, Eric Appel, Jimmy Kaczmarek, Heloise Ragelle, Faryal Mir, Jung Yang, Matt Webber, Omar Khan, Roman Bogorad, Hao Yin, Arturo Vegas, Katie Whitehead, Abigail Lyton-Jean, Rose Kanasty, Sid Jhunjhunwala, Ben Tang, Angie DiCiccio, Karsten Olejnik, Luke Ceo, Robert Dorkin, Volkan Yesilyurt, Suman Bose, Tara Fawaz, Asha Patel, Kevin Daniel, Giovanni Traverso, Abel Cortinas, Matthias Oberli, Keith Hearon, Lisa Freed, Omar Khan, Alexis Coste, and Nicolas Boyer.

I would also like to thank my undergraduate advisor Professor Bianca R. Sculimbrene. Without your guidance I would never be where I am today – you provided such an incredible laboratory experience for me during my time at Holy Cross. I would also like to thank Professors Sarah Petty and Kimberley A. Frederick who also shaped me tremendously during my time in Haberman Hall.

Finally, I would like to thank my family, to whom this thesis is dedicated. Mom, Dad, PJ, Stef, and Emerie – thank you for all of your support and guidance for my entire life – I am so fortunate to have you as family. An additional thank you to my extended family, many of whom I had the opportunity to grow up with and learn from in my youth. To all of you, this thesis is dedicated.

## Table of Contents

Abstract.....	3
Acknowledgements.....	4
Table of Contents.....	5
List of Figures.....	6
List of Tables.....	7
List of Abbreviations.....	8
<b>Chapter 1. Background, significance, and thesis overview</b>	
A. Introduction.....	10
B. Barriers to the Systemic Delivery of mRNA.....	12
C. References.....	17
<b>Chapter 2. Bioinspired Alkenyl Amino Alcohol Ionizable Lipid Materials for Highly Potent In Vivo mRNA Delivery</b>	
A. Discussion.....	22
B. Experimental.....	31
C. References.....	48
<b>Chapter 3. Fatty Acid Derived Lipid Nanoparticles Deliver mRNA to B Lymphocytes In Vivo</b>	
A. Discussion.....	52
B. Experimental.....	62
C. References.....	71
<b>Chapter 4. Non-Toxic Ionizable Lipid Materials for mRNA Delivery In Vitro and In Vivo</b>	
A. Discussion.....	75
B. Experimental.....	89
C. References.....	99
<b>Curriculum Vitae.....</b>	<b>102</b>

## List of Figures

Figure 2-1	Cartoon of alkenyl amino alcohol ionizable lipids	24
Figure 2-2a	Synthesis of <b>OF-00</b> through <b>OF-03</b>	25
Figure 2-2b	Cryogenic transmission electron microscopy of <b>OF-02</b> LNPs	25
Figure 2-3a	In vivo mRNA screen of <b>OF-00</b> through <b>OF-03</b> mRNA LNPs	27
Figure 2-3b	Batch-to-batch consistency of <b>OF-02</b> mRNA LNPs	27
Figure 2-3c	In vivo dose response of <b>OF-02</b> mRNA LNPs	27
Figure 2-3d	Time course of <b>OF-02</b> mRNA LNPs	27
Figure 2-4a	Luciferase biodistribution of <b>cKK-E12</b> mRNA LNPs	30
Figure 2-4b	Luciferase biodistribution of <b>OF-02</b> mRNA LNPs	30
Figure 2-4c	Percent biodistribution of <b>cKK-E12</b> and <b>OF-02</b> mRNA LNPs	30
Figure 2-5	Percent weight loss with <b>cKK-E12</b> and <b>OF-02</b> mRNA LNPs	46
Figure 3-1a	Cartoon of <b>OF-77</b> mRNA LNPs targeting the spleen	54
Figure 3-1b	Cartoon of <b>OF-77</b> mRNA LNPs accessing B lymphocytes	54
Figure 3-1c	Chemical structure of <b>OF-77</b>	54
Figure 3-1d	Cryogenic transmission electron microscopy of <b>OF-77</b> LNPs	54
Figure 3-1e	Dynamic light scattering of <b>OF-77</b> mRNA LNPs	54
Figure 3-2a	In vitro dose response of <b>OF-77</b> mRNA LNPs	56
Figure 3-2b	Luciferase biodistribution of <b>OF-77</b> mRNA LNPs	56
Figure 3-2c	Percent biodistribution of <b>OF-77</b> mRNA LNPs	56
Figure 3-2d	TNS assay of <b>OF-77</b> mRNA LNPs	56
Figure 3-3a	FACS plots for cell populations labeled with <b>OF-77</b> LNPs	59
Figure 3-3b	Labeling for immune cell populations with <b>OF-77</b> LNPs	59
Figure 3-4a	In vivo dose response of functional protein in B lymphocytes	61
Figure 3-4b	In vivo dose response of functional protein in splenic cells	61
Figure 3-5	Synthesis of <b>OF-TBS</b> and <b>OF-77</b>	63
Figure 3-6	<sup>1</sup> H NMR of <b>OF-TBS</b>	64
Figure 3-7	<sup>1</sup> H NMR of <b>OF-77</b>	65
Figure 3-8	Luciferase calibration curve for <b>OF-77</b> mRNA LNPs	70
Figure 4-1	Synthesis of <b>OF-71</b> through <b>OF-77</b>	78
Figure 4-2	In vitro screen of <b>OF-71</b> through <b>OF-77</b> siRNA LNPs	81
Figure 4-3	In vitro screen of <b>OF-71</b> through <b>OF-77</b> mRNA LNPs	82
Figure 4-4a	In vitro dose response for <b>OF-77</b> siRNA LNPs	83
Figure 4-4b	In vitro dose response for <b>OF-77</b> mRNA LNPs	83
Figure 4-5a	In vivo ALP, ALT, and AST levels for <b>OF-77</b> siRNA LNPs	84
Figure 4-5b	Percent weight gain for <b>OF-77</b> siRNA LNPs	84
Figure 4-5c	Cytokine response for <b>OF-77</b> siRNA LNPs	84
Figure 4-6a	CD4 T cell activation with <b>OF-77</b> mRNA LNPs	86
Figure 4-6b	CD8 T cell activation with <b>OF-77</b> mRNA LNPs	86
Figure 4-7	Structure of <b>OF-C4-TBS</b> and synthesis of <b>OF-C4-77</b>	87
Figure 4-8a	TNS Assay for <b>OF-C4-77</b> mRNA LNPs	88
Figure 4-8b	Luciferase Biodistribution for <b>OF-C4-77</b> mRNA LNPs	88
Figure 4-8c	Percent biodistribution of <b>OF-C4-77</b> mRNA LNPs	88

### List of Tables

Table 2-1	LNP characterization data for <b>OF-00</b> to <b>OF-03</b> LNPs	46
Table 4-1	LNP characterization data for <b>OF-71</b> to <b>OF-77</b> siRNA LNPs	79
Table 4-2	LNP characterization data for <b>OF-71</b> to <b>OF-77</b> mRNA LNPs	79

## Abbreviations

Standard 1-letter codes are used for amino acids

AAA – Alkenyl Amino Alcohol  
ALP – Alkaline Phosphatase  
ALT – Alanine Transaminase  
ApoE – Apolipoprotein E  
AST – Aspartate Transaminase  
Cy5.5 – Cyanine 5.5  
DOPE - 1,2-dioleoyl-sn-glycero-3-phosphoethanolamine  
DSPE - 1,2-distearoyl-sn-glycero-3-phosphoethanolamine  
DSPC - 1,2-distearoyl-sn-glycero-3-phosphocholine  
EC<sub>50</sub> – half maximal effective concentration  
EPO – Erythropoietin  
FVII – Factor VII serum clotting protein  
LNP – Lipid nanoparticle  
Luc – Luciferase  
mRNA – Messenger RNA  
siRNA – Short interfering RNA  
TBAF – tetrabutyl ammonium fluoride  
TNS – 2-(p-toluidinyl)naphthalene-6-sulphonic acid



**Chapter 1:**

**Background, significance, and thesis overview**

## **A. Introduction**

Nearly all examples of disease, including diabetes, cancers, and even the common cold, involve the abnormal expression of specific proteins. Whether it is the undesirable upregulation of an oncogene, the absence of a tumor suppressor, or the presence of an exogenous viral protein, protein expression often determines the phenotypes observed in individuals suffering from disease. Having the ability to regulate individual protein concentrations, therefore, could allow scientists and physicians to study, prevent, and even treat disease.<sup>[1]</sup> Towards this end, great interest resides in the development of therapeutics that can eliminate, modify, or increase the amount of specific proteins within the body.

Historically, numerous therapeutic classes have been examined and studied for their ability to regulate protein expression in humans. Even before the mechanism of action was understood, for example, natural remedies derived from plants and animals were administered that could inhibit, degrade, modify, activate, or even upregulate specific proteins associated with disease.<sup>[2]</sup> Tremendous advances in molecular isolation, purification, and characterization have since identified thousands of small molecules that are capable of selectively interacting with proteins in the body. While many of these small molecules are effective and serve as the foundation of modern medicine, many more bind to off-target proteins or to proteins in untargeted cells, resulting in a wide array of potential side effects.<sup>[3]</sup> Furthermore, not all proteins are easily targeted, and small molecules cannot be used to introduce proteins that are necessary but absent in a given individual.

As an alternative to small molecule drugs, the direct delivery of therapeutic proteins has been explored to increase intracellular protein concentrations. For example, patients suffering from diabetes and hemophilia are regularly injected with insulin or Factor IX to help manage disease.<sup>[4]</sup> Generally speaking, however, protein based therapeutics are rather limited. For example, it is extremely difficult to obtain the correct cellular distribution for nuclear, cytoplasmic, or transmembrane proteins *in vivo*. Moreover, high and/or continual dosing regimens are hallmarks of protein replacement therapies; this is because many proteins have narrow half-lives and/or may not be catalytic, thereby limiting the generality of their clinical application.

To address these limitations, gene therapy was proposed as yet another means to regulate the intracellular concentration of proteins. Inspired by the central dogma of biochemistry (namely that DNA is transcribed into messenger RNA (mRNA) which is, in turn, translated into proteins), scientists demonstrated that by delivering DNA into the nucleus, a cell could produce a specific protein for its entire lifetime.<sup>[1]</sup> Moreover, this protein could be produced with the appropriate post-translational modifications and in the correct area within the cell. In this sense, DNA could be thought of as a drug – its successful delivery could be used to produce specific protein with high levels of selectivity.<sup>[5]</sup> Translating DNA delivery *in vitro* to *in vivo*, however, has proven extremely difficult, which has ultimately limited its successful transition into the clinic.<sup>[6]</sup> Obstacles include, but are not limited to, tissue biodistribution, cellular uptake, endosomal escape, and finally, entry into the nucleus.<sup>[7]</sup>

Given the limited clinical translation of DNA, mRNA has recently gained much interest as a therapeutic cargo.<sup>[8]</sup> Much like DNA, mRNA encodes for a specific protein, allowing for selective production of a therapeutic protein with the appropriate cell localization and post-translational modifications. Unlike DNA, however, mRNA need only access the cytoplasm of a cell to achieve therapeutic effect. Additionally, mRNA carries no risk of genomic integration, one of the many potential safety concerns surrounding the use of DNA.<sup>[9]</sup> DNA and mRNA also present varying durations of therapeutic effect; while mRNA is capable of producing a significant amount of protein, it is also degraded more quickly than DNA. This difference can be regarded as either an advantage or a disadvantage, as some disease treatments require constitutive protein expression whereas others are better managed in a transient fashion. Given these properties, there is great interest in developing mRNA based drugs, as having dose-dependent control over protein expression could have profound impact in fields such as protein replacement therapy, vaccine development, and immune tolerization wherein the selective expression of proteins could treat disease.<sup>[10]</sup> However, several questions and obstacles must still be overcome before mRNA can be successfully implemented in clinical applications. The goal of this thesis, therefore, is to contribute to the understanding of mRNA delivery *in vivo*, with the hope that these findings may someday contribute to the eventual study, prevention, and even treatment of human disease.

## **B. Barriers to the Systemic Delivery of Messenger RNA**

Over the past few decades, countless examples detailing the successful use of mRNA to produce protein *in vitro* have been described. Interestingly, however, when these mRNAs are administered *in vivo*, they either do not result in functional protein

production or are so minimally potent that their use is not considered clinically viable. This discrepancy between *in vitro* and *in vivo* activity of mRNAs suggests that the problem is not the efficacy of the mRNA itself, but rather the difficulty of delivering mRNA to the cytoplasm of diseased cells *in vivo*. Here, we aim to delineate some of the challenges associated with mRNA delivery to better frame why it is so challenging to create mRNA-based therapeutics.

For the purposes of this discussion, our conversation will focus around the systemic delivery of mRNA (i.e. delivery that passes through the circulatory system). Systemic delivery is a desirable route of administration for drugs because nearly every organ/tissue of interest comes into contact with the blood. If implemented successfully, therefore, systemic mRNA delivery could theoretically treat disease found in nearly every cell population within the body. However, systemic delivery of any drug is difficult, and mRNA based therapeutics are no exception to this rule.

Upon injection into the bloodstream, mRNA must first avoid degradation by a plethora of exo- and endonucleases.<sup>[11]</sup> Although the plasma stability of siRNAs has been improved through the fluorination or methylation of the 2'-hydroxy group along the ribose backbone,<sup>[12]</sup> this strategy is not practical for mRNA stabilization; whereas siRNAs are approximately 19-25 base pairs in length,<sup>[13]</sup> mRNAs are considerably longer and can include upwards of thousands of nucleobases. Alternative strategies have attempted to disguise mRNA from the immune system by substituting alternative nucleotides (i.e. swapping uridine with pseudouridine). However, this modification can affect the translational efficiency of mRNA into the desired protein.<sup>[14]</sup>

If by some mechanism the mRNA is not degraded during circulation, the next obstacle facing its *in vivo* delivery is biodistribution. Exogenously delivered mRNAs are most commonly cleared by the liver and/or kidneys.<sup>[15]</sup> While these two tissues are implicated in several forms of disease, having the ability to target other organs would dramatically increase the number of clinical applications available for mRNA. However, as all mRNAs consist of the same chemical building blocks, the resultant biodistribution profile remains limited at best.

The final obstacles involved with systemic mRNA delivery are cellular uptake and endosomal escape.<sup>[16]</sup> The high anionic charge density, size, and hydrophilicity of nucleic acids prevent meaningful levels of passive diffusion of mRNA across cell membranes.<sup>[17]</sup> Although cells can internalize material from their surrounding environment through a variety of different pathways (including macropinocytosis, caveolae mediated endocytosis, and clathrin mediated endocytosis), mRNA is not taken up by any appreciable extent. Even if mRNA is endocytosed, however, it still must somehow exit the endosome, enter the cytoplasm, and finally bind to a ribosomal complex before protein production can begin. This final process is still not well understood, even in the case of siRNA which has been studied for more than two decades.

To overcome the limitations with systemic mRNA delivery, several strategies have been either proposed or explored to improve mRNA delivery *in vivo*. For example, the direct chemical modification of nucleic acids with targeting ligands, polymeric chains, or non-natural base pairs has demonstrated remarkable success in the field of siRNA delivery.<sup>[13b]</sup> However, mRNA is difficult to selectively modify because it can

consist of hundreds of thousands of nucleobases. Moreover, both modified and unmodified nucleic acids lack a mechanism to escape the endosome – some research even suggests that between 95 to 98% of total siRNA entering an endosome is degraded by nucleases or expunged through exocytosis, even when a biological response is observed.<sup>[18]</sup> Instead, efforts have focused on the development of both biological and synthetic drug delivery vehicles that are capable of complexing and protecting nucleic acids. Viruses, for example, have been examined as potential delivery vehicles due to their natural capacity to deliver RNAs to specific cell populations *in vivo*.<sup>[19]</sup> However, safety concerns regarding their potential immunogenicity and practical considerations regarding their limited scalability have limited their promise for clinical application.<sup>[20]</sup> Several classes of polymers that exploit electrostatic interactions between cationic amines and the phosphate rich RNA backbone have also been explored for nucleic acid delivery. But these materials, which include protamine,<sup>[21]</sup> poly-lysine,<sup>[22]</sup> and poly(beta-amino esters),<sup>[23]</sup> face potential issues with efficacy, biodistribution, and toxicity.

Alternatively, lipid nanoparticles (LNPs) have been considered as potential candidates for systemic mRNA delivery. Previously, LNPs have demonstrated tremendous potential for the *in vivo* delivery of siRNAs, achieving EC<sub>50</sub> values as low as 0.02 mg/kg.<sup>[24]</sup> However, given the differences between the size (i.e. number of nucleobases), hybridization (i.e. double vs. single strand), and charge density between siRNA and mRNA, it was not readily obvious whether or not LNPs would be able to complex and deliver mRNA *in vivo*. Recent work from other groups and from our own lab has established LNPs as viable mRNA delivery vehicles; much like siRNA LNPs,

these particles are roughly 50-200 nm in size, are uni- or multilamellar in nature, and are capable of producing biological response in the liver.<sup>[8, 15]</sup>

While this work validates LNPs for systemic mRNA delivery, relatively little is known about the structure-function relationships relating mRNA delivery properties (i.e. efficacy, biodistribution, and toxicity) to specific chemical functionality found within the LNP. In practice, LNPs are composed of cholesterol (aids in stability),<sup>[25]</sup> a phospholipid (modifies bilayer structure),<sup>[26]</sup> a polyethylene glycol (PEG) derivative (decreases aggregation and nonspecific uptake),<sup>[27]</sup> and an ionizable lipid (complexes negatively charged RNA and enhances endosomal escape).<sup>[16, 24b]</sup> Evidence within the siRNA delivery community has implicated the chemical structure and identity of the ionizable lipid as the most pivotal component for efficacy, but this finding has not yet been validated for mRNA delivery. This lack of knowledge significantly reduces the pace at which new and potentially more efficacious compounds for mRNA delivery can be discovered.

Towards this end, the overarching theme of my work has focused on the design, synthesis, and characterization of novel ionizable lipid materials for use in the systemic delivery of mRNA LNPs. Notably, our efforts have focused on the incorporation of previously unexplored functional group combinations within ionizable lipids, ultimately providing modular chemical intermediates, precise molecular characterization, and scalable synthetic protocols along the way. Through our work, which sits at the interface of synthetic chemistry and biological engineering, we humbly propose the following: subtle chemical modifications profoundly impact biological activity.

This affirmation is observed in each of the following sections:



In **Chapter 2**, we pioneer the synthesis of a new series of alkenyl amino alcohol (AAA) based ionizable lipids. When formulated into LNPs with mRNA coding for human erythropoietin (EPO), our materials result in high concentrations of expressed protein in the liver. Notably, LNPs derived from our lead compound **OF-02** are the most potent mRNA delivery vehicle yet reported in the scientific literature.

In **Chapter 3**, we design and synthesize ionizable lipid **OF-77**. Interestingly, both **OF-02** and **OF-77** share the same bis-lysine-diketopiperazine core; however, **OF-02** is AAA based whereas **OF-77** incorporates ester linkages. Unlike other materials (including **OF-02**) that target the liver, **OF-77** LNPs produce more than 85% of total functional protein in the spleen. Notably, **OF-77** mRNA LNPs also demonstrate the first example of functional protein production within B lymphocytes.

Finally, in **Chapter 4** we modulate the tail length, linker spacing, and total degrees of unsaturation in **OF-77** to afford a new series of materials. *In vitro* and *in vivo* experiments detail interesting trends correlating structural properties to mRNA delivery potency. We also demonstrate that these materials are also capable of delivering siRNA, a structurally-distinct nucleic acid cargo that can silence protein production within cells.

### C. References

- [1] R. W. Herzog, O. Cao, A. Srivastava, *Discov Med* **2010**, *45*, 105-111.
- [2] F. E. Koehn, G. T. Carter, *Nat Rev Drug Discov* **2005**, *4*, 206-220.
- [3] A. Bender, J. Scheiber, M. Glick, J. W. Davies, K. Azzaoui, J. Hamon, L. Urban, S. Whitebread, J. L. Jenkins, *Chemmedchem* **2007**, *2*, 861-873.
- [4] D. E. DeWitt, I. B. Hirsch, *Jama-J Am Med Assoc* **2003**, *289*, 2254-2264.

- [5] V. Escriou, C. Ciolina, A. Helbling-Leclerc, P. Wils, D. Scherman, *Cell Biol Toxicol* **1998**, *14*, 95-104.
- [6] S. S. Jiao, P. Williams, R. K. Berg, B. A. Hodgeman, L. J. Liu, G. Repetto, J. A. Wolff, *Hum Gene Ther* **1992**, *3*, 21-33.
- [7] S. N. Tamkovich, A. V. Cherepanova, E. V. Kolesnikova, E. Y. Rykova, D. V. Pyshnyi, V. V. Vlassov, P. P. Laktionov, *Ann Ny Acad Sci* **2006**, *1075*, 191-196.
- [8] U. Sahin, K. Kariko, O. Tureci, *Nat Rev Drug Discov* **2014**, *13*, 759-780.
- [9] S. Hacein-Bey-Abina, C. von Kalle, M. Schmidt, F. Le Deist, N. Wulffraat, E. McIntyre, I. Radford, J. L. Villeval, C. C. Fraser, M. Cavazzana-Calvo, A. Fischer, *New Engl J Med* **2003**, *348*, 255-256.
- [10] B. Leader, Q. J. Baca, D. E. Golan, *Nat Rev Drug Discov* **2008**, *7*, 21-39.
- [11] S. Sorrentino, *Cell Mol Life Sci* **1998**, *54*, 785-794.
- [12] Y. L. Chiu, T. M. Rana, *Rna* **2003**, *9*, 1034-1048.
- [13] a) R. L. Kanasty, K. A. Whitehead, A. J. Vegas, D. G. Anderson, *Mol Ther* **2012**, *20*, 513-524; b) K. A. Whitehead, R. Langer, D. G. Anderson, *Nat Rev Drug Discov* **2009**, *8*, 129-138; c) K. A. Whitehead, J. E. Dahlman, R. S. Langer, D. G. Anderson, *Annu Rev Chem Biomol* **2011**, *2*, 77-96.
- [14] a) A. Thess, S. Grund, B. L. Mui, M. J. Hope, P. Baumhof, M. Fotin-Mleczek, T. Schlake, *Mol Ther* **2015**, *23*, 1456-1464; b) K. Kariko, H. Muramatsu, F. A. Welsh, J. Ludwig, H. Kato, S. Akira, D. Weissman, *Mol Ther* **2008**, *16*, 1833-1840.
- [15] K. J. Kauffman, J. R. Dorkin, J. H. Yang, M. W. Heartlein, F. DeRosa, F. F. Mir, O. S. Fenton, D. G. Anderson, *Nano Lett* **2015**, *15*, 7300-7306.

- [16] G. Sahay, W. Querbes, C. Alabi, A. Eltoukhy, S. Sarkar, C. Zurenko, E. Karagiannis, K. Love, D. L. Chen, R. Zoncu, Y. Buganim, A. Schroeder, R. Langer, D. G. Anderson, *Nat Biotechnol* **2013**, *31*, 653-U119.
- [17] M. S. D. Kormann, G. Hasenpusch, M. K. Aneja, G. Nica, A. W. Flemmer, S. Herber-Jonat, M. Huppmann, L. E. Mays, M. Illenyi, A. Schams, M. Griese, I. Bittmann, R. Handgretinger, D. Hartl, J. Rosenecker, C. Rudolph, *Nat Biotechnol* **2011**, *29*, 154-U196.
- [18] M. W. Tibbitt, J. E. Dahlman, R. Langer, *J Am Chem Soc* **2016**, *138*, 704-717.
- [19] M. Giacca, S. Zacchigna, *J Control Release* **2012**, *161*, 377-388.
- [20] I. M. Verma, N. Somia, *Nature* **1997**, *389*, 239-242.
- [21] B. Scheicher, A. L. Schachner-Nedherer, A. Zimmer, *Eur J Pharm Sci* **2015**, *75*, 54-59.
- [22] T. Bettinger, R. C. Carlisle, M. L. Read, M. Ogris, L. W. Seymour, *Nucleic Acids Res* **2001**, *29*, 3882-3891.
- [23] J. J. Green, R. Langer, D. G. Anderson, *Accounts Chem Res* **2008**, *41*, 749-759.
- [24] a) Y. Z. Dong, K. T. Love, J. R. Dorkin, S. Sirirungruang, Y. L. Zhang, D. L. Chen, R. L. Bogorad, H. Yin, Y. Chen, A. J. Vegas, C. A. Alabi, G. Sahay, K. T. Olejnik, W. H. Wang, A. Schroeder, A. K. R. Lytton-Jean, D. J. Siegwart, A. Akinc, C. Barnes, S. A. Barros, M. Carioto, K. Fitzgerald, J. Hettinger, V. Kumar, T. I. Novobrantseva, J. N. Qin, W. Querbes, V. Kotliansky, R. Langer, D. G. Anderson, *P Natl Acad Sci USA* **2014**, *111*, 5753-5753; b) K. T. Love, K. P. Mahon, C. G. Levins, K. A. Whitehead, W. Querbes, J. R. Dorkin, J. Qin, W. Cantley, L. L. Qin, T. Racie, M. Frank-Kamenetsky, K. N. Yip, R. Alvarez, D. W.

- Y. Sah, A. de Fougerolles, K. Fitzgerald, V. Koteliansky, A. Akinc, R. Langer, D. G. Anderson, *P Natl Acad Sci USA* **2010**, *107*, 9915-9915; c) K. A. Whitehead, J. R. Dorkin, A. J. Vegas, P. H. Chang, O. Veisch, J. Matthews, O. S. Fenton, Y. L. Zhang, K. T. Olejnik, V. Yesilyurt, D. L. Chen, S. Barros, B. Klebanov, T. Novobrantseva, R. Langer, D. G. Anderson, *Nat Commun* **2014**, *5*.
- [25] a) J. J. Lu, R. Langer, J. Z. Chen, *Mol Pharmaceut* **2009**, *6*, 763-771; b) T. M. Allen, P. R. Cullis, *Adv Drug Deliver Rev* **2013**, *65*, 36-48.
- [26] I. S. Zuhorn, U. Bakowsky, E. Polushkin, W. H. Visser, M. C. A. Stuart, J. B. F. N. Engberts, D. Hoekstra, *Mol Ther* **2005**, *11*, 801-810.
- [27] B. L. Mui, Y. K. Tam, M. Jayaraman, S. M. Ansell, X. Y. Du, Y. Y. C. Tam, P. J. C. Lin, S. Chen, J. K. Narayanannair, K. G. Rajeev, M. Manoharan, A. Akinc, M. A. Maier, P. Cullis, T. D. Madden, M. J. Hope, *Mol Ther-Nucl Acids* **2013**, *2*.

## CHAPTER 2

### Bioinspired Alkenyl Amino Alcohol Ionizable Lipid Materials for Highly Potent In Vivo mRNA Delivery

The work presented in this chapter was published in the following manuscript and is reproduced with kind permission from Wiley Periodicals, Inc (Copyright © 2016)

Fenton, O.S.; Kauffman, K.J.; McClellan, R.L.; Appel, E.A.; Dorkin, J.R.; Tibbitt, M.W.; Heartlein, M.W.; DeRosa, F.; Langer, R.; Anderson, D.G.\* Bioinspired Alkenyl Amino Alcohol Ionizable Lipid Materials for Highly Potent In Vivo mRNA Delivery. *Adv. Mat.*, **2016**, *in press*.

The work presented in this chapter has been filed with the United States Patent and Trademark Office:

Anderson, D.G.; Dorkin, J.R.; Fenton, O.S.; Kauffman, K.J.; McClellan, R.L.  
“Alkenyl Substituted 2,5-Piperazinediones, Compositions, and Uses Thereof. US  
Provisional Application Number: 62/182,264. Filing Date: June 19, 2015

## A. Discussion

Nucleic acid therapies could be leveraged to treat thousands of genetic disorders, many of which are difficult or impossible to manage with present day therapeutic approaches. For example, the successful delivery of short interfering RNAs (siRNA) to cells in both rodents and non-human primates has been widely used for the treatment of hereditary diseases and cancer.<sup>[1]</sup> By contrast, the delivery of messenger RNA (mRNA) remains largely unexplored. Whereas siRNA sequences are employed to silence gene expression, mRNA therapeutics could be used to treat diseases caused by deficiencies in specific proteins.<sup>[2]</sup> This is because mRNA sequences can be translated into proteins once they are successfully transported into the cytoplasm of target cells. The implementation of mRNA therapeutics, therefore, could profoundly impact fields such as protein replacement therapy, vaccine development, and immune tolerization wherein the selective expression of proteins *in vivo* could treat disease.<sup>[3]</sup>

Before clinical translation can be realized, however, serious limitations with the *in vivo* delivery of mRNA must still be overcome. The high anionic charge density, size, and hydrophilicity of nucleic acids prevent meaningful levels of passive diffusion of mRNA across cell membranes.<sup>[4]</sup> To circumvent this barrier, our group and others have developed and implemented an array of lipid nanoparticles (LNPs) for the entrapment and subsequent delivery of nucleic acids *in vivo*.<sup>[1]</sup> Although these LNPs have been largely optimized for siRNA sequences, both Schlake's group<sup>[5]</sup> and our research team<sup>[6]</sup> have recently employed LNPs derived from previously described components to deliver mRNA *in vivo*. Successful delivery was confirmed by quantifying serum protein levels, thereby establishing LNPs as viable delivery vehicles for mRNA.

Inspired by these results, we sought to design and synthesize novel LNP components capable of delivering mRNA with unprecedented levels of *in vivo* efficacy. In practice, LNPs are comprised of cholesterol (aids in stability),<sup>[7]</sup> a phospholipid (modifies bilayer structure),<sup>[1a, 8]</sup> a polyethylene glycol (PEG) derivative (decreases aggregation and non-specific uptake),<sup>[9]</sup> and an ionizable lipid (complexes negatively charged RNA and enhances endosomal escape).<sup>[10]</sup> Evidence within the siRNA delivery community has implicated the chemical structure and identity of the ionizable lipid as the most pivotal component for efficacy. Accordingly, several rationally designed<sup>[11]</sup> and combinatorial chemistry<sup>[10b, 12]</sup> methodologies have been explored to discover novel series of ionizable lipid materials capable of maximizing gene silencing at the lowest possible dose. This strategy both conserves precious therapeutic nucleic acid cargo and also serves to mitigate any possible issues with the toxicity of the LNPs themselves.

Interestingly, however, no reports detailing the creation of a new series of ionizable lipids for the expressed purpose of improving mRNA LNP delivery *in vivo* have yet been reported. We hypothesized that ionizable lipids based upon alkenyl amino alcohols (AAA), a functional group combination found in sphingosine and other bioactive molecules, could promote high levels of *in vivo* protein expression when formulated into mRNA LNPs (**Figure 2-1**).<sup>[13]</sup> We envisioned that we could furnish AAA ionizable lipids *via* a ring opening reaction between alkenyl epoxides (AE) with a polyamine core (**Figure 2-2a**).<sup>[12]</sup> It is important to note, however, that no AEs of suitable tail length are commercially available, nor are they trivial to synthesize on account of the difficulty of selectively oxidizing singular alkenes in the presence of electronically-similar carbon-carbon double bonds. As such, we report the first detailed procedures for AE synthesis and characterization beginning from

biologically relevant fatty acid starting materials (**Experimental Section 4**). **AE-00** through **AE-03** were then each reacted in turn with polyamine **1** to afford AAA ionizable lipids **OF-00** through **OF-03**. While **OF-00** through **OF-03** represent the first four members of this series of materials, we hope that the chemical versatility of **AE-00** through **AE-03** will serve as inspiration for future generations of AAA ionizable lipids for nucleic acid delivery.

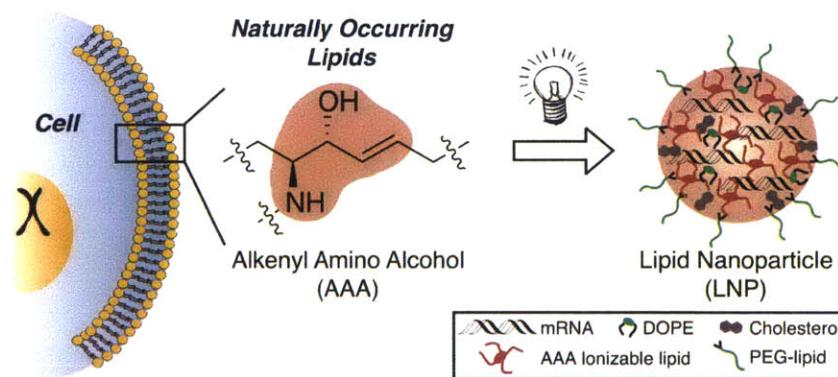


**Figure 2-1.** Naturally occurring components of the cell membrane contain alkenyl amino alcohol (AAA) functionality serving as the inspiration for the development of AAA ionizable lipids. These lipids form the basis of lipid nanoparticles exhibiting highly efficient *in vivo* delivery of mRNA.



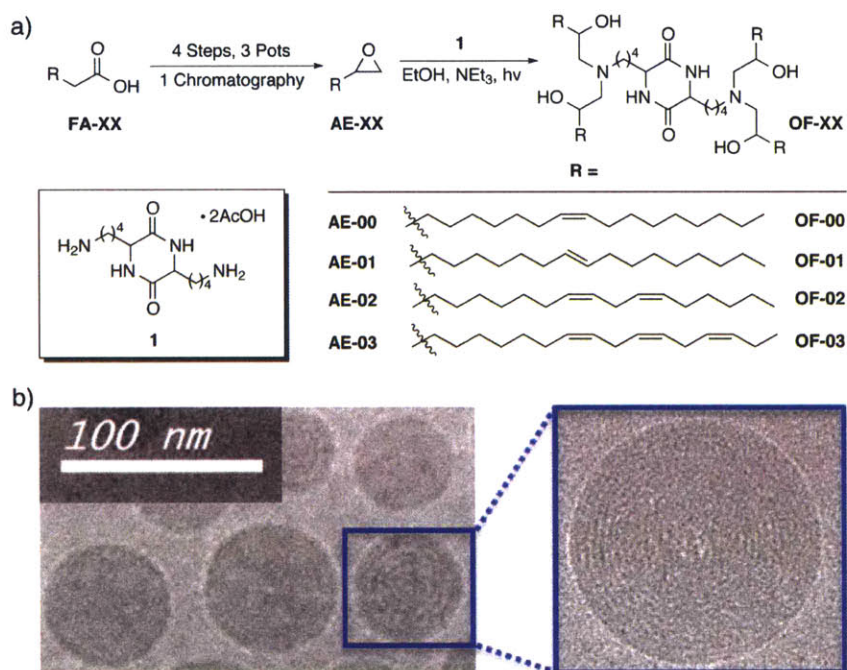


**Figure 2-2.** a) Synthesis of **OF-00** through **OF-03**, seminal members of the AAA class of ionizable lipids. b) Representative cryogenic transmission electron microscopy of **OF-02** LNPs.

Lipids **OF-00** through **OF-03** were then formulated with cholesterol, 1,2-dioleoyl-sn-glycero-3-phosphoethanolamine (DOPE), C14-PEG-2000, and unmodified mRNA coding for human erythropoietin (EPO) into mRNA LNPs.<sup>[6]</sup> EPO was selected as a model protein to evaluate the relationship between ionizable lipid identity and mRNA LNP efficacy for two reasons: 1) the associated protein is secreted directly into the bloodstream allowing for robust protein quantification, and 2) EPO has potential therapeutic applications in such areas as anemia.<sup>[4, 14]</sup> Cryogenic transmission electron microscopy images of **OF-02** LNPs detail a spherical morphology and a multilamellar structure (**Figure 2-2b**). Additional physical properties include a narrow polydispersity index (0.130) and an average particle diameter around 100 nm.

The nanoparticle diameters, polydispersity indices, and encapsulation efficiencies for each **OF-00** through **OF-03** LNP formulation can be found in **Table**

**2-1 (Experimental Section 5).** Ionizable lipid **cKK-E12** was also formulated alongside these compounds to be used as a positive control in our study. **cKK-E12** was chosen because it is capable of silencing Factor VII expression in mice at siRNA doses as low as 0.002 mg/kg, and as such it represents a benchmark ionizable lipid in the field of nucleic acid delivery.<sup>[12]</sup> Each resultant mRNA loaded LNP was then injected intravenously at a 0.75 mg/kg dose in C57BL/6 mice alongside phosphate buffered saline (PBS) as a negative control. At six hours, the serum EPO levels were quantified (**Figure 2-3a**). The PBS control imparted no significant EPO production *in vivo*, whereas positive control **cKK-E12** LNPs promoted a serum EPO concentration of 7100 ± 700 ng/mL. Excitingly, **OF-02** LNPs significantly outperformed benchmark lipid **cKK-E12** LNPs, promoting an approximate two-fold increase in EPO concentration to 14200 ± 1500 ng/mL. Additionally, **OF-02** outperformed two other benchmark ionizable lipids from the nucleic acid delivery field, namely **503013**<sup>[15]</sup> and **C12-200**,<sup>[10b]</sup> whose respective LNP promoted *in vivo* EPO concentrations were 2800 ± 200 ng/mL and 7100 ± 500 ng/mL at an identical dose. To the best of our knowledge, therefore, **OF-02** LNPs represent the most potent mRNA delivery vehicle reported to date in the scientific literature.

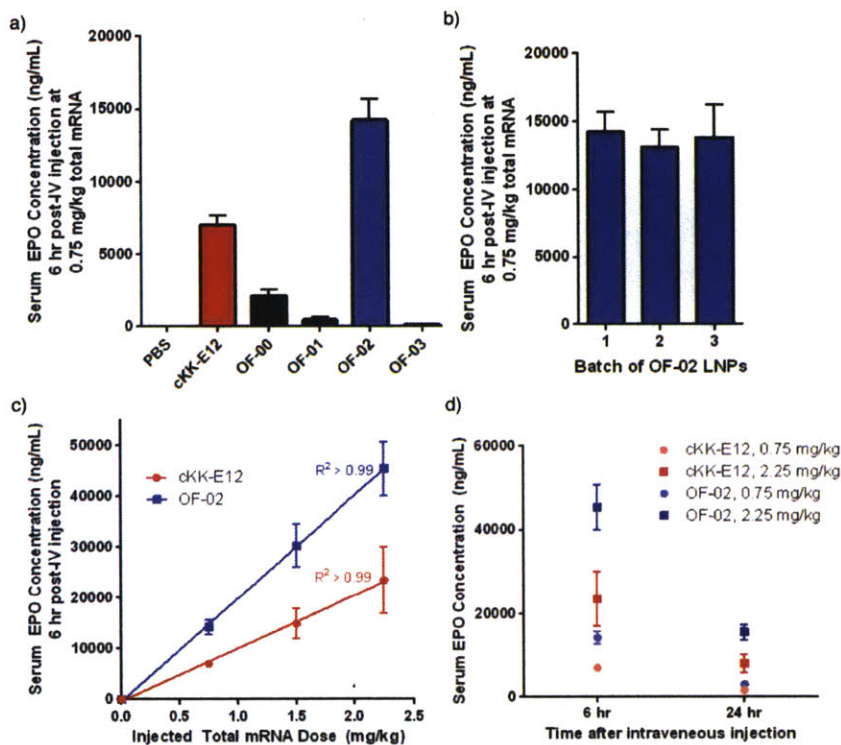


**Figure 2-3.** a) *In vivo* expression of EPO following administration of AAA LNPs for delivery of mRNA. b) Batch-to-batch variability of **OF-02** LNPs for EPO mRNA delivery *in vivo*. c) *In vivo* dose response curves for **OF-02** and **cKK-E12** LNPs. d) EPO expression following administration of **OF-02** and **cKK-E12** LNPs at 6 and 24 h. Data presented as mean + standard deviation (n = 3).

The **OF-00**, **OF-01**, and **OF-03** LNPs also allow the deduction of structure/function relationships within this new series of AAA ionizable lipids. We note two general structure/function trends of interest. First, we note that only alkenes with a *cis* geometry promote *in vivo* efficacy – **OF-00** and **OF-01** exclusively differ in the *cis/trans* geometry of their alkenes, and only **OF-00** produces meaningful EPO concentrations. Second, the optimal number and placement of two *cis* alkenes per tail matches those observed in optimized siRNA LNPs.<sup>[11, 16]</sup> While we are still discerning why these specific trends are observed, these empirical findings could potentially shape subsequent generations of AAA lipids. It is interesting to note, therefore, that only the linoleic acid derivative **OF-02** promotes significantly higher levels of EPO expression than the positive control, although oleic acid derivative **OF-00** also

demonstrates modest activity promoting a serum EPO concentration of  $2100 \pm 500$  ng/mL using the same dose.

With this information in hand, our attention then shifted from exploring the general properties of the new AAA series of ionizable lipids to further characterizing LNPs made from our lead material **OF-02**. The clinical translation of nucleic acid delivery vehicles is in part predicated on high reproducibility of the chemical constituents and formulation of LNPs. To test this, three independent batches of **OF-02** were synthesized and then formulated into LNPs. The average serum concentration among all batches was found to be  $13700 \pm 1700$  ng/mL and demonstrated minimal batch-to-batch variability (**Figure 2-3b**). Next, a dose response curve was collected at  $0.75$  mg/kg,  $1.5$  mg/kg, and  $2.25$  mg/kg total EPO mRNA dose for both **OF-02** and **cKK-E12** LNPs (**Figure 2-3c**). **OF-02** LNPs outperformed their **cKK-E12** counterparts roughly two-fold across all doses studied, reaching a maximum EPO concentration of  $45400 \pm 5300$  ng/mL at the  $2.25$  mg/kg dose. It is also interesting to note that both sets of LNPs promote EPO production in a linear fashion with respect to dose. This trend implies that we have not yet reached a saturation point for the intracellular translation machinery, suggesting protein production is currently only limited by the dose of mRNA. Moreover, it is important to note that no animal mortality was observed at all doses studied, and that mice treated with both **cKK-E12** and **OF-02** LNPs displayed similar weight loss profiles at identical doses (**Figure 2-5, Experimental Section 5**). **OF-02** LNPs therefore represent a tunable handle for *in vivo* EPO production readily capable of exceeding normal human EPO levels (40 - 250 pg/mL) in our chosen mouse model.<sup>[17]</sup> Finally, **OF-02** LNPs also outperformed their **cKK-E12** counterparts at 24 hours, independent of dose (**Figure 2-3d**). The sharp decrease in EPO concentration as a function of time highlights one of the many

exciting potential therapeutic advantages of mRNA delivery *in vivo*; in contrast to permanent gene replacement therapies, mRNA delivery offers transient, dose-response dependent protein expression *in vivo*, a property that could one day prove useful for a variety of genetic disorders.

Finally, we were interested to determine if the efficacy differences observed between **ckk-E12** and **OF-02** LNPs were due to variations in biodistribution. mRNA coding for luciferase was independently formulated with both **ckk-E12** and **OF-02** in the same fashion as for EPO delivery, and mouse organs were harvested 24 hours post injection. The tissues were subsequently imaged *ex-vivo* to measure the total luminescence per organ, demonstrating that mRNA from both **ckk-E12** and **OF-02** LNPs is predominantly translated in the liver with minimal translation in the spleen and negligible translation in other organs (**Figure 2-4a,b**). Quantification of this data also confirms nearly identical biodistribution profiles for the two formulations, suggesting that the increased efficacy of **OF-02** LNPs is not due to a difference in tissue targeting (**Figure 2-4c**). Since more than 4000 human diseases are caused by liver genetic disorders such as hemophilias A and B, **OF-02** LNPs represent a promising delivery vehicle for therapeutic mRNA delivery to the liver.<sup>[18]</sup>

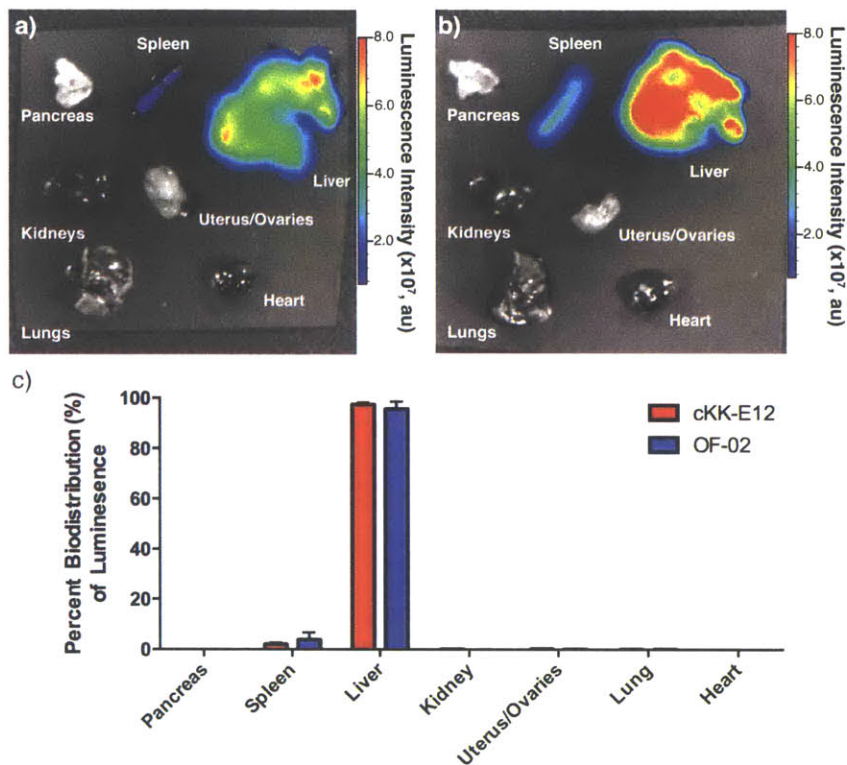


**Figure 2-4.** Representative luminescence biodistribution of a) **cKK-E12** and b) **OF-02** LNPs with luciferase mRNA *ex-vivo* and c) associated quantification. Data presented as mean + standard deviation (n = 3).

In summary, we have synthesized a new series of AAA ionizable lipid materials for mRNA LNP delivery. To the best of our knowledge, compounds **OF-00** through **OF-03** represent the first examples of AAA ionizable lipids in the scientific literature, and we hope that their alkene-epoxide precursors **AE-00** through **AE-03** can serve as versatile scaffolds for the synthesis of future generations of these ionizable lipids. **OF-02** LNPs yielded a two-fold increase in EPO production *in vivo* as compared to benchmark LNPs in the literature across a broad linear dose-response window. This illustrates that **OF-02** presents a tunable handle over *in vivo* protein expression, which is important in protein replacement therapies.<sup>[2]</sup> Batch-to-batch variability, dose response curves, and time course studies were coupled with biodistribution data, highlighting the exceptional potency with which these LNPs can

deliver mRNA to the liver. Future work will study the potential of **OF-02** LNPs for therapeutic applications and establish further groundwork necessary for translating this novel mRNA delivery vehicle to the clinic. In total, this study demonstrates efficient mRNA delivery with **OF-02** as well as the importance of utilizing synthetic chemistry in tandem with biological inspirations to further improve and understand nucleic acid delivery *in vivo*.

## **B. Experimental**

### ***1. Instrumentation, Materials, and Animal Protocols***

Microwave reactions were performed in a Biotage Initiator. Other reactions were performed in round bottom flasks. Proton nuclear magnetic resonance ( $^1\text{H}$  NMR) spectra were recorded with a Varian inverse probe INOVA-500 spectrometer (with a Magnex Scientific superconducting actively-shielded magnet), are reported in parts per million on the  $\delta$  scale, and are referenced from the residual protium in the NMR solvent ( $\text{CDCl}_3$ :  $\delta$  7.24; DMSO:  $\delta$  2.50). Data are reported as follows: chemical shift [multiplicity (br = broad, s = singlet, d = doublet, t = triplet, sp = septet, m = multiplet), integration, assignment. All commercial reagents and solvents were used as received.

All animal studies were approved by the M.I.T. Institutional Animal Care and Use Committee and were consistent with local, state and federal regulations as applicable. LNPs were intravenously injected in female C57BL/6 mice (Charles River Labs, 18-22 grams) via the tail vein. After six or 24 hours, blood was collected via the tail vein and serum was isolated by centrifugation in serum separation tubes. Serum EPO levels were quantified with an ELISA assay (Human Erythropoietin Quantikine IVD ELISA Kit, R&D Systems, Minneapolis, MD). 24 hours after injection of Luc-mRNA LNPs, mice were injected intraperitoneally with 130  $\mu\text{L}$  of D-luciferin (30

mg/mL in PBS). After fifteen minutes, mice were sacrificed and the organs were isolated (pancreas, spleen, liver, kidneys, lungs, heart, uterus and ovaries) and imaged with an IVIS imaging system (Perkin Elmer, Waltham, MA). Luminescence was quantified using LivingImage software (Perkin Elmer).

## **2. General Lipid Nanoparticle Synthesis**

The organic phase was prepared by solubilizing with ethanol a mixture of ionizable lipid, 1,2-dioleoyl-*sn*-glycero-3-phosphoethanolamine (DOPE, Avanti), cholesterol (Sigma), and 1,2-dimyristoyl-*sn*-glycero-3-phosphoethanolamine-N-[methoxy-(polyethyleneglycol)-2000] (ammonium salt) (C14-PEG 2000, Avanti) at a molar ratio of 35:16:46.5:2.5 and an ionizable lipid:mRNA weight ratio of 10:1. All ethanolic stock solutions were prepared at a concentration of 10 mg/mL. The aqueous phase was prepared in 10 mM citrate buffer (pH 3) with either EPO mRNA (human Erythropoietin mRNA, courtesy of Shire Pharmaceuticals, Cambridge, MA) or Luc mRNA (Firefly luciferase mRNA, Shire). All mRNAs were stored at -80 °C, and were allowed to thaw on ice prior to use. The ethanol and aqueous phases were mixed at a 3:1 ratio in a microfluidic chip device using syringe pumps as previously described at a final mRNA concentration of 0.1 mg/mL. Resultant LNPs were dialyzed against 1X PBS in a 20,000 MWCO cassette at 4°C for 2 hours and were stored at 4°C prior to injection.

## **3. General Lipid Nanoparticle Characterization**

To calculate the mRNA encapsulation efficiency, a modified Quant-iT RiboGreen RNA assay (Invitrogen) was used as previously described. Briefly, RiboGreen fluorescence was compared in the presence and absence of 2% Triton X-100 in TE buffer. The fluorescence was quantified using a Tecan infinite M200 Pro. The diameter and polydispersity (PDI) of the LNPs were measured using dynamic



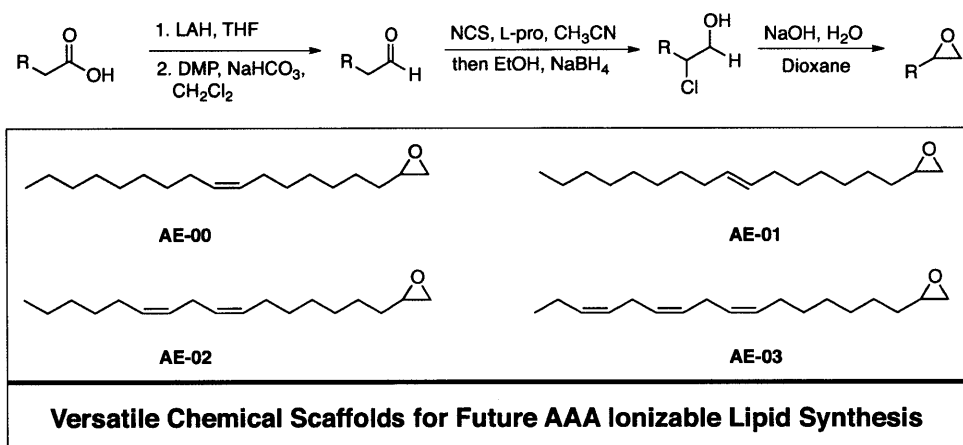
light scattering (ZetaPALS, Brookhaven Instruments). LNP diameters are reported as the largest intensity mean peak average, which constituted >95% of the nanoparticles present in the sample.

#### ***4. Synthetic Procedures for AE-00 through AE-03, all synthetic intermediates, and OF-00 through OF-03***

One of the most common and facile synthetic methods to afford epoxides relies on the oxidation of alkenes using meta-chloroperbenzoic acid (mcpba). However, we immediately recognized this as a poor synthetic strategy for synthesizing alkenyl epoxides **AE-00** through **AE-03** because the selective oxidation of a terminal alkene in the presence of electronically similar alkenes would be extremely difficult if not impossible. Purification of the reaction medium would also be highly challenging due to the similar polarity of products and the complexity of the mixture ensuing from the reaction. In order to circumvent this problem, we elected to use biologically relevant fatty acids as our general synthetic starting material. We envisioned that fatty acids would serve as excellent synthetic building blocks for our study because they are abundant in large quantities from many commercial vendors and they also offer high levels of regiochemical fidelity in their alkenes. Additionally, fatty acids would allow us to circumvent the forecasted issue with mcpba oxidation; we envisioned that the carboxylic acid termini could be used to directly furnish the epoxide while leaving the alkenes in the substrate fully intact.

Having selected fatty acids as an ideal starting material, we executed our synthesis of alkenyl epoxides. For a general scheme and the fully drawn products, see below. Briefly, fatty acids were subjected to a lithium aluminum hydride reduction followed by Dess-Martin Periodinane oxidation to afford their corresponding aldehydes. Proline catalyzed alpha-chlorination followed by sodium borohydride

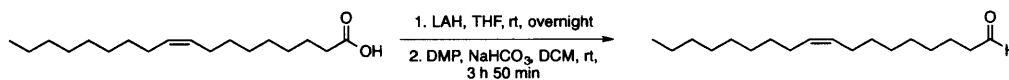
reduction in the same reaction flask afforded the 1,2-chloroalcohols in moderate yields. Finally, gentle heating of these 1,2-chloroalcohols at 35 °C in basic dioxane promoted ring closure to furnish the desired alkenyl epoxides **AE-00** through **AE-03** in moderate yields in 4 steps with only a single chromatographic purification. Excitingly, these alkene-containing epoxides represent a virtually unexplored synthetic scaffold for ionizable lipid development. We hope this synthetic route will broadly add to the creation of future generations of ionizable lipids for nucleic acid therapy. Full synthetic procedures and molecular characterization data for each step of the synthetic procedures for **AE-00** through **AE-03** are available below, as are the final syntheses of **OF-00** through **OF-03**.



### Scheme 2-1: Synthesis of AAA Ionizable Lipid Alkenyl Epoxide Precursors

#### 4.1. *AE-00* Synthesis; (*Z*)-2-(hexadec-7-en-1-yl)oxirane

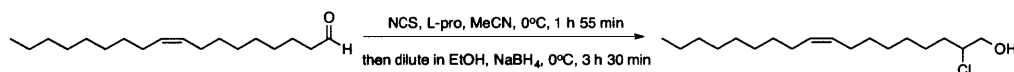
##### 4.1.1 Synthesis of *AE-00*-aldehyde



To a solution of oleic acid (5.01 ml, 15 mmol, 1 eq) in THF (190 ml) at 0°C was added lithium aluminum hydride (1 M in THF, 22.5 ml, 22.5 mmol, 1.5 eq) dropwise. The solution was allowed to warm to room temperature and was stirred

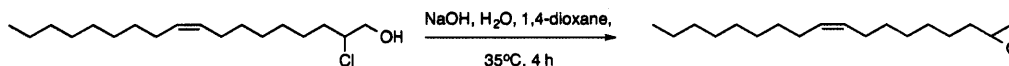
overnight. The reaction was quenched with sequential additions of water (0.85 ml), 1N NaOH (0.85 ml), and water (2.6 ml) dropwise. The mixture was filtered through celite, and the filtrate was concentrated under reduced pressure. The crude product, **AE-00-aldehyde**, a yellow oil, was then dissolved in CH<sub>2</sub>Cl<sub>2</sub> (160 ml). NaHCO<sub>3</sub> (8.821 g, 105 mmol, 7 eq) was added followed by Dess-Martin Periodinane (7.63 g, 18 mmol, 1.2 eq). The mixture was stirred for 3 hours, 50 minutes. It was then diluted in petroleum ether, washed sequentially with saturated NaHCO<sub>3</sub> and brine, dried over anhydrous sodium sulfate, filtered, and concentrated under reduced pressure. The crude product, a yellow oil, was used without further purification.

#### 4.1.2. Synthesis of AE-00-chloroalcohol



To a solution of **AE-00-aldehyde** (3.91 g, 14.7 mmol, 1 eq) in MeCN (40 ml) cooled to 0°C was added L-proline (0.507 g, 4.41 mmol, 0.3 eq) and *N*-chlorosuccinimide (1.8657 g, 14.0 mmol, 0.95 eq). The solution was stirred at 0°C for 1 hour, 55 minutes. It was then diluted in ethanol (23 mL) and to it was added NaBH<sub>4</sub> (71 mg, 1.875 mmol, 2.5 eq). The mixture was stirred at 0°C for 3 hours, 30 minutes. It was then diluted in ethyl acetate, washed with brine, dried over anhydrous sodium sulfate, filtered, and concentrated under reduced pressure. The crude product **AE-00-chloroalcohol**, a yellow oil, was used without further purification.

### 4.1.3. Synthesis of AE-00

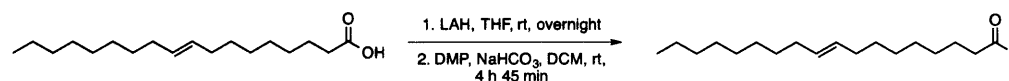


To a solution of **AE-00-chloroalcohol** (3.495 g, 11.6 mmol, 1 eq) in 1,4-dioxane (35 ml) was added a solution of NaOH (10.44 g, 261 mmol, 22.5 eq) in water (45 ml). The reaction mixture was heated to 35°C and allowed to stir for 4 hours. The resulting mixture was then diluted in hexanes, washed with brine, dried over anhydrous sodium sulfate, filtered, and concentrated under reduced pressure. The crude product was purified by flash chromatography on silica gel using acetone/hexanes (0:100 → 6:94) to yield **AE-00** (0.441 g, 1.65 mmol, 14% yield over 4 steps) as a pale yellow oil.

<sup>1</sup>H NMR (500 MHz, CDCl<sub>3</sub>, 20 °C): 5.34 (m, 2H, CHCH), 2.90 (m, 1H, CH<sub>2</sub>OCH), 2.74 (ddd, 1 H, CH<sub>2</sub>OCH), 2.46 (m, 1H, CH<sub>2</sub>OCH), 2.01 (pd, 4H, CHCHCH<sub>2</sub>), 1.68-1.18 (m, 22H, CH<sub>2</sub>), 0.88 (t, 3H, CH<sub>3</sub>)

## 4.2. AE-01 Synthesis; (E)-2-(hexadec-7-en-1-yl)oxirane

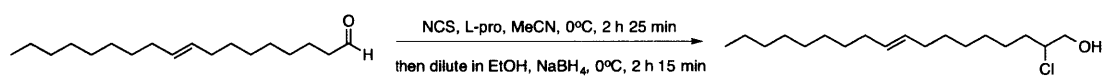
### 4.2.1. Synthesis of AE-01-aldehyde



To a solution of elaidic acid (4.717 g, 16.7 mmol, 1 eq) in THF (210 ml) at 0°C was added Lithium Aluminum Hydride (1 M in THF, 25 ml, 25 mmol, 1.5 eq) dropwise. The solution was allowed to warm to room temperature and was stirred overnight. The reaction was quenched with sequential additions of water (0.95 ml), 1N NaOH (0.95 ml), and water (2.9 ml) dropwise. The mixture was filtered through celite, and the filtrate was concentrated under reduced pressure. The crude product,

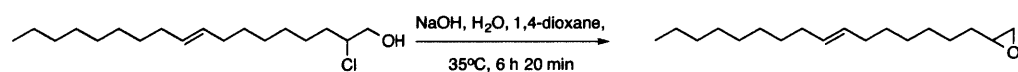
(E)-octadec-9-en-1-ol, was then dissolved in CH<sub>2</sub>Cl<sub>2</sub> (180 ml). NaHCO<sub>3</sub> (9.820 g, 116.9 mmol, 7 eq) was added followed by Dess Martin Periodinane (8.5 g, 20 mmol, 1.2 eq). The mixture was stirred for 4 hours, 45 minutes. It was then diluted in petroleum ether, washed sequentially with saturated NaHCO<sub>3</sub> and brine, dried over anhydrous sodium sulfate, filtered, and concentrated under reduced pressure. The crude product **AE-01-aldehyde**, a white solid, was used without further purification.

#### 4.2.2. Synthesis of AE-01-chloroalcohol



To a solution **AE-01-aldehyde** (16.7 mmol, 1 eq) in MeCN (46 ml) cooled to 0°C was added L-proline (0.577 g, 5.01 mmol, 0.3 eq) and *N*-chlorosuccinimide (2.118 g, 15.8 mmol, 0.95 eq). The solution was stirred at 0°C for 2 hours, 25 minutes. It was then diluted in ethanol (26 ml) and to it was added NaBH<sub>4</sub> (1.579 g, 41.75 mmol, 2.5 eq). The mixture was stirred at 0°C for 2 hours, 15 minutes. It was then diluted in ethyl acetate, washed with brine, dried over anhydrous sodium sulfate, filtered, and concentrated under reduced pressure. The crude product **AE-01-chloroalcohol**, a white solid, was used without further purification.

#### 4.2.3. Synthesis of AE-01



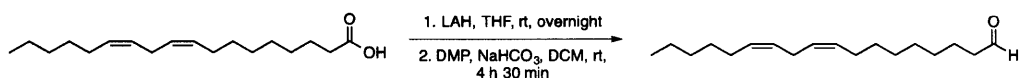
To a solution of **AE-01-chloroalcohol** in 1,4-dioxane (50 ml) was added a solution of NaOH (15.03 g, 376 mmol, 22.5 eq) in water (65 ml). The reaction mixture was heated to 35°C and allowed to stir for 6 hours, 20 minutes. The resulting mixture was then diluted in hexanes, washed with brine, dried over anhydrous sodium

sulfate, filtered, and concentrated under reduced pressure. The crude product was purified by flash chromatography on silica gel using acetone/hexanes (0:100 → 10:90) to yield **AE-01** as an off-white oil (19% yield over 4 steps).

<sup>1</sup>H NMR (500 MHz, CDCl<sub>3</sub>, 20 °C): 5.37 (m, 2H, CHCH), 2.87 (tq, 1H, CH<sub>2</sub>OCH), 2.71 (m, 1H, CH<sub>2</sub>OCH), 2.43 (dt, 1H, CH<sub>2</sub>OCH), 1.95 (m, 4 H, CHCHCH<sub>2</sub>), 1.36-1.16 (m, 22 H, CH<sub>2</sub>), 0.86 (t, 3 H, CH<sub>3</sub>)

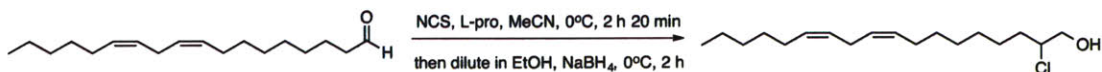
### 4.3. AE-02 Synthesis; ((7Z,10Z)-hexadeca-7,10-dien-1-yl)oxirane

#### 4.3.1. Synthesis of AE-02-aldehyde



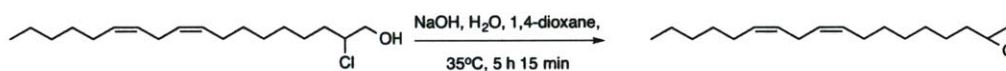
To a solution of linoleic acid (4.66 ml, 15 mmol, 1 eq) in THF (190 ml) at 0°C was added Lithium Aluminum Hydride (1 M in THF, 22.5 ml, 22.5 mmol, 1.5 eq) dropwise. The solution was allowed to warm to room temperature and was stirred overnight. The reaction was quenched with sequential additions of water (0.85 ml), 1N NaOH (0.85 ml), and water (2.6 ml) dropwise. The mixture was filtered through celite, and the filtrate was concentrated under reduced pressure. The crude product was subsequently dissolved in CH<sub>2</sub>Cl<sub>2</sub> (160 ml). NaHCO<sub>3</sub> (8.821 g, 105 mmol, 7 eq) was added followed by Dess-Martin-Periodinane (7.63 g, 18 mmol, 1.2 eq). The mixture was stirred for 4 hours, 30 minutes. It was then diluted in petroleum ether, washed sequentially with saturated NaHCO<sub>3</sub> and brine, dried over anhydrous sodium sulfate, filtered, and concentrated under reduced pressure. The crude product **AE-02-aldehyde**, a yellow oil, was used without further purification.

#### 4.3.2. Synthesis of AE-02-chloroalcohol



To a solution **AE-02-aldehyde** (3.3955 g, 12.7 mmol, 1 eq) in MeCN (35 ml) cooled to 0°C was added L-proline (518 mg, 4.5 mmol, 0.3 eq) and *N*-chlorosuccinimide (1.903 g, 14.25 mmol, 0.95 eq). The solution was stirred at 0°C for 2 hours 20 minutes. It was then diluted in ethanol (20 ml) and to it was added NaBH<sub>4</sub> (1.418 g, 37.5 mmol, 2.5 eq). The mixture was stirred at 0°C for 2 hours. It was then diluted with ethyl acetate, washed with brine, dried over anhydrous sodium sulfate, filtered, and concentrated under reduced pressure. The crude product **AE-02-chloroalcohol**, a yellow oil was used without further purification.

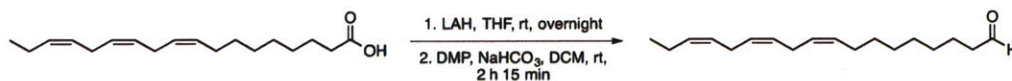
#### 4.3.3. Synthesis of AE-02



To a solution of **AE-02-chloroalcohol** (1.4768 g, 4.91 mmol, 1 eq) in 1,4-dioxane (14.7 ml) was added a solution of NaOH (4.417 g, 110.4 mmol, 22.5 eq) in water (19.4 ml). The reaction mixture was heated to 35°C and allowed to stir for 5 hours, 15 minutes. The resulting mixture was then diluted in hexanes, washed with brine, dried over anhydrous sodium sulfate, filtered, and concentrated under reduced pressure. The crude product was purified by flash chromatography on silica gel using ether/petroleum ether (0:100 → 20:80) to yield **AE-02** (in 41% yield over 4 steps).  
<sup>1</sup>H NMR (500 MHz, CDCl<sub>3</sub>, 20 °C): 5.33 (m, 4 H, CHCH), 2.88 (tdd, 1H, CH<sub>2</sub>OCH), 2.73 (m, 3H, CH<sub>2</sub>OCH and CHCH<sub>2</sub>CH), 2.44 (m, 1H, CH<sub>2</sub>OCH), 2.04 (qd, 4H, CH<sub>2</sub>CH<sub>2</sub>CHCH), 1.58-1.19 (m, 14H, CH<sub>2</sub>), 0.87 (t, 3H, CH<sub>3</sub>)

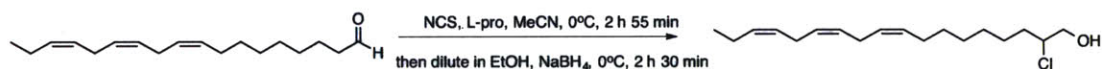
#### 4.4. Synthesis of AE-03; 2-((7Z,10Z,13Z)-hexadeca-7,10,13-trien-1-yl)oxirane

##### 5.4.1. Synthesis of AE-03-aldehyde



To a solution of linolenic acid (4.57 ml, 15 mmol, 1 eq) in THF (190 ml) at 0 °C was added Lithium Aluminum Hydride (1 M in THF, 22.5 ml, 22.5 mmol, 1.5 eq) dropwise. The solution was allowed to warm to room temperature and was stirred overnight. The reaction was quenched with sequential additions of water (0.85 ml), 1N NaOH (0.85 ml), and water (2.6 ml) dropwise. The mixture was filtered through celite, and the filtrate was concentrated under reduced pressure. The crude product was then dissolved in CH<sub>2</sub>Cl<sub>2</sub> (160 ml). NaHCO<sub>3</sub> (8.821 g, 105 mmol, 7 eq) was added followed by Dess-Martin-Periodinane (7.63 g, 18 mmol, 1.2 eq). The mixture was stirred for 2 hours, 15 minutes. It was then diluted in petroleum ether, washed sequentially with saturated NaHCO<sub>3</sub> and brine, dried over anhydrous sodium sulfate, filtered, and concentrated under reduced pressure. The crude product **AE-03-aldehyde**, a yellow oil, was used without further purification.

##### 4.4.2. Synthesis of AE-03-chloroalcohol

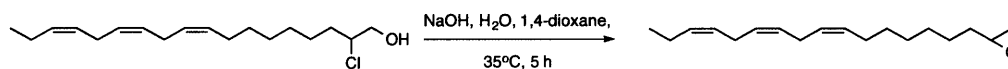


To a solution of **AE-03-aldehyde** (5.131, 1 eq) in MeCN (14 ml) cooled to 0 °C was added L-proline (177 mg, 1.54 mmol, 0.3 eq) and *N*-chlorosuccinimide (650 mg, 4.87 mmol, 0.95 eq). The solution was stirred at 0 °C for 2 hours 55 minutes. It was then diluted in ethanol (8 ml) and to it was added NaBH<sub>4</sub> (484 mg, 12.8 mmol, 2.5 eq). The solution was stirred at 0 °C for 2 hours, 30 minutes. It was then diluted in ethyl acetate, washed with brine, dried over anhydrous sodium sulfate, filtered, and



concentrated under reduced pressure. The crude product **AE-03-chloroalcohol**, a yellow oil, was used without further purification.

#### 4.4.3. Synthesis of AE-03

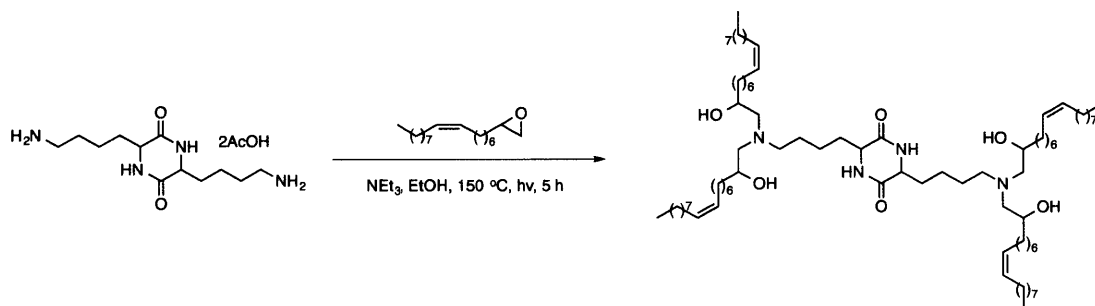


To a solution of **AE-03-chloroalcohol** (5.13 mmol, 1 eq) in 1,4-dioxane (15.5 ml) was added a solution of NaOH (4.617 g, 115.4 mmol, 22.5 eq) in H<sub>2</sub>O (20 ml). The reaction mixture was heated to 35°C and allowed to stir for 5 hours. The resulting mixture was then diluted in hexanes, washed with brine, dried over anhydrous sodium sulfate, filtered, and concentrated under reduced pressure. The crude product was purified by flash chromatography on silica gel using acetone/hexanes (0:100 → 10:90) to yield **AE-03** as a pale yellow oil (9% yield over 4 steps).

<sup>1</sup>H NMR (500 MHz, CDCl<sub>3</sub>, 20 °C): 5.33 (m, 6H, CH), 2.88 (tdd, 1H, CH<sub>2</sub>OCH), 2.80 (m, 5H, CHCH<sub>2</sub>CH), 2.73 (m, 1 H, CH<sub>2</sub>OCH), 2.44 (m, 1H CH<sub>2</sub>OCH), 2.04 (m, 4H, CH<sub>2</sub>CH<sub>2</sub>CH), 1.58-1.19 (m, 10H, CH<sub>2</sub>), 0.87 (t, 3H, CH<sub>3</sub>)

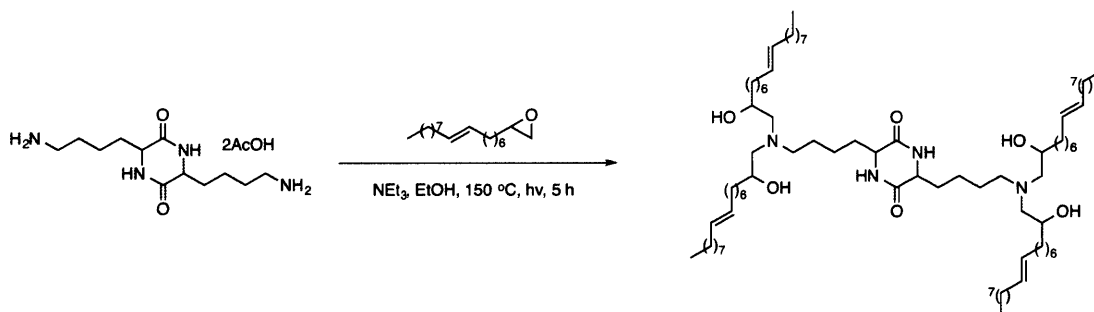
#### 4.5. Synthesis of AAA Ionizable Lipids OF-00 through OF-03

##### 4.5.1. Synthesis of OF-00



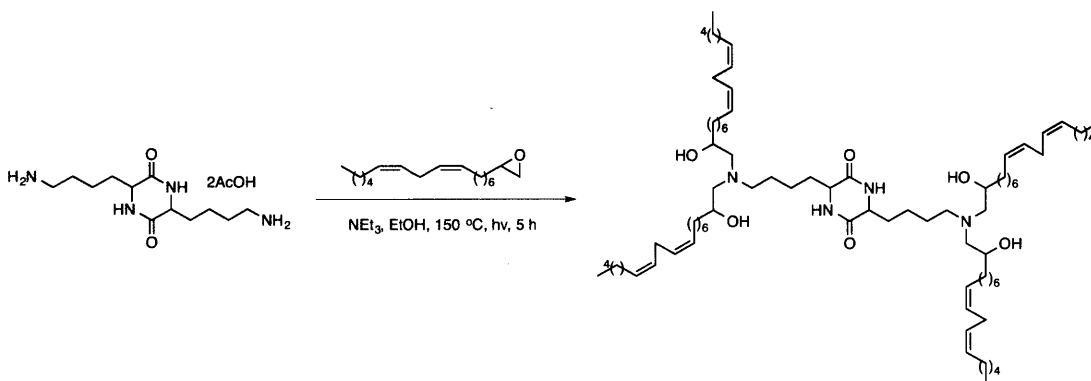
To a solution of **AE-00** (359 mg, 1.35 mmol, 6 eq) in ethanol (2 ml) was added diketopiperazine **1** (84.7 mg, 0.225 mmol, 1 eq) followed by triethylamine (125  $\mu$ l, 0.9 mmol, 4 eq). The mixture was stirred at room temperature for 5 minutes before being irradiated, with stirring, in a microwave for 5 hours at 150 °C. The crude product was purified by flash chromatography to yield the product as a viscous yellow oil (19% yield). <sup>1</sup>H NMR (500 MHz, DMSO-d<sub>6</sub>, 20 °C) 8.11 (br, 2H, CONH), 5.15-5.2 (m, 8H, CH<sub>2</sub>CH), 4.21 (dd, 4H, OH), 3.79 (br, 2H, COCH), 3.44 (br, 4H, CHOH), 2.25-2.44 (m, 12H, NCH<sub>2</sub>), 2.1 (m, 16H, CHCH<sub>2</sub>CH<sub>2</sub>), 1.64-1.67 (m, 4H, CH<sub>2</sub>), 1.21-1.39 (m, 96H, CH<sub>2</sub>), 0.88 (t, 12H, CH<sub>3</sub>). HRMS (DART) (m/z): calc'd for C<sub>84</sub>H<sub>160</sub>N<sub>4</sub>O<sub>6</sub> [M + H]<sup>+</sup>: 1322.23; found: 1322.04.

#### 4.5.2. Synthesis of OF-01



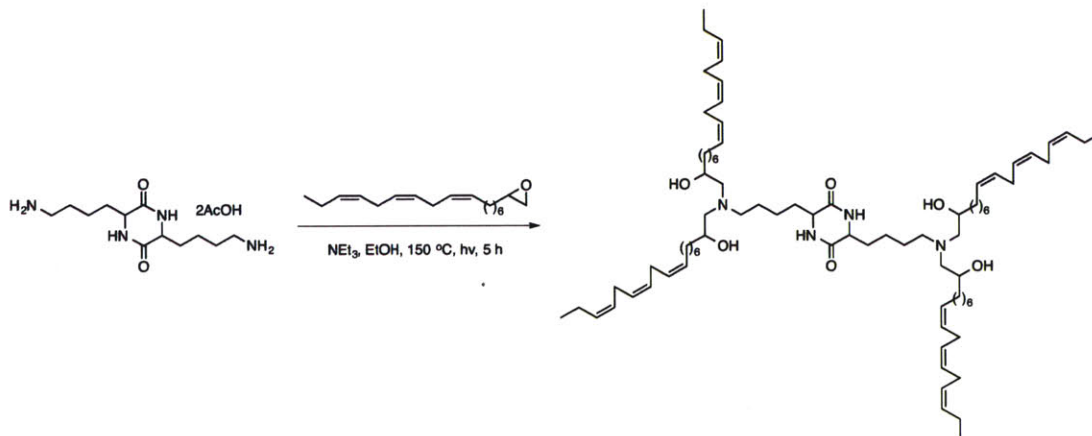
To a solution of **AE-01** (359 mg, 1.35 mmol, 6 eq) in ethanol (2 ml) was added diketopiperazine **1** (84.7 mg, 0.225 mmol, 1 eq) followed by triethylamine (125  $\mu$ l, 0.9 mmol, 4 eq). The mixture was stirred at room temperature for 5 minutes before being irradiated, with stirring, in a microwave for 5 hours at 150 °C. The crude product was purified by flash chromatography to yield the product as a yellow oil (9% yield). <sup>1</sup>H NMR (500 MHz, DMSO-d<sub>6</sub>, 20 °C) 8.11 (br, 2H, CONH), 5.15-5.2 (m, 8H, CH<sub>2</sub>CH), 4.21 (dd, 4H, OH), 3.79 (br, 2H, COCH), 3.44 (br, 4H, CHOH), 2.25-2.44 (m, 12H, NCH<sub>2</sub>), 2.1 (m, 16H, CHCH<sub>2</sub>CH<sub>2</sub>), 1.64-1.67 (m, 4H, CH<sub>2</sub>), 1.21-1.39 (m, 96H, CH<sub>2</sub>), 0.88 (t, 12H, CH<sub>3</sub>). HRMS (DART) (m/z): calc'd for C<sub>84</sub>H<sub>160</sub>N<sub>4</sub>O<sub>6</sub> [M + H]<sup>+</sup>: 1322.23; found: 1322.09.

#### 4.5.3. Synthesis of OF-02



To a solution of **AE-02** (357 mg, 1.35 mmol, 6 eq) in ethanol (2 ml) was added diketopiperazine **1** (84.7 mg, 0.225 mmol, 1 eq) followed by triethylamine (125  $\mu$ l, 0.9 mmol, 4 eq). The mixture was stirred at room temperature for 7 minutes before being irradiated, with stirring, in a microwave for 5 hours at 150 °C. The crude product was purified by flash chromatography to yield the product as a yellow oil (33% yield).  $^1\text{H}$  NMR (500 MHz, DMSO- $d_6$ , 20 °C) 8.11 (br, 2H, CONH), 5.15-5.2 (m, 16H,  $\text{CH}_2\text{CH}$ ), 4.21 (dd, 4H, OH), 3.79 (br, 2H, COCH), 3.44 (br, 4H, CHOH), 2.7 (m, 8H,  $\text{CHCH}_2\text{CH}$ ), 2.25-2.44 (m, 12H,  $\text{NCH}_2$ ), 2.1 (m, 16H,  $\text{CHCH}_2\text{CH}_2$ ), 1.64-1.67 (m, 4H,  $\text{CH}_2$ ), 1.21-1.39 (m, 72H,  $\text{CH}_2$ ), 0.88 (t, 12H,  $\text{CH}_3$ ). HRMS (DART) ( $m/z$ ): calc'd for  $\text{C}_{84}\text{H}_{152}\text{N}_4\text{O}_6$  [ $\text{M} + \text{H}$ ] $^+$ : 1314.17; found: 1314.93.

#### 4.5.4. Synthesis of OF-03



To a solution of **AE-03** (357 mg, 1.35 mmol, 6 eq) in ethanol (2 ml) was added diketopiperazine **1** (84.7 mg, 0.225 mmol, 1 eq) followed by triethylamine (125  $\mu$ l, 0.9 mmol, 4 eq). The mixture was stirred at room temperature for 10 minutes before being irradiated, with stirring, in a microwave for 5 hours at 150 °C. The crude product was purified by flash chromatography to yield the product, as a mix of the desired product and the tri-substituted product, as a yellow oil (6% yield). <sup>1</sup>H NMR (500 MHz, DMSO-d<sub>6</sub>, 20 °C) 8.11 (br, 2H, CONH), 5.15-5.2 (m, 24H, CH<sub>2</sub>CH), 4.21 (dd, 4H, OH), 3.79 (br, 2H, COCH), 3.44 (br, 4H, CHOH), 2.7 (m, 16H, CHCH<sub>2</sub>CH), 2.25-2.44 (m, 12H, NCH<sub>2</sub>), 2.1 (m, 16H, CHCH<sub>2</sub>CH<sub>2</sub>), 1.64-1.67 (m, 4H, CH<sub>2</sub>), 1.21-1.39 (m, 48H, CH<sub>2</sub>), 0.88 (t, 12H, CH<sub>3</sub>). HRMS (DART) (m/z): calc'd for C<sub>84</sub>H<sub>144</sub>N<sub>4</sub>O<sub>6</sub> [M + H]<sup>+</sup>: 1306.11; found: 1306.87.

5. Additional Data from Text

Ionizable Lipid LNP	Average EPO (ng/mL)	Encapsulation Efficiency (%)	LNP Diameter (nm)	PDI
ckk-E12	7100 ± 700	54	83	0.217
OF-00	2100 ± 500	74	92	0.147
OF-01	500 ± 200	81	78	0.194
OF-02	14200 ± 1500	55	122	0.130
OF-03	140 ± 3	76	75	0.239

**Table 2-1:** LNP Formulation Characterization. Serum EPO concentrations reported as mean ± SD (n = 3) 6 hr after a 0.75 mg/kg dose intravenous injection into mice. Encapsulation efficiencies, LNP diameter, and PDI were collected as described above for each representative LNP formulation.

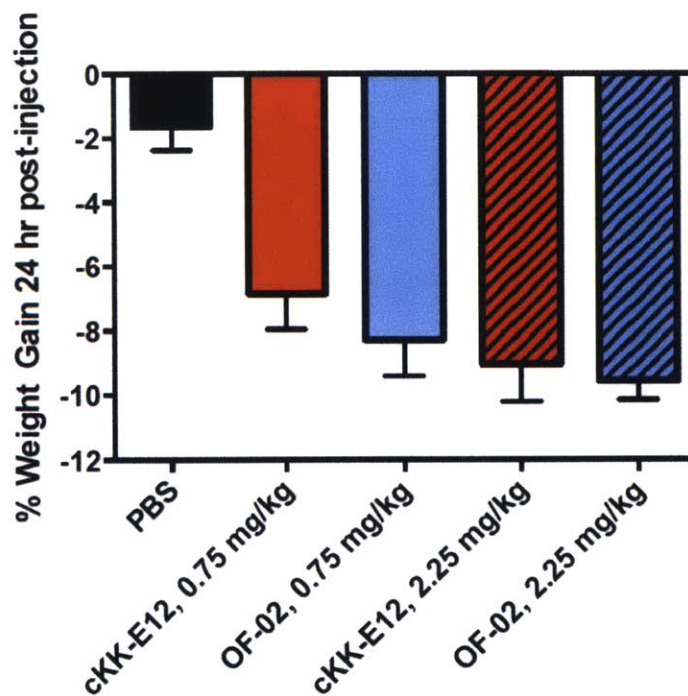


**Figure 2-5.** Percent weight gain reported as mean – SD (n=3) 24 hours after respective intravenous dose into mice.

## ***6. Cryogenic Transmission Electron Microscopy of Lipid Nanoparticles***

LNPs were prepared as previously described in section 2 (General Lipid Nanoparticle Synthesis), with the exception that they were dialyzed against 0.1X PBS instead of 1X PBS. The batch of LNPs was then split, and the encapsulation efficiency was calculated for a subpopulation of the LNPs using the aforementioned method (section 3: General Lipid Nanoparticle Characterization, Quanti-iT RiboGreen RNA assay from Invitrogen, see above). The remaining LNPs were then prepared for Cryogenic TEM. Briefly, 3  $\mu$ L of the LNP solution was diluted with buffer and was placed onto a lacey copper grid coated with a continuous carbon film. Excess sample was blotted off using a Gatan Cryo Plunge III. The grid was then mounted on a Gatan 626 cryo-holder equipped within the TEM column. The specimen and holder tip were continually cooled by liquid nitrogen during transfer into the microscope and subsequent imaging. Imaging was performed using a JEOL 2100 FEG microscope using a minimum dose method that was essential to avoiding sample damage under the electron beam. The microscope was operated at 200 kV and with a magnification setting of 60,000 for assessing particle size and distribution. All images were recorded on a Gatan 2kx2k UltraScan CCD camera.

### C. References

- [1] a) R. Kanasty, J. R. Dorkin, A. Vegas, D. Anderson, *Nat Mater* **2013**, *12*, 967-977; b) K. A. Whitehead, R. Langer, D. G. Anderson, *Nat Rev Drug Discov* **2009**, *8*, 516-516.
- [2] U. Sahin, K. Kariko, O. Tureci, *Nat Rev Drug Discov* **2014**, *13*, 759-780.
- [3] B. Leader, Q. J. Baca, D. E. Golan, *Nat Rev Drug Discov* **2008**, *7*, 21-39.
- [4] M. S. D. Kormann, G. Hasenpusch, M. K. Aneja, G. Nica, A. W. Flemmer, S. Herber-Jonat, M. Huppmann, L. E. Mays, M. Illenyi, A. Schams, M. Griese, I. Bittmann, R. Handgretinger, D. Hartl, J. Rosenecker, C. Rudolph, *Nat Biotechnol* **2011**, *29*, 154-U196.
- [5] A. Thess, S. Grund, B. L. Mui, M. J. Hope, P. Baumhof, M. Fotin-Mleczek, T. Schlake, *Mol Ther* **2015**, *23*, S55-S55.
- [6] K. J. Kauffman, J.R. Dorkin, J.H. Yang, M.W. Heartlein, F. DeRosa, F.F. Mir, O.S. Fenton, D.G. Anderson, *Nano Lett.*, **2015**, 7300-7306.
- [7] a) J. J. Lu, R. Langer, J. Z. Chen, *Mol Pharmaceut* **2009**, *6*, 763-771; b) T. M. Allen, P. R. Cullis, *Adv Drug Deliver Rev* **2013**, *65*, 36-48.
- [8] I. S. Zuhorn, U. Bakowsky, E. Polushkin, W. H. Visser, M. C. A. Stuart, J. B. F. N. Engberts, D. Hoekstra, *Mol Ther* **2005**, *11*, 801-810.
- [9] B. L. Mui, Y. K. Tam, M. Jayaraman, S. M. Ansell, X. Y. Du, Y. Y. C. Tam, P. J. C. Lin, S. Chen, J. K. Narayanannair, K. G. Rajeev, M. Manoharan, A. Akinc, M. A. Maier, P. Cullis, T. D. Madden, M. J. Hope, *Mol Ther-Nucl Acids* **2013**, *2*.
- [10] a) G. Sahay, W. Querbes, C. Alabi, A. Eltoukhy, S. Sarkar, C. Zurenko, E. Karagiannis, K. Love, D. L. Chen, R. Zoncu, Y. Buganim, A. Schroeder, R. Langer, D. G. Anderson, *Nat Biotechnol* **2013**, *31*, 653-U119; b) K. T. Love,



- K. P. Mahon, C. G. Levins, K. A. Whitehead, W. Querbes, J. R. Dorkin, J. Qin, W. Cantley, L. L. Qin, T. Racie, M. Frank-Kamenetsky, K. N. Yip, R. Alvarez, D. W. Y. Sah, A. de Fougères, K. Fitzgerald, V. Kotliansky, A. Akinc, R. Langer, D. G. Anderson, *P Natl Acad Sci USA* **2010**, *107*, 9915-9915.
- [11] S. C. Semple, A. Akinc, J. X. Chen, A. P. Sandhu, B. L. Mui, C. K. Cho, D. W. Y. Sah, D. Stebbing, E. J. Crosley, E. Yaworski, I. M. Hafez, J. R. Dorkin, J. Qin, K. Lam, K. G. Rajeev, K. F. Wong, L. B. Jeffs, L. Nechev, M. L. Eisenhardt, M. Jayaraman, M. Kazem, M. A. Maier, M. Srinivasulu, M. J. Weinstein, Q. M. Chen, R. Alvarez, S. A. Barros, S. De, S. K. Klimuk, T. Borland, V. Kosovrasti, W. L. Cantley, Y. K. Tam, M. Manoharan, M. A. Ciufolini, M. A. Tracy, A. de Fougères, I. MacLachlan, P. R. Cullis, T. D. Madden, M. J. Hope, *Nat Biotechnol* **2010**, *28*, 172-U118.
- [12] Y. Z. Dong, K. T. Love, J. R. Dorkin, S. Sirirungruang, Y. L. Zhang, D. L. Chen, R. L. Bogorad, H. Yin, Y. Chen, A. J. Vegas, C. A. Alabi, G. Sahay, K. T. Olejnik, W. H. Wang, A. Schroeder, A. K. R. Lytton-Jean, D. J. Siegwart, A. Akinc, C. Barnes, S. A. Barros, M. Carioto, K. Fitzgerald, J. Hettinger, V. Kumar, T. I. Novobrantseva, J. N. Qin, W. Querbes, V. Kotliansky, R. Langer, D. G. Anderson, *P Natl Acad Sci USA* **2014**, *111*, 5753-5753.
- [13] a) N. Bartke, Y. A. Hannun, *J Lipid Res* **2009**, *50*, S91-S96; b) Y. A. Hannun, L. M. Obeid, *Nat Rev Mol Cell Bio* **2008**, *9*, 139-150.
- [14] a) K. Kariko, H. Muramatsu, J. M. Keller, D. Weissman, *Mol Ther* **2012**, *20*, 948-953; b) S. Liu, J. A. Ren, Z. W. Hong, D. S. Yan, G. S. Gu, G. Han, G. F. Wang, H. J. Ren, J. Chen, J. S. Li, *Nutr Clin Pract* **2013**, *28*, 120-127.

- [15] K. A. Whitehead, J. R. Dorkin, A. J. Vegas, P. H. Chang, O. Veiseh, J. Matthews, O. S. Fenton, Y. L. Zhang, K. T. Olejnik, V. Yesilyurt, D. L. Chen, S. Barros, B. Klebanov, T. Novobrantseva, R. Langer, D. G. Anderson, *Nat Commun* **2014**, *5*.
- [16] J. Heyes, L. Palmer, K. Bremner, I. MacLachlan, *J Control Release* **2005**, *107*, 276-287.
- [17] M. Cazzola, F. Mercuriali, C. Brugnara, *Blood* **1997**, *89*, 4248-4267.
- [18] J. McClellan, M. C. King, *Cell* **2010**, *142*, 353-355.

## CHAPTER 3

### Fatty Acid Derived Lipid Nanoparticles Deliver mRNA to B Lymphocytes In Vivo

The work presented in this chapter has been filed with the United States Patent and Trademark Office:

Fenton, O.S.; Dorkin, J.R.; Anderson, D.G.; McClellan, R.M. "Polyamine-Fatty Acid Derived Lipidoids and Uses Thereof". US Patent Number: 20,160,002,178. Filing Date: July 1, 2015

The work presented in this chapter will be published in the following manuscript:

Fenton, O.S.; Kauffman, K.J.; Kaczmarek, J.C.; McClellan, R.L.; Jhunjhunwala, S; Zeng, M.D.; Appel, E.A.; Dorkin, J.R.; Mir, F.; Yang, J.; Tibbitt, M.W.; Heartlein, M.W.; DeRosa, F.; Langer, R.; Anderson, D.G. \* Fatty Acid Derived Lipid Nanoparticles Deliver mRNA to B Lymphocytes In Vivo

## A. Discussion

B lymphocytes (commonly referred to as B cells) are a versatile subpopulation of white blood cells that originate in the bone marrow, mature in the spleen, and circulate throughout the vasculature and lymphatic system in healthy individuals.<sup>[1]</sup> While B cells perform a wide range of biological functions, they are predominantly responsible for three critical tasks *in vivo*: *i.* producing and secreting antibodies to fight infections; *ii.* generating memory cells that mitigate the deleterious effects of pathogen re-exposure; and *iii.* stimulating T cell production through antigen presentation via the MHC I (killer T cell) or MHC II (helper T cell) complexes.<sup>[2]</sup> Despite their essential role in disease prevention and management, B cell dysfunction can also serve as the root of disease. For example, misregulated B lymphocyte proliferation can result in non-Hodgkin's B-cell lymphoma, from which nearly 20,000 patients die each year in the US alone.<sup>[3]</sup> Moreover, a cure for lymphomas and cancers of the circulation, in general, remains elusive. As a result, B cells represent an interesting target for drug delivery, as having the ability to modulate their function *in vivo* could have profound impact on the study, prevention, and treatment of disease.<sup>[4]</sup>

Recently, the delivery of messenger RNA (mRNA) cargo encapsulated in lipid nanoparticles (LNPs) has emerged as one potential strategy to modulate cell activity *in vivo*.<sup>[5]</sup> LNPs serve to shield the mRNA from nucleases, prevent unwanted clearance, and promote cellular uptake. Upon accessing the cytosol, LNPs can decomplex from the mRNAs, allowing them to be translated into multiple copies of bioactive proteins whose presence in the cytoplasm can modulate cellular function.<sup>[6]</sup> While several mRNA LNPs have recently been developed, they are currently limited by their biodistribution. Indeed,

all current lead mRNA LNPs target the liver predominantly, resulting in more than 99% of total protein expression in this organ.<sup>[5a, 5b]</sup> The targeting of non-liver cell populations with mRNA LNPs remains challenging and overcoming this limitation in biodistribution is paramount to the eventual clinical translation of mRNA based therapeutics for non-liver-based cell populations. Further, off-site protein production can result in toxicity issues in otherwise healthy cells and tissues.<sup>[7]</sup>

Here, we report a novel LNP system that affords the first *in vivo* example of mRNA-induced protein expression in B lymphocytes (**Figure 3-1a,b**). In contrast to previous mRNA LNP systems that produce protein primarily in the liver, our system, afforded by the synthesis of ionizable lipid **OF-77**, results in more than 85% of total protein production in the spleen following a routine intravenous injection. We demonstrate that the development of **OF-77** LNPs represents a significant advance in the field of mRNA delivery to B lymphocytes, wherein intracellular protein expression in B cells, induced by **OF-77** LNPs, is limited only by the dose of mRNA provided *in vivo*.

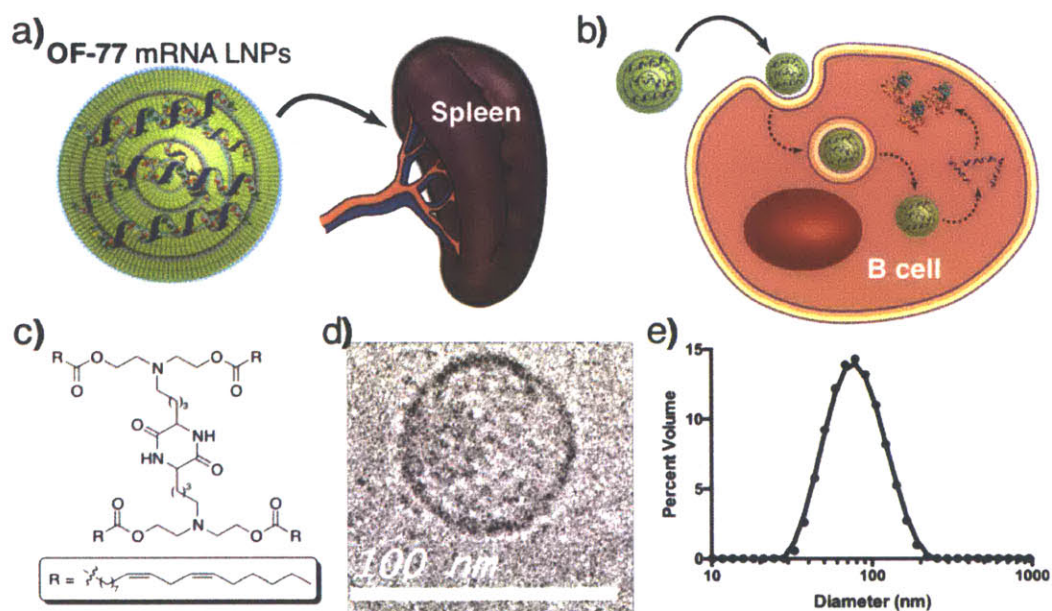


**Figure 3-1.** a) **OF-77** LNPs target the spleen *in vivo*. b) B lymphocytes are transfected with **OF-77** LNPs, with resultant protein expression. c) chemical structure of **OF-77**. d) Representative cryogenic transmission electron microscopy of **OF-77** LNPs. e) Dynamic Light Scattering Trace of **OF-77** LNPs.

Our study began with the synthesis of **OF-77**, an amino-acid-derived diketopiperazine<sup>[8]</sup> with ester-appended linoleic acid tails (**Figure 3-1c**). Briefly, this material was accessed in 5 synthetic steps from a bis-lysine diketopiperazine, with key steps including a deprotection/Steglich esterification protocol.<sup>[9]</sup> Complete synthetic procedures and molecular characterization details can be found in **Experimental Section 2**. **OF-77** was then formulated into LNPs with 1,2-dioleoyl-*sn*-glycero-3-phosphoethanolamine (DOPE, to modify bilayer structure), C14-PEG-2000 (to prevent LNP aggregation), cholesterol (to aid in membrane stability), and unmodified mRNA coding for firefly luciferase (FLuc).<sup>[5a]</sup> LNP formation was confirmed using cryogenic transmission electron microscopy (**Figure 3-1d**); interesting structural features include a spherical morphology similar to that observed for previously described liver-targeting

mRNA LNPs. Furthermore, dynamic light scattering was used to quantify the size distribution of **OF-77** mRNA LNPs, highlighting an average particle diameter of 84 nm with a narrow polydispersity of 0.118 (**Figure 3-1e**). Finally, the encapsulation efficiency of these **OF-77** LNPs was measured as approximately 56% for the FLuc mRNA.<sup>[10]</sup>

With mRNA-loaded **OF-77** LNPs in hand, we sought to characterize their ability to induce functional translation of FLuc in mammalian cells, validating them as a viable delivery vehicle for mRNA. Towards this end, American Type HeLa cells were treated with **OF-77** FLuc-mRNA LNPs at doses ranging from 12.5 to 200 ng of total mRNA per 15,000 cells. After 24 hours, total luminescence levels were quantified, demonstrating near-linear protein production over the entire dosing range (**Figure 3-2a**). Notably, cell viability was 100% across all doses studied; this stands in contrast to other cellular transfection techniques including electroporation,<sup>[11]</sup> mechanical disruption of the cellular membrane,<sup>[12]</sup> and viruses.<sup>[13]</sup> Further, these results suggest that translation of the desired protein with our system *in vitro* is limited only by the dose of mRNA applied.

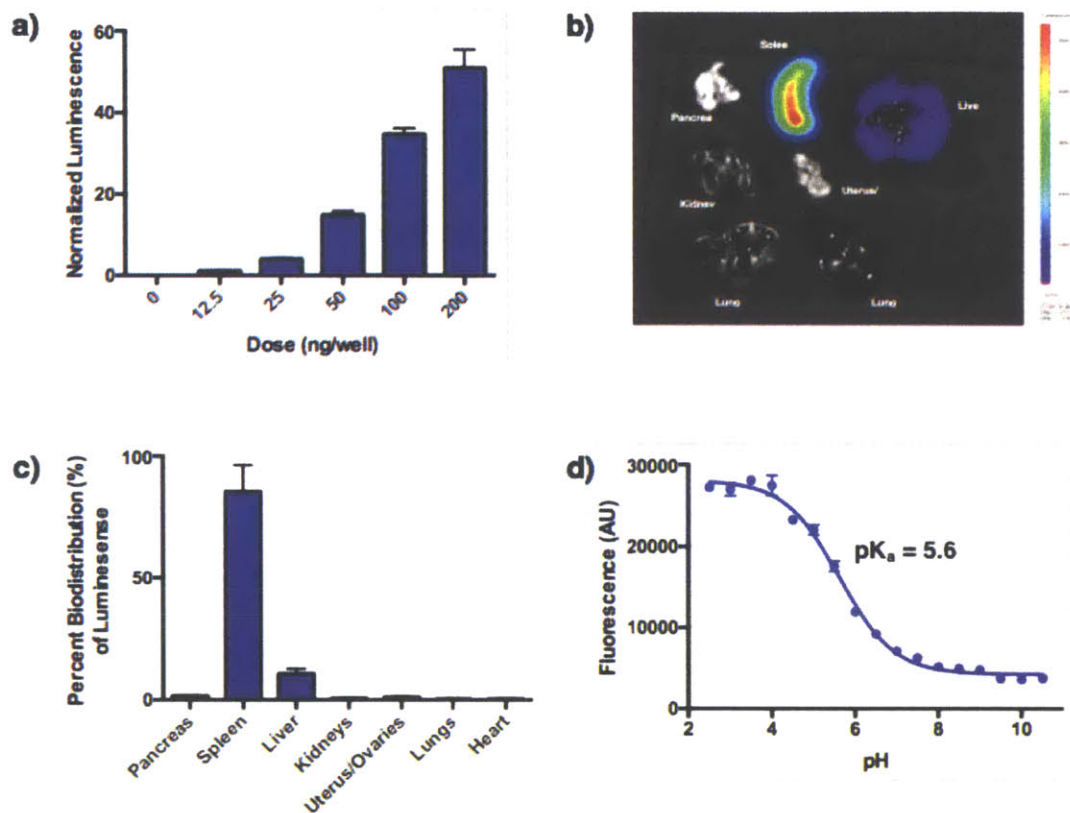


**Figure 3-2.** a) In vitro dose-response for OF-77 LNPs. b) Representative luminescence biodistribution of OF-77 LNPs with luciferase mRNA *ex-vivo*. c) Percent Biodistribution of Luminescence. d) TNS Assay of OF-77 LNPs and corresponding pK<sub>a</sub>.

Having established OF-77 LNPs as a viable delivery vehicle for mRNA transfection *in vitro*, our attention then shifted to validating OF-77 LNP mRNA delivery *in vivo*. The clinical translation of mRNA LNPs is in part predicated on the ability to promote selective protein expression in specific tissues, whether healthy or diseased, while simultaneously avoiding potential complications caused by off-target protein production. FLuc mRNA was therefore selected as a model therapeutic cargo for our study for two reasons: 1) the associated protein can be directly imaged in whole organs, allowing us to verify whether or not OF-77 LNPs demonstrate requisite levels of non-



liver tissue specificity for protein production and 2) the total luminescent signal can be directly correlated to the total number of individual protein molecules, allowing for robust protein quantification. Towards this end, **OF-77** FLuc-mRNA LNPs were injected intravenously at a 0.75 mg/kg dose in C57BL/6 mice alongside a phosphate buffered saline (PBS) negative control. At 6 hours post-injection, each mouse was treated intraperitoneally with D-Luciferin and then sacrificed. The organs (pancreas, spleen, kidneys, lungs, heart, uterus/ovaries) were isolated by standard necropsy and then imaged with an IVIS imaging system (**Figure 3-2b**). **OF-77** FLuc-mRNA LNPs demonstrated a unique protein expression profile when compared with other mRNA LNPs described in the literature. Whereas current mRNA LNPs target the liver with greater than 99% specificity, **OF-77** mRNA LNPs promote protein expression predominantly in the spleen, with minimal translation in the liver, and negligible translation in other organs. Quantification of this data further substantiated this observation, with more than 85% of total protein production occurring in the spleen (**Figure 3-2c**). While we are still discerning why this unique biodistribution profile is observed, one possible explanation is that the  $pK_a$  (defined as the inflection point on previously described TNS assay curves for LNPs) of **OF-77** FLuc-mRNA LNPs appears to be considerably lower ( $\sim 5.6$ ) than those observed for liver-targeting mRNA LNPs ( $\sim 7.3$ ) (**Figure 3-2d**).<sup>[5a]</sup> We hope that this empirical finding will help to inspire future generations of non-liver targeting mRNA LNPs, as well as contribute to the development of enhanced understanding as to how LNP surface properties impact efficacy and biodistribution.

Having established that **OF-77** LNPs target the spleen, we were optimistic that **OF-77** LNPs may indeed target B cells *in vivo*, largely because the spleen is the primary

residence site of nearly all immune cells. To test this hypothesis, fluorescence assisted cell sorting (FACS) was performed on cells isolated from the spleen.<sup>[14]</sup> Briefly, **OF-77** LNPs were formulated as before, with the exception that the mRNA sequence was modified to contain a Cy5 dye molecule approximately every 16<sup>th</sup> base pair. These LNPs were then injected at a 0.75 mg/kg intravenous dose, alongside a PBS control group. After 1 hour, the mice were sacrificed, the spleens were isolated, red blood cells were lysed, and the remaining cells were analyzed via FACS. For completeness, FACS analysis was performed on four discrete CD45+ cell populations: B cells (CD19+), T cells (TCR-β+), neutrophils (Ly-6G+), and monocytes/macrophages (CD11b+/Ly-6G-) (**Figure 3-3a**). Interestingly, these **OF-77** Cy5-Fluc LNPs predominantly label the B cell and monocyte/macrophage populations, minimally label neutrophils, and have negligible labeling of T cells relative to cell populations in PBS treated mice. This qualitative observation was determined for each individual cell population by gating the CD45+/Cy5+ cells at an appropriate cutoff relative to the PBS standard. Quantification of this data further supported this observation, with roughly 8% of the total B cell population uptaking the Cy5-labeled mRNA (**Figure 3-3b**). To the best of our knowledge, this was the first example of mRNA LNPs transfecting B cells in an *in vivo* context.

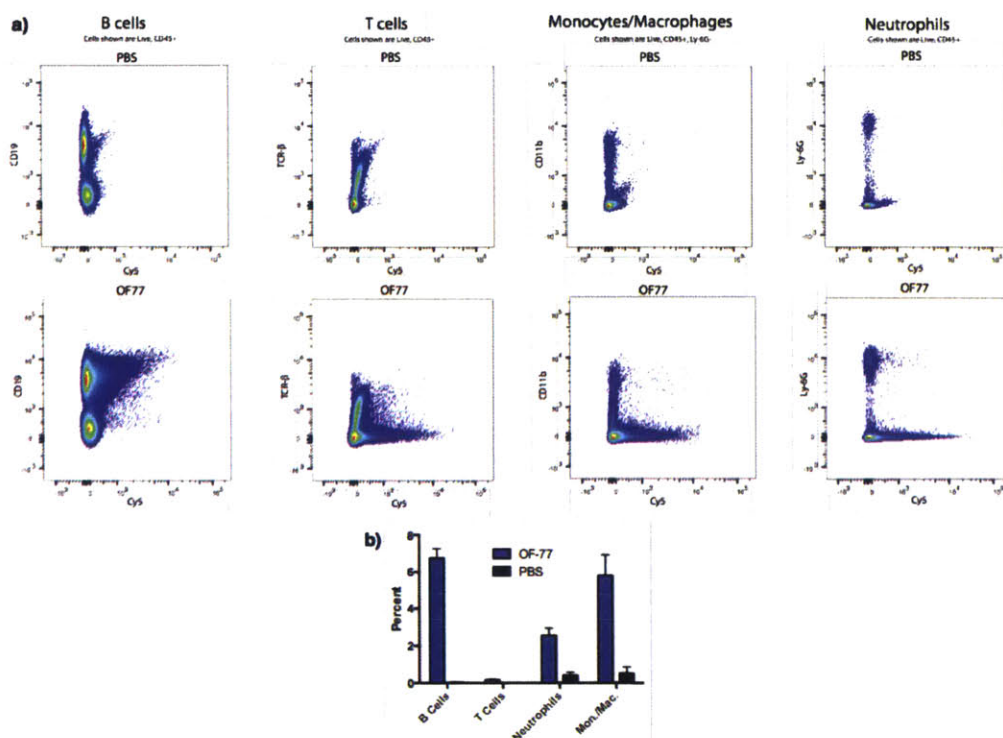


**Figure 3-3.** a) FACS plots for B cells, T cells, Monocytes/Macrophages, and Neutrophils for mice treated with PBS and **OF-77** LNPs and b) Associated quantification.

Our final goal in this study was to directly measure levels of functional protein production within B cells induced by **OF-77** mRNA LNPs. As mentioned, the clinical translation of mRNA LNPs is predicated not solely on their ability to transport mRNA into a given cell; rather, these LNPs must also release the mRNA cargo so that it may be translated into therapeutic proteins.<sup>[15]</sup> Our FACS data, while valuable, only confirms that the mRNA is present in the cell. Towards this end, we performed an *in vivo* dose-response study specifically on the B cell population of mice treated with **OF-77** FLuc-mRNA LNPs (**Figure 3-4a**). Briefly, mice were injected intravenously with **OF-77** FLuc-mRNA LNPs at doses ranging from 0.75 mg/kg to 2.25 mg/kg. After six hours, the mice were sacrificed, and the spleens were isolated and processed. Following red blood cell lysis, a primary antibody cocktail containing antibodies against all splenic cells

except for B cells was added. The B cells were then isolated from the mixture by using a magnet provided by the manufacturer that removed all non-B cells from the cell suspension. B cells were then verified to be greater than 98% pure by flow cytometry, and were then plated at a seeding density of approximately 2 million B lymphocytes per well. Luciferase expression was then quantified using a Bright-Glo Luciferase Assay kit (Promega, Madison, WI) directly on the isolated B cells, with the total luminescent signal being converted into total mass of protein produced per million cells by utilizing a calibration curve (**Figure 3-8, Experimental Section 9**). Interestingly, protein production across all doses studied within these B cells was linear, suggesting that protein production is currently only limited by the administered dose of mRNA. Approximately 70 pg/luciferase protein was produced per million B cells at the highest **OF-77** LNP dose. To the best of our knowledge, this is the first example of functional protein production in B cells induced by mRNA LNP delivery *in vivo*. Interestingly, this linear dose-response trend was not observed when luciferase expression was quantified for the mixture of all isolated spleen cells (**Figure 3-4b**), wherein the total amount of luciferase produced appeared to plateau after the 1.5 mg/kg dose of mRNA. As current methods to introduce proteins into B cells rely on patient-specific B cell isolation, *ex-vivo* manipulation via electroporation,<sup>[16]</sup> viral transfection,<sup>[17]</sup> or mechano-poration,<sup>[12a, 12b]</sup> and subsequent re-introduction of the engineered B cells into the body, we hope that **OF-77** LNPs represent a significant advancement towards manipulating B cell activity in an on-demand and routine manner.

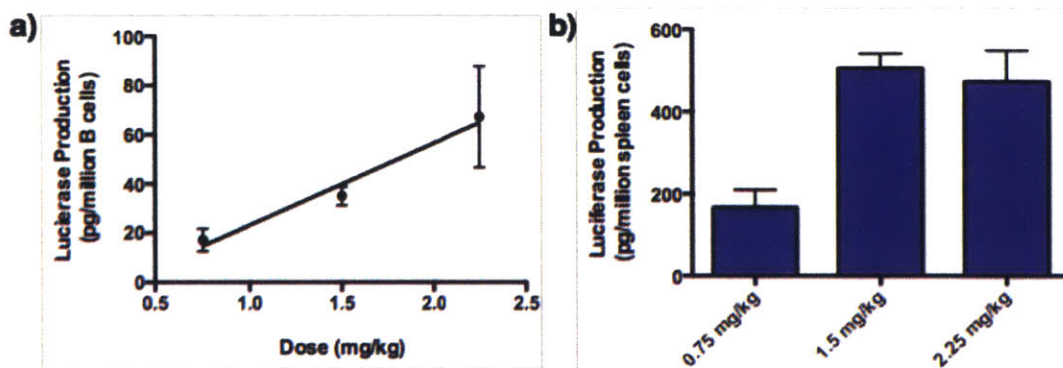


**Figure 3-4.** a) In vivo dose-response curve detailing protein expression within B cells resulting from tail vein injections of **OF-77** mRNA LNPs in mice and b) Total luciferase production in all spleen cells resulting from tail vein injections of **OF-77** mRNA LNPs in mice.

In summary, we report on the design, synthesis, and characterization of a novel mRNA based LNP system designated **OF-77**. Unlike other mRNA LNPs, **OF-77** LNPs promote predominant protein expression in the spleen as opposed to the liver. We also demonstrate that these novel LNPs specifically target immune cells, including the mature B cell population. In contrast to current methods, typically relying on patient specific immune cell isolation, ex-vivo manipulation, and subsequent reintroduction *in vivo*, **OF-77** LNPs afford on-demand protein expression in B cells following a routine intravenous injection. Future work will focus on the introduction of both therapeutic proteins and mRNA sequences coding for specific antigen sequences that could potentially be used to activate T cells for immune therapy *in vivo*. In sum, this report highlights the importance of creating new materials in conjunction with LNP delivery to afford tissue and cell specific targeting for the future clinical translation of mRNA therapeutics.

## **B. Experimental**

### ***1. Instrumentation, Materials, and Animal Protocols***

Reactions were performed in round bottom flasks. Proton nuclear magnetic resonance ( $^1\text{H}$  NMR) spectra were recorded with a Varian inverse probe INOVA-500 spectrometer (with a Magnex Scientific superconducting actively-shielded magnet), are reported in parts per million on the  $\delta$  scale, and are referenced from the residual protium in the NMR solvent ( $\text{CDCl}_3$ :  $\delta$  7.24). Data are reported as follows: chemical shift [multiplicity (br = broad, s = singlet, d = doublet, t = triplet, sp = septet, m = multiplet), integration, assignment. All commercial reagents and solvents were used as received.

All animal studies were approved by the M.I.T. Institutional Animal Care and Use Committee and were consistent with local, state and federal regulations as applicable. LNPs were intravenously injected in female C57BL/6 mice (Charles River Labs, 18-22 grams) via the tail vein. After six or 24 hours, blood was collected via the tail vein and serum was isolated by centrifugation in serum separation tubes. Serum EPO levels were quantified with an ELISA assay (Human Erythropoietin Quantikine IVD ELISA Kit, R&D Systems, Minneapolis, MD). 24 hours after injection of Luc-mRNA LNPs, mice were injected intraperitoneally with 130  $\mu\text{L}$  of D-luciferin (30 mg/mL in PBS). After fifteen minutes, mice were sacrificed and the organs were isolated (pancreas, spleen, liver, kidneys, lungs, heart, uterus and ovaries) and imaged with an IVIS imaging system (Perkin Elmer, Waltham, MA). Luminescence was quantified using LivingImage software (Perkin Elmer).

## 2. Synthetic Procedures for OF-77 and Molecular Characterizations of Intermediates

OF-77 was synthesized beginning from the bis-lysine **diketopiperazine** depicted below (**Figure 3-5**). Key intermediate **OF-TBS** was accessed via a tetra-reductive amination on **diketopiperazine** using a tert-butyldimethylsilyl protected aldehyde derivative in the presence of sodium triacetoxyborohydride. **OF-TBS** was then tetra-deprotected using tetrabutylammonium fluoride desilylation, and the intermediate tetra-ol was then subjected to an EDC coupling reaction in the presence of linoleic acid to afford **OF-77**. Full synthetic details and protocols can be found below.

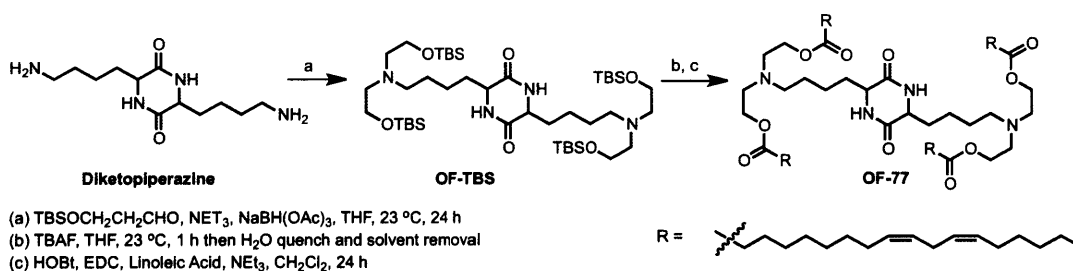


**Figure 3-5.** Synthesis of key intermediate **OF-TBS** and **OF-77**.

### **OF-TBS Synthesis**

To **diketopiperazine** (1.000 g, 2.66 mmol, 1 eq) in THF (88 ml) was added NEt<sub>3</sub> (823  $\mu$ L, 5.90 mmol, 2.2 eq). The reaction mixture was stirred for 1.5 h, until the solid was nearly fully dissolved, and then to it was added the protected aldehyde TBSOCH<sub>2</sub>CH<sub>2</sub>CHO (3.49 mL, 18.3 mmol, 6.9 eq), followed by NaB(OAc)<sub>3</sub>H (2.814 g, 13.3 mmol, 5 eq). The solution was stirred overnight. It was then diluted in EtOAc and washed with brine. The organic layer was then dried over Na<sub>2</sub>SO<sub>4</sub>, was filtered, and then concentrated under reduced pressure to afford yellow oil **OF-TBS** in 58% yield.

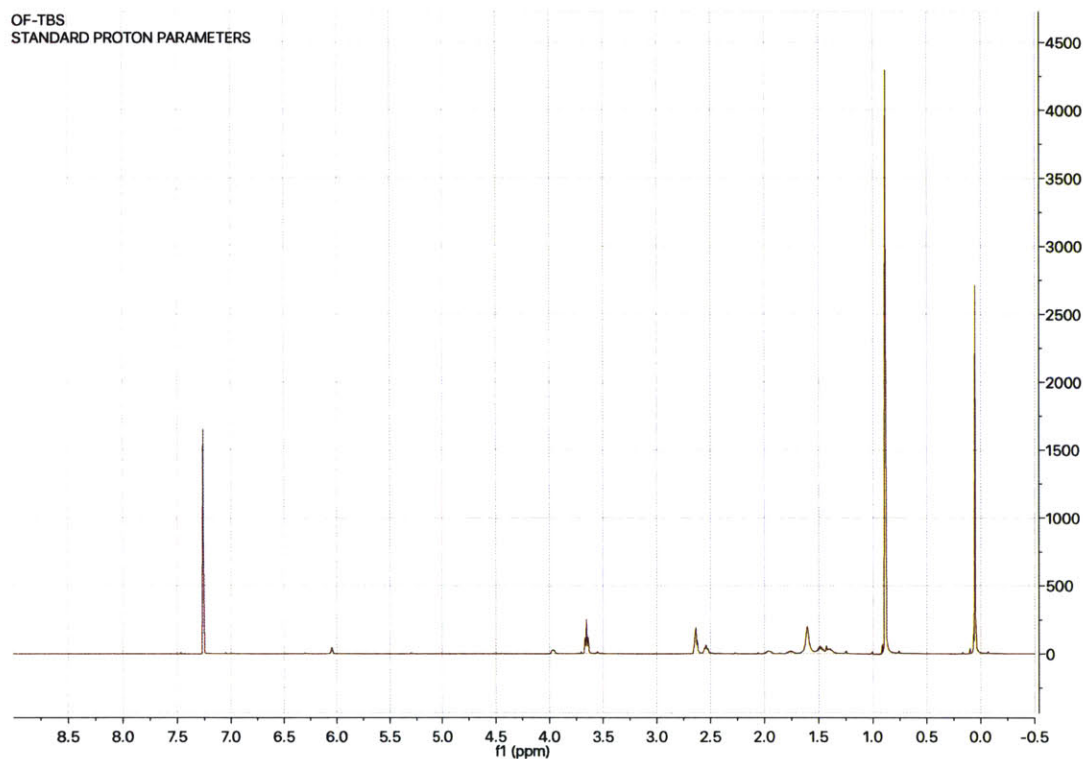


**Figure 3-6.**  $^1\text{H}$  NMR spectrum of **OF-TBS**

$^1\text{H}$  NMR (500 MHz,  $\text{CDCl}_3$ ): 6.15 (br, 2H, NH), 3.99 (br, 2H, COCHN), 3.8 (t, 8H,  $\text{NCH}_2\text{CH}_2\text{OSi}$ ), 2.65 (t, 8H,  $\text{NCH}_2\text{CH}_2\text{OSi}$ ), 2.55 (t, 4 H,  $\text{NCH}_2$ ), 1.99 (m, 2H,  $\text{COCHCH}_2$ ), 1.8 (m, 2H,  $\text{COCHCH}_2$ ), 1.45 (m, 4H,  $\text{NCH}_2\text{CH}_2\text{CH}_2\text{CH}_2$ ), 1.40 (m, 4H,  $\text{NCH}_2\text{CH}_2\text{CH}_2\text{CH}_2$ ), 0.89 (s, 36H,  $\text{OSi}(\text{CH}_3)_2\text{C}(\text{CH}_3)_3$ ), 0.04 (s, 36H,  $\text{OSi}(\text{CH}_3)_2\text{C}(\text{CH}_3)_3$ )

### **OF-77 Synthesis**

To **OF-TBS** (0.088 mmol, 1 eq) in THF (6 ml) was added a solution of tetrabutyl ammonium fluoride (TBAF) (1.75 ml, 1M in THF, 1.75 mmol, 12 equiv). The solution was stirred for one hour at room temperature and was then quenched via the addition of a single drop of distilled water. The reaction was then concentrated to dryness under



reduced pressure. The crude product was then dissolved in  $\text{CH}_2\text{Cl}_2$  (6 mL) was added hydroxybenzotriazole (120.7 mg, 0.88 mmol, 10 eq), 1-Ethyl-3-(3-dimethylaminopropyl)carbodiimide (168.7 mg, 0.88 mmol, 10 eq), linoleic acid (0.88 mmol, 10 eq), and then triethylamine (178  $\mu\text{L}$ , 2.2 mmol, 25 eq). The reaction was allowed to stir overnight at room temperature, and was then concentrated under reduced pressure. The crude product was purified using silica gel chromatography eluting with a gradient (0-100%) Ultra (3% concentrated ammonium hydroxide, 22% methanol, 75% dichloromethane):dichloromethane to afford **OF-77**.

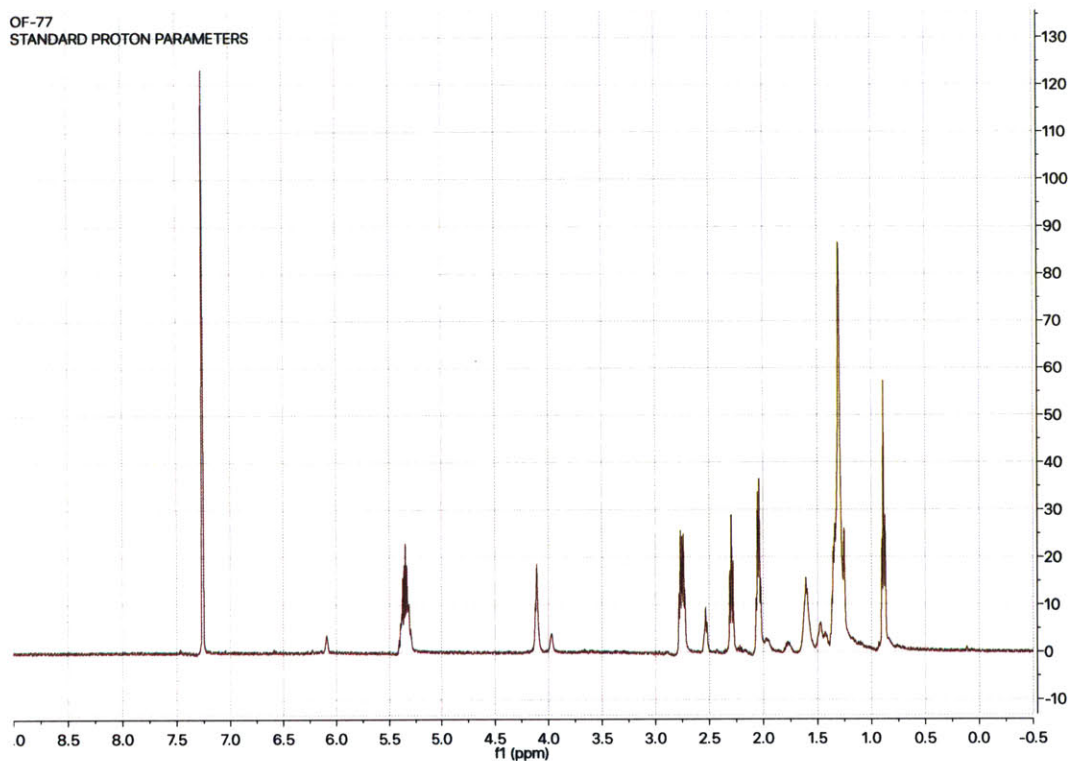


**Figure 3-7.**  $^1\text{H}$  NMR spectrum of **OF-77**.

$^1\text{H}$  NMR (500 MHz, solvent, ppm): 6.15 (br, 2H, NH), 3.99 (br, 2H, COCHN), 3.8 (t, 8H,  $\text{NCH}_2\text{CH}_2\text{OSi}$ ), 2.65 (t, 8H,  $\text{NCH}_2\text{CH}_2\text{OSi}$ ), 2.55 (t, 4 H,  $\text{NCH}_2$ ), 1.99 (m, 2H,

COCHCH<sub>2</sub>), 1.8 (m, 2H, COCHCH<sub>2</sub>), 1.45 (m, 4H, NCH<sub>2</sub>CH<sub>2</sub>CH<sub>2</sub>CH<sub>2</sub>), 1.40 (m, 4H, NCH<sub>2</sub>CH<sub>2</sub>CH<sub>2</sub>CH<sub>2</sub>), 0.89 (s, 36H, OSi(CH<sub>3</sub>)<sub>2</sub>C(CH<sub>3</sub>)<sub>3</sub>), 0.04 (s, 36H, OSi(CH<sub>3</sub>)<sub>2</sub>C(CH<sub>3</sub>)<sub>3</sub>)  
HRMS (ESI) (m/z): calc'd for C<sub>92</sub>H<sub>160</sub>N<sub>4</sub>O<sub>10</sub> [M + H]<sup>+</sup>:1482.21; found: 1482.34

### **3. General Lipid Nanoparticle Synthesis**

An organic phase was prepared by solubilizing with ethanol a mixture of **OF-77**, 1,2-dioleoyl-*sn*-glycero-3-phosphoethanolamine (DOPE, Avanti), cholesterol (Sigma), and 1,2-dimyristoyl-*sn*-glycero-3-phosphoethanolamine-N-[methoxy-(polyethyleneglycol)-2000] (ammonium salt) (C14-PEG 2000, Avanti) at a molar ratio of 35:16:46.5:2.5 and an **OF-77**:mRNA weight ratio of 10:1. All ethanolic stock solutions were prepared at a concentration of 10 mg/mL. The aqueous phase was prepared in 10 mM citrate buffer (pH 3) with either Luc mRNA (Firefly luciferase mRNA, Shire) or Cy5-labelled Luc mRNA (TriLink BioTechnologies). All mRNAs were stored at -80 °C, and were allowed to thaw on ice prior to use. The ethanol and aqueous phases were mixed at a 3:1 ratio in a microfluidic chip device using syringe pumps as previously described<sup>2</sup> at a final mRNA concentration of 0.1 mg/mL. Resultant LNPs were dialyzed against 1X PBS in a 20,000 MWCO cassette at 4°C for 2 hours and were stored at 4°C prior to injection.

### **4. General Lipid Nanoparticle Characterization**

To calculate the mRNA encapsulation efficiency, a modified Quant-iT RiboGreen RNA assay (Invitrogen) was used as previously described. Briefly, RiboGreen fluorescence was compared in the presence and absence of 2% Triton X-100 in TE buffer. The fluorescence was quantified using a Tecan infinite M200 Pro. The diameter and polydispersity (PDI) of the LNPs were measured using dynamic light scattering

(ZetaPALS, Brookhaven Instruments). LNP diameters are reported as the largest intensity mean peak average, which constituted >95% of the nanoparticles present in the sample.

### ***5. Cryogenic Transmission Electron Microscopy of Lipid Nanoparticles***

LNPs were prepared as previously described in Section 3 (General Lipid Nanoparticle Synthesis), with the exception that they were dialyzed against 0.1X PBS instead of 1X PBS. The resultant LNPs were then prepared for Cryogenic TEM. Briefly, 3  $\mu$ L of the LNP solution was diluted with buffer and was placed onto a lacey copper grid coated with a continuous carbon film. Excess sample was blotted off using a Gatan Cryo Plunge III. The grid was then mounted on a Gatan 626 cryo-holder equipped within the TEM column. The specimen and holder tip were continually cooled by liquid nitrogen during transfer into the microscope and subsequent imaging. Imaging was performed using a JEOL 2100 FEG microscope using a minimum dose method that was essential to avoiding sample damage under the electron beam. The microscope was operated at 200 kV and with a magnification setting of 60,000 for assessing particle size and distribution. All images were recorded on a Gatan 2kx2k UltraScan CCD camera.

### ***6. In Vitro Dose Response With Luciferase mRNA***

HeLa cells (American Type Culture Collection, Manassas, VA) were maintained at 37 °C in high glucose Dulbecco's Modified Eagles Medium with phenol red (Invitrogen) supplemented with 10% fetal bovine serum (Invitrogen). 12–24 h before transfection, cells were seeded in white 96-well plates at a density of 20,000 cells per well. Cells were transfected with a relevant dose Luc mRNA (Firefly luciferase mRNA, Shire) that had been formulated with **OF-77** into lipid nanoparticles as described above. After 24 hours, cell viability was first assessed using a MultiTox-Fluor multiplex

cytotoxicity assay (Promega, Madison, WI). Then luciferase expression was quantified using a Bright-Glo Luciferase Assay kit (Promega, Madison, WI) using a Tecan multiplate reader. Expression levels were normalized to live cell signal.

### ***7. In Vivo Luciferase Expression/IVIS Imaging***

All animal studies were approved by the M.I.T. Institutional Animal Care and use Committee and were consistent with local, state, and federal regulations as applicable. **OF-77** Luc mRNA LNPs were injected via the tail vein of female C57BL/6 mice (Charles River Labs, 18-22 g) at a dose of 0.75 mg/kg. After 6 hours, the mice were injected intraperitoneally with 130  $\mu$ L of D-Luciferin (30 mg/mL in PBS). After 15 minutes, mice were sacrificed and the organs were isolated (pancreas, spleen, liver, kidneys, lungs, heart, uterus, and ovaries) and imaged with an IVIS imaging system (Perkin Elmer, Waltham, MA). Luminescence was quantified using LivingImage software (Perkin Elmer).

### ***8. Fluorescence Activated Cell Sorting***

**OF-77** Cy5 Luc mRNA LNPs were formulated as described above, and were injected at a 0.75 mg/kg dose via the tail vein. After 1 hour the mice were sacrificed, and the spleens were isolated. Following red blood cell lysis, single cell suspensions from the spleens were then generated in PBS containing 0.5% BSA and 2 mM EDTA. Cells were stained with a combination of the following antibodies at 1:300 dilution in 1 ng/ $\mu$ L propidium iodide – Ly-6G (clone 1A8), CD11b (clone M1/70), CD19 (clone 6D5), TCR $\beta$  (clone H57-597), CD45 (clone 30-F11). All antibodies were purchased from Biolegend (San Diego, CA). FACS was performed using an BD LSR II cytometer (BD Biosciences). Cy5 fluorescence was measured using the 633 nm excitation laser and the

670/30 emission filter. The following identifications of cell populations were used:

1) Neutrophils: Live, CD45+, CD11b+, Ly-6G+, 2) Monocytes/Macrophages: Live, CD45+, CD11b+, Ly-6G-, 3) T cells: Live, CD45+, CD11b-, Ly-6G-, TCR-β+, 4) B cells: Live, CD45+, CD11b-, Ly-6G-, CD19+.

### ***9. B Cell Isolation/Luciferase Quantification Dose Response***

OF-77 Luc mRNA LNPs were formulated as described above, and were injected in triplicate at either a 0.75 mg/kg, 1.5 mg/kg, or 2.25 mg/kg dose via the tail vein. After 6 hours, the mice were sacrificed, and the spleens were isolated. B cells were isolated from the spleen using kits from Stemcell Technologies® according to the manufacturer's instructions. Briefly, single cell suspensions from the spleen were generated in PBS containing 5% fetal calf serum (isolation buffer). Following red blood cell lysis, cells were suspended at  $10 \times 10^6$  cells per mL in isolation buffer. A primary antibody cocktail, containing antibodies against all splenic cells except for B cells (as provided by manufacturer) were added at appropriate concentration. After incubating for 10 minutes at room temperature, isolation magnetic beads (provided by manufacturer) were added. Following a 5 minute incubation at room temperature, untouched B cells were retrieved using a magnet provided by the manufacturer. The cell purity was verified by flow cytometry to be greater than 98% pure B cells in all samples. B cells were then plated in white 96-well plates at a seeding of 2 million cells per well. Luciferase expression was then quantified using a Bright-Glo Luciferase Assay kit (Promega, Madison, WI) using a Tecan multiplate reader. The luminescence values were converted into total protein per million cells by utilizing a calibration curve that correlates total luminescence against authentic luciferase protein concentration (**Figure 3-8**).

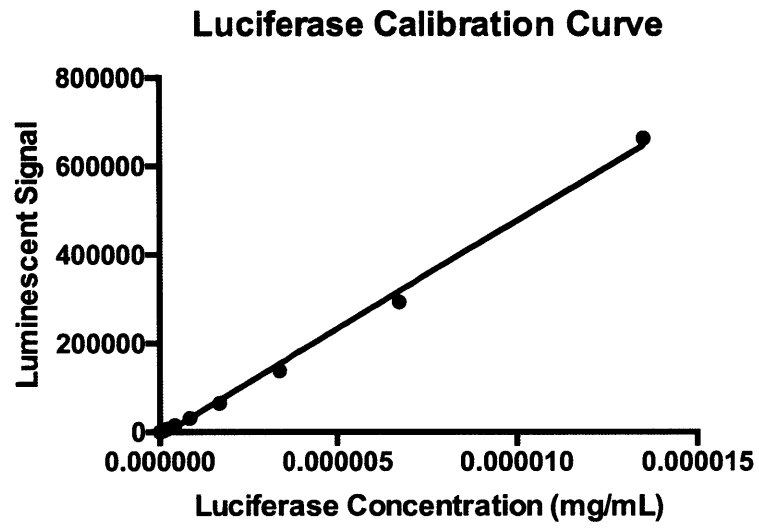


**Figure 3-8.** Luciferase Calibration Curve Correlating Total Protein to Total Luminescent Signal

### C. References

- [1] K. Murphy, *Janeway's Immunobiology 8th Edition*, **2012**.
- [2] M. D. Cooper, *Nat Rev Immunol* **2015**, *15*, 191-197.
- [3] C. M. Knapp, K. A. Whitehead, *Expert opinion on drug delivery* **2014**, *11*, 1923-1937.
- [4] a) T. Ahmadi, A. Flies, Y. Efebera, D. H. Sherr, *Immunology* **2008**, *124*, 129-140; b) P. Castiglioni, M. Gerloni, M. Zanetti, *Vaccine* **2004**, *23*, 699-708; c) A. O. Kamphorst, P. Guermonprez, D. Dudziak, M. C. Nussenzweig, *J Immunol* **2010**, *185*, 3426-3435; d) K. Wennhold, A. Shimabukuro-Vornhagen, S. Theurich, M. von Bergwelt-Baildon, *Expert Rev Vaccines* **2013**, *12*, 631-637.
- [5] a) K. J. Kauffman, J. R. Dorkin, J. H. Yang, M. W. Heartlein, F. DeRosa, F. F. Mir, O. S. Fenton, D. G. Anderson, *Nano Lett* **2015**, *15*, 7300-7306; b) B. Li, X. Luo, B. B. Deng, J. F. Wang, D. W. McComb, Y. M. Shi, K. M. L. Gaensler, X. Tan, A. L. Dunn, B. A. Kerlin, Y. Z. Dong, *Nano Lett* **2015**, *15*, 8099-8107; c) M. Baba, K. Itaka, K. Kondo, T. Yamasoba, K. Kataoka, *J Control Release* **2015**, *201*, 41-48; d) P. Midoux, C. Pichon, *Expert Rev Vaccines* **2015**, *14*, 221-234; e) I. E. Palama, B. Cortese, S. D'Amone, G. Gigli, *Biomater Sci-Uk* **2015**, *3*, 144-151; f) C. Pollard, S. De Koker, X. Saelens, G. Vanham, J. Grooten, *Trends Mol Med* **2013**, *19*, 705-713; g) J. Rejman, G. Tavernier, N. Bavarsad, J. Demeester, S. C. De Smedt, *J Control Release* **2010**, *147*, 385-391; h) X. F. Su, J. Fricke, D. G. Kavanagh, D. J. Irvine, *Mol Pharmaceut* **2011**, *8*, 774-787.
- [6] a) A. Calabretta, P. A. Kupfer, C. J. Leumann, *Nucleic Acids Res* **2015**, *43*, 4713-4720; b) R. W. Herzog, O. Cao, A. Srivastava, *Discov Med* **2010**, *45*, 105-111; c)

- K. Kariko, H. Muramatsu, F. A. Welsh, J. Ludwig, H. Kato, S. Akira, D. Weissman, *Mol Ther* **2008**, *16*, 1833-1840; d) C. Lorenz, M. Fotin-Mleczek, G. Roth, C. Becker, T. C. Dam, W. P. R. Verdurmen, R. Brock, J. Probst, T. Schlake, *Rna Biol* **2011**, *8*, 627-636.
- [7] U. Sahin, K. Kariko, O. Tureci, *Nat Rev Drug Discov* **2014**, *13*, 759-780.
- [8] Y. Z. Dong, A. A. Eltoukhy, C. A. Alabi, O. F. Khan, O. Veiseh, J. R. Dorkin, S. Sirirungruang, H. Yin, B. C. Tang, J. M. Pelet, D. L. Chen, Z. Gu, Y. Xue, R. Langer, D. G. Anderson, *Adv Healthc Mater* **2014**, *3*, 1392-1397.
- [9] a) J. W. Gillard, R. Fortin, H. E. Morton, C. Yoakim, C. A. Quesnelle, S. Daignault, Y. Guindon, *J Org Chem* **1988**, *53*, 2602-2608; b) B. Neises, W. Steglich, *Angew Chem Int Edit* **1978**, *17*, 522-524.
- [10] J. Heyes, L. Palmer, K. Bremner, I. MacLachlan, *J Control Release* **2005**, *107*, 276-287.
- [11] a) M. Gerloni, M. Rizzi, P. Castiglioni, M. Zanetti, *Mol Ther* **2004**, *9*, S213-S213; b) G. Filaci, M. Gerloni, M. Rizzi, P. Castiglioni, H. D. Chang, M. C. Wheeler, R. Fiocca, M. Zanetti, *Gene Ther* **2004**, *11*, 42-51; c) C. M. Coughlin, B. A. Vance, S. A. Grupp, R. H. Vonderheide, *Pediatr Res* **2004**, *55*, 285A-285A.
- [12] a) A. Sharei, R. Trifonova, S. Jhunjunwala, G. C. Hartoularos, A. T. Eyerman, A. Lytton-Jean, M. Angin, S. Sharma, R. Poceviciute, S. Mao, M. Heimann, S. Liu, T. Talkar, O. F. Khan, M. Addo, U. H. von Andrian, D. G. Anderson, R. Langer, J. Lieberman, K. F. Jensen, *Plos One* **2015**, *10*; b) A. Sharei, J. Zoldan, A. Adamo, W. Y. Sim, N. Cho, E. Jackson, S. Mao, S. Schneider, M. J. Han, A. Lytton-Jean, P. A. Basto, S. Jhunjunwala, J. Lee, D. A. Heller, J. W. Kang, G. C.



- Hartoularos, K. S. Kim, D. G. Anderson, R. Langer, K. F. Jensen, *P Natl Acad Sci USA* **2013**, *110*, 2082-2087; c) G. L. Szeto, D. Van Egeren, H. Worku, A. Sharei, B. Alejandro, C. Park, K. Frew, M. Brefo, S. Mao, M. Heimann, R. Langer, K. Jensen, D. J. Irvine, *Sci Rep-Uk* **2015**, *5*.
- [13] a) E. Kondo, M. S. Topp, H. P. Kiem, Y. Obata, Y. Morishima, K. Kuzushima, M. Tanimoto, M. Harada, T. Takahashi, Y. Akatsuka, *J Immunol* **2002**, *169*, 2164-2171; b) Y. S. Kim, Y. J. Kim, J. M. Lee, S. H. Han, H. J. Ko, H. J. Park, A. Pereboev, H. H. Nguyen, C. Y. Kang, *Hum Gene Ther* **2010**, *21*, 1697-1706.
- [14] D. R. Parks, V. M. Bryan, V. T. Oi, L. A. Herzenberg, *P Natl Acad Sci USA* **1979**, *76*, 1962-1966.
- [15] R. S. McIvor, *Mol Ther* **2011**, *19*, 822-823.
- [16] S. X. Shen, Z.; Qian, X.; Ding, Y.; Yu, L.; Liu, B., *Exp. Oncol.* **2007**, *29*, 137-143.
- [17] M. Giacca, S. Zacchigna, *J Control Release* **2012**, *161*, 377-388.

## CHAPTER 4

### Non-Toxic Ionizable Lipid Materials for mRNA Delivery In Vitro and In Vivo

The work presented in this chapter has been filed with the United States Patent and Trademark Office:

Fenton, O.S.; Dorkin, J.R.; Anderson, D.G.; McClellan, R.M. "Polyamine-Fatty Acid Derived Lipidoids and Uses Thereof". US Patent Number: 20,160,002,178. Filing Date: July 1, 2015

The work presented in this chapter will be published in the following manuscript:

Fenton, O.S.; Kauffman, K.J.; Kaczmarek, J.C.; McClellan, R.M.; Jhunjhunwala, S.; Zeng, M.D.; Oberli, M.A.; Appel, E.A.; Dorkin, J.R.; Mir, F.; Yang, J.; Tibbitt, M.W.; Heartlein, M.W.; DeRosa, F.; Langer, R.; Anderson, D.G.\* Non-toxic Ionizable Lipid Materials for mRNA Delivery In Vitro and In Vivo.

## A. Discussion

Nearly all disease, independent of severity, is related by a simple concept – abnormal protein levels in the body. For example, protein over-expression is the root of nearly all cancers, with high levels of oncogenic proteins causing rapid and uncontrolled cell division. On the other extreme, illnesses such as hemophilia and diabetes are caused by a complete lack of or a significant deficiency in specific proteins. As a result, there is significant interest in the development and implementation of drugs that can eliminate, modify, or even increase the amount of specific proteins within the body.<sup>[1]</sup>

Recently, several classes of RNAs have demonstrated the potential to either silence (siRNA) or express (mRNA) specific proteins with limited off target effects.<sup>[2]</sup> As such, there is great interest in the development of siRNA or mRNA based drugs that could potentially be leveraged to treat disease. However, significant difficulties associated with the intracellular delivery of RNAs currently limits the clinical application of RNA based therapeutics.<sup>[3]</sup> Without a carrier or substantial chemical modification, both siRNA and mRNA are rapidly cleared from the body or degraded, resulting in little or no cellular uptake and a corresponding lack of biological response.<sup>[4]</sup>

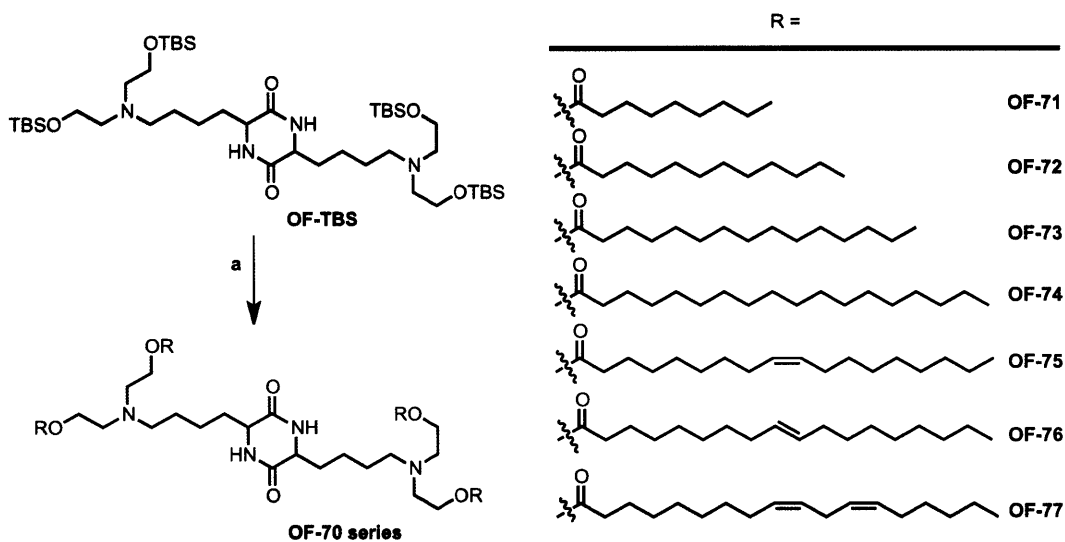
To overcome these issues, several delivery vehicles (including viruses<sup>[5]</sup> and polymers<sup>[6]</sup>) have been developed that can complex RNAs, transfect the cellular membrane through a number of potential mechanisms, and deliver the RNA cargo into the cytoplasm of target cells. However, each of these RNA delivery systems displays limited clinical potential for reasons including, but not limited to, undesired potential for genomic integration,<sup>[7]</sup> lack of scalability,<sup>[5]</sup> and limited potency.<sup>[8]</sup> Instead, lipid

nanoparticles (LNPs) currently display the most potential for clinical translation, with some RNA LNPs already undergoing clinical trials.<sup>[9]</sup>

However, despite their potential for therapeutic use, there are still numerous issues with and questions surrounding RNA LNPs that must still be answered. For example, many LNPs are toxic, causing cell death *in vitro*, and cytokine response, weight loss, and liver-specific enzyme upregulation *in vivo*.<sup>[6b, 10]</sup> Moreover, relatively little is known about the structure-function relationships relating RNA delivery properties to specific chemical functionality found within the LNP. While efficacious LNPs have been discovered,<sup>[3, 11]</sup> this lack of structure-function knowledge significantly reduces the pace at which new and potentially more efficacious compounds for RNA delivery can be discovered.

In practice, LNPs are composed of cholesterol (aids in stability),<sup>[12]</sup> a phospholipid (modifies bilayer structure),<sup>[13]</sup> a polyethylene glycol (PEG) derivative (decreases aggregation and nonspecific uptake),<sup>[14]</sup> and an ionizable lipid (complexes negatively charged RNA and enhances endosomal escape).<sup>[9a, 15]</sup> Evidence within the siRNA delivery community has implicated the chemical structure and identity of the ionizable lipid as the most pivotal component for efficacy and toxicity. As such, we sought to design, synthesize, and characterize a new series of ionizable lipids with precise variations in molecular structure. Once in hand, these ionizable lipids would each be formulated into LNPs that either incorporated siRNA or mRNA, and biological response in mammalian cells would be measured and compared amongst the series to glean insight into structure-function relationships in our LNPs.

To begin our study, we drew inspiration from the previously described ionizable lipid **OF-77**. We chose **OF-77** as our starting point for several reasons: 1) its structure incorporates hydrolysable ester bonds, a structural motif that is associated with low toxicity in ionizable lipids,<sup>[16]</sup> 2) the hydrophobic tails derive from fatty acids, important (and non-toxic) synthetic intermediates that can be purchased with varying tail lengths, geometries, and total number of alkenes, and 3) it is synthesized by route of common intermediate **OF-TBS**, a highly scalable and readily modified intermediate whose synthesis we pioneered in an earlier study. Following our established protocol, **OF-TBS** was converted into each member **OF-71** through **OF-77** employing a 2 step, 1 pot desilylation/Steglich esterification protocol (**Figure 4-1**).<sup>[17]</sup> Importantly, we were unable to synthesize stearic acid derivative **OF-74** due to solubility issues related to the extreme hydrophobicity of the fully saturated C18 tails. As such, it is not included in any further biological screening. Complete synthetic details including molecular characterization can be found in **Experimental Section 2**.



(a) TBAF, THF, 23 °C, 1 h then H<sub>2</sub>O quench to concentration under reduced pressure; HOBt, EDC-HCl, Fatty Acid, NEt<sub>3</sub>, 24 h

#### Figure 4-1. Synthesis of Ionizable Lipids OF-71 through OF-77

Next, we formulated each respective ionizable lipid with either Luc-mRNA or anti-Luc siRNA in accord with previously established protocols to form LNPs. Briefly, cholesterol, C14-PEG-2000, the requisite ionizable lipid from the OF-70 series, and either 1,2-distearoyl-*sn*-glycero-3-phosphocholine (DSPC) (for siRNA) or 1,2-dioleoyl-*sn*-glycero-3-phosphoethanolamine (DOPE) (for mRNA) were solubilized in ethanol, and the siRNA or mRNA was solubilized in 10 mM citrate buffer (pH = 3).<sup>[11]</sup> The organic and aqueous phases were then mixed at a 3:1 ratio in a microfluidic chip device using syringe pumps as previously described.<sup>[18]</sup> The resultant LNPs were then dialyzed against 1X PBS for 2 hours. The nanoparticle diameters, polydispersity indices, and encapsulation efficiencies for both the siRNA and mRNA formulations can be found in **Table 4-1** and **Table 4-2** respectively.

Ionizable Lipid	EE (%)	Size (nm)	PDI	Fatty Acid Tail
OF-71	55	111	0.358	C9
OF-72	58	81	0.370	C12
OF-73	43	62	0.266	C15
OF-75	57	64	0.334	C18-Oleic
OF-76	58	58	0.351	C18-Elaidic
OF-77	42	124	0.361	C18-Linoleic

**Table 4-1.** siRNA Lipid Nanoparticle Encapsulation Efficiency, Size, and PDI. Note: **OF-74** is insoluble in ethanol and therefore was not formulated into LNPs

Ionizable Lipid	EE (%)	Size (nm)	PDI	Fatty Acid Tail
OF-71	60	121	0.307	C9
OF-72	65	90	0.385	C12
OF-73	60	81	0.241	C15
OF-75	64	71	0.320	C18-Oleic
OF-76	64	64	0.287	C18-Elaidic
OF-77	42	145	0.355	C18-Linoleic

**Table 4-2.** mRNA Lipid Nanoparticle Encapsulation Efficiency, Size, and PDI. Note: **OF-74** is insoluble in ethanol and therefore was not formulated into LNPs.

With these LNPs in hand, we first sought to characterize their ability to induce functional gene silencing in mammalian cells using siRNA. Towards this end, each OF-70 series siRNA LNP was applied to HeLa cells at a dose of 50 ng/well that stably expressed two reporter luciferase proteins: firefly (target gene) and Renilla (control gene). Given that many LNPs have demonstrated dependence on apolipoprotein E

(ApoE),<sup>[9c]</sup> additional HeLa cells were treated with an identical dose of LNP but also with ApoE. Relative luciferase activity, which is the normalized value of firefly activity, is shown in **Figure 4-2**. Interestingly, there are several key trends to note within this series of molecules. Generally speaking, it appears that varying the ionizable lipid in each LNP can result in profound differences in silencing. It also appears that increasing the length of saturated tails (**OF-71** through **OF-73**) decreases the potency of the LNPs. Moreover, there is virtually no difference between having a single *cis*-alkene per tail (**OF-75**) versus a single *trans*-alkene per tail (**OF-76**). Finally, it appears that having two *cis*-alkenes per tail (**OF-77**) is optimal for siRNA delivery, which matches results found by both our group and others. Perhaps most interestingly, though, is that there appears to be virtually no increase in silencing with the addition of ApoE. While we are still discerning why these specific trends exist, we hope that these empirical findings may help to shape future generations of LNPs. Notably, virtually no toxicity was observed for any LNPs at these doses, as Renilla levels were consistent with those observed in untreated and PBS treated cells.



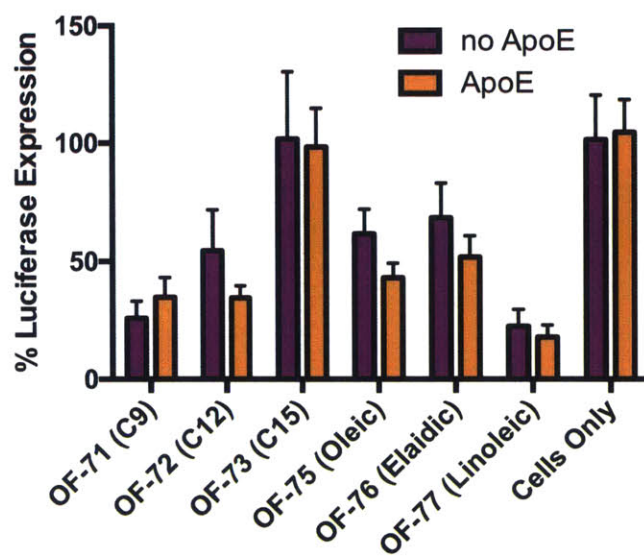


**Figure 4-2.** In vitro siRNA screen of Ionizable Lipid **OF-71** through **OF-77**. Note: **OF-74** is insoluble in ethanol and therefore could not be screened *in vitro*.

Having assessed their potential for gene silencing, we then sought to characterize the ability of OF-70 series LNPs to induce functional expression of firefly luciferase. Briefly, American type HeLa cells were treated with the OF-70series mRNA LNPs, both with and without the presence of ApoE. Total luminescence was quantified, and values were normalized to live cell count (**Figure 4-3**). Interestingly, it appears that only some of the structure-function trends observed in siRNA LNP delivery hold for mRNA LNPs. For example, there still appears to be little to no difference between having one *cis*-alkene per tail (**OF-75**) versus one *trans*-alkene per tail (**OF-76**). Once again, **OF-77** appears to be the most potent compound, containing two *cis*-alkenes per tail. Interestingly, however, it does not appear that tail length in fully saturated systems (**OF-71** through **OF-73**) plays as significant a role in potency as it does for siRNA delivery. Finally, it appears that ApoE plays a slightly more pronounced role in promoting expression, albeit small at these doses and best observed for **OF-77** LNPs.

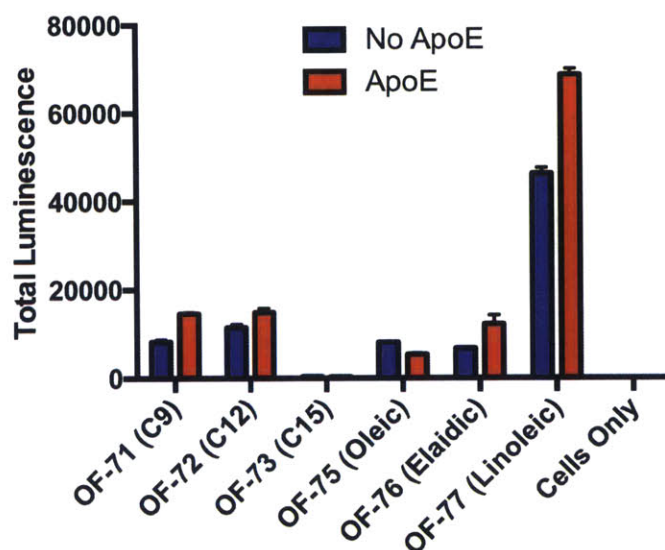


**Figure 4-3.** In vitro mRNA screen of ionizable lipids **OF-71** through **OF-77**. Note: **OF-74** is insoluble in ethanol and therefore could not be screened *in vitro*.

Given that LNPs derived from **OF-77** displayed the highest levels of potency for both siRNA and mRNA delivery, we sought to further understand their dosing potential. Towards this end, appropriate HeLa cell populations were treated with **OF-77** siRNA LNPs ranging in dose from 0 to 100 ng/well (**Figure 4-4a**) and **OF-77** mRNA LNPs ranging in dose from 0 to 200 ng/well (**Figure 4-4b**). Once again, ApoE potency was also measured with and without the incorporation of ApoE. Interestingly, it appears that **OF-77** LNPs display a much larger dependence on ApoE at higher doses, independent of the nucleic acid cargo. For example, the EC<sub>50</sub> for siRNA is roughly 50 ng/well without ApoE, and only 25 ng/well with ApoE. This ApoE dependence is even further pronounced for mRNA delivery; at doses of 100 and 200 ng/well of **OF-77** mRNA LNPs, for example, the inclusion of ApoE affords 8.8 and 9.6 fold more protein expression respectively. Importantly, this relative protein expression level with the incorporation of ApoE is higher than that can be achieved using **ckk-E12** or **OF-02** mRNA LNPs alone, or with

the incorporation of ApoE; for this reason, **OF-77** mRNA LNP/ApoE mixes could potentially one day serve as a new benchmark for *in vitro* transfection reagents.

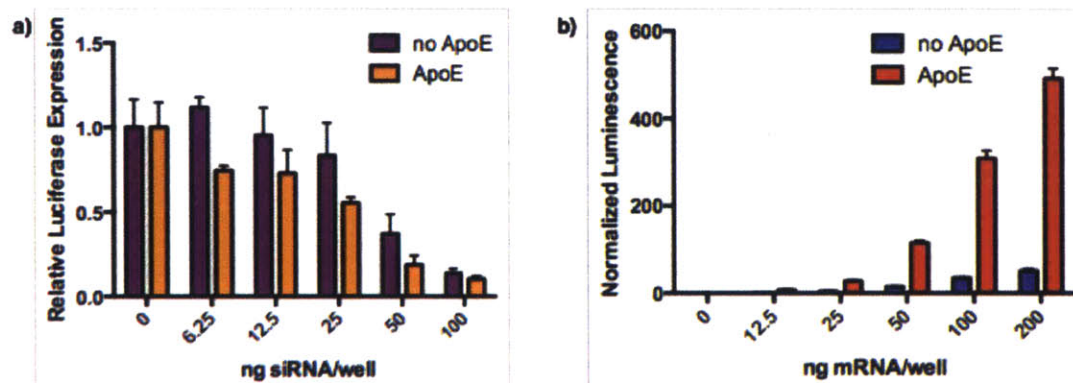


**Figure 4-4.** a) **OF-77** *in vitro* siRNA dose response screen with and without ApoE and b) **OF-77** *in vitro* mRNA dose response screen with and without ApoE.

With this data in hand, we also wanted to ensure that **OF-77** LNPs are non-toxic *in vivo*, as we specifically incorporated structural motifs within the lipid to be biocompatible. Towards this end, **OF-77** was formulated as previously described. The LNPs were injected at a 4 mg/kg intravenous dose, and all toxicity is reported as relative to a PBS control group. Blood levels of alkaline phosphatase (ALP), alanine transaminase (ALT), and aspartate transaminase (AST) were quantified (**Figure 4-5a**), as was the total weight loss was recorded for both test and control groups of mice (**Figure 4-5b**). Both of these sets of data showed no statistical difference in toxicity for **OF-77** LNPs and PBS. Moreover, a cytokine profile was also collected relative to the PBS control group, albeit at lower dose of 0.75 mg/kg (**Figure 4-6c**). Once again, no statistical difference between LNPs and PBS was observed. These data sets stand in contrast to other cationic lipid based materials for RNA transfection that cause toxicity both *in vitro* and *in vivo*.<sup>[10]</sup>

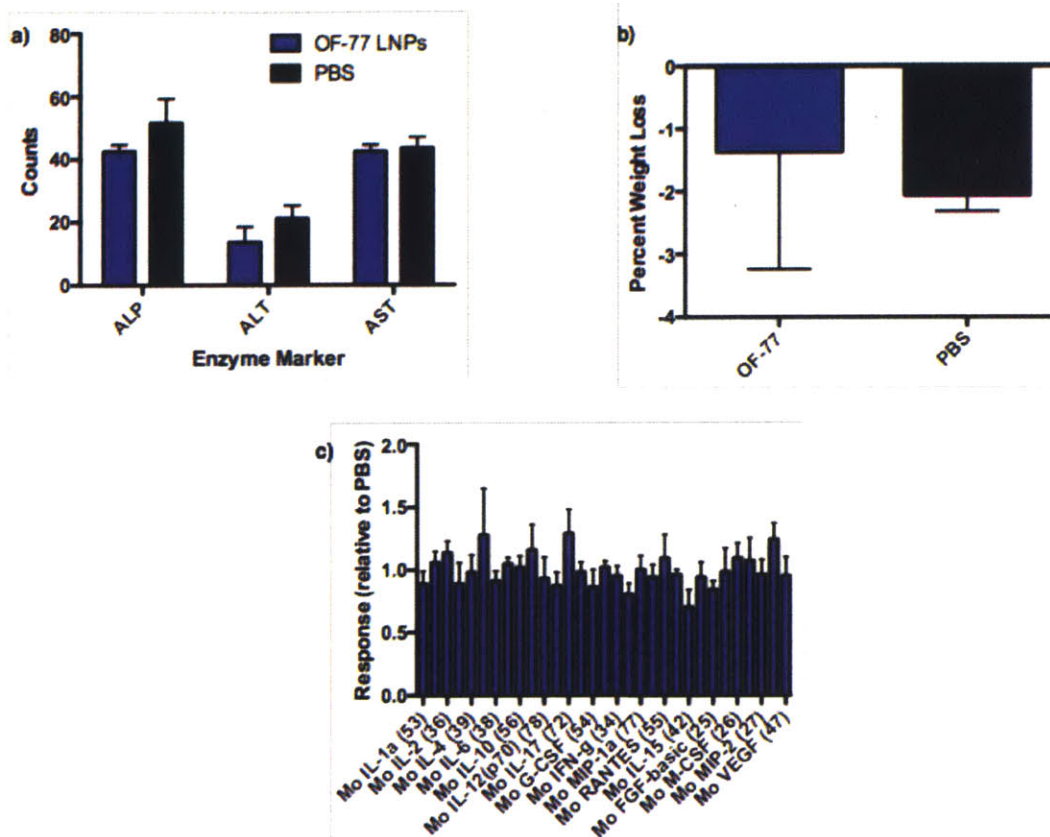


**Figure 4-5.** a) ALP, ALT, and AST levels in mice treated with a 4 mg/kg intravenous dose of **OF-77** siRNA LNPs compared to a PBS control group. b) Weight loss for a 4 mg/kg dose of **OF-77** siRNA LNPs and PBS. C) cytokine response at a 0.75 mg/kg dose of **OF-77** siRNA LNPs relative to the PBS response.

Excited by this toxicity data, we sought to establish whether or not we could activate the immune system with **OF-77** mRNA LNPs. We have previously established that **OF-77** mRNA LNPs can produce functional protein within B cells after an intravenous dose. While B lymphocytes perform a wide range of biological functions (including producing/secreting antibodies and generating memory cells), they can also stimulate T cell production through antigen presentation via the MHC I (killer T cell) or MHC II (helper T cell) complexes. As such, having the ability to induce protein

production within B cells *in vivo* could have broad impact on the field of cancer immunotherapy.

Towards this end, we once again formulated **OF-77** as described previously, but in lieu of mRNA coding for Luciferase, the mRNA coded for model immunology protein ovalbumin (OVA). The resultant **OF-77** OVA LNPs were then injected into five C57BL/6 mice via the tail vein at a dose of 0.5 mg/kg. A second 0.5 mg/kg dose was administered 72 hours after the initial injection. A control group of **OF-77** Luc LNPs were also administered to 5 mice with the same dosing regimen. The mice were bled ten days post first injection, the red blood cells were lysed (RBC buffer), and the monocytes were stained using a tetramer conjugate for either the OVA-epitope ISQAVHAAHAEINEAGR (CD4 T cells) or SIINFEKL (CD8 T cells). Flow cytometry was performed to determine the percentage of OVA specific CD4 T cells and CD8 T cells for both the control (Luc) and test (OVA) groups (**Figure 4-6a,b**). Control and test mice exhibited nearly identical levels of antigen-specific CD4 T cells. Excitingly, however, preliminary results suggest that these same LNPs may activate the CD8 T cells, with **OF-77** OVA LNPs promoting approximately  $0.6\% \pm 0.5\%$  of antigen specific cells.

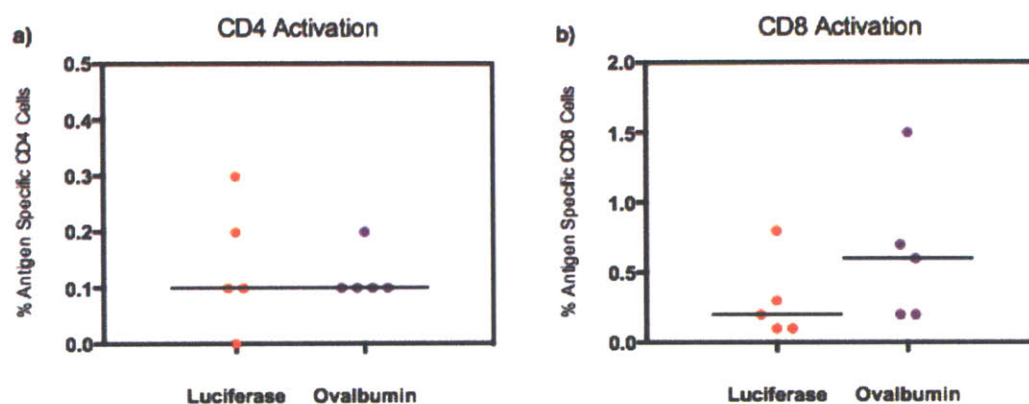
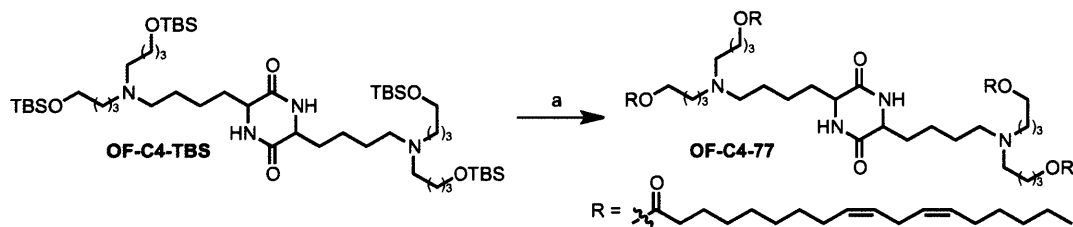


**Figure 4-6.** a) Percent antigen specific CD4 T Cells with luciferase and ovalbumin **OF-77** LNPs. b) Percent antigen specific CD8 T Cells with luciferase and ovalbumin **OF-77** LNPs.

Future efforts to improve the immune response will focus on increasing the administered dose as well as the number of injections. Additionally, we are also synthesizing new **OF-77** derivatives that may increase functional protein expression within the B cell population. Evidence in the literature suggests that LNPs with a surface  $pK_a$  between 6.6 and 7.4 may have enhanced endosomal escape properties. As previously described in Chapter 3, however, **OF-77** LNPs have a notably lower  $pK_a$  of 5.6. We hypothesized that by increasing the number of carbons between the lysinyl amines and the hydroxyl groups in the **OF-70** series because it would render the amines more basic. Towards this end, we synthesized **OF-C4-TBS** following the same protocol as for **OF-TBS**. **OF-C4-TBS** was then converted into ionizable lipid **OF-C4-77** using the same two step, one pot protocol (**Figure 4-7**).



(a) TBAF, THF, 23 °C, 1 h then H<sub>2</sub>O quench to concentration under reduced pressure; HOBt, EDC-HCl, Fatty Acid, NEt<sub>3</sub>, 24 h

**Figure 4-7.** Structures and synthesis of **OF-C4-TBS** and **OF-C4-77**.

For preliminary studies, we have formulated **OF-C4-77** with mRNA coding for luciferase. A TNS assay was performed, demonstrating a pK<sub>a</sub> of 7.1 (**Figure 4-8a**); this increased pK<sub>a</sub> confirmed our hypothesis that increasing the number of carbons would increase the pK<sub>a</sub> of the nanoparticle. The luciferase biodistribution for **OF-C4-77** Luc LNPs was also collected for these compounds (**Figure 4-8b**), and the associated quantification (**Figure 4-8c**) demonstrated spleen specific protein expression much like parent compound **OF-77** LNPs. Future experiments will both isolate B cells to directly quantify internal luciferase levels as well as test its ability to activate the immune system *in vivo*.

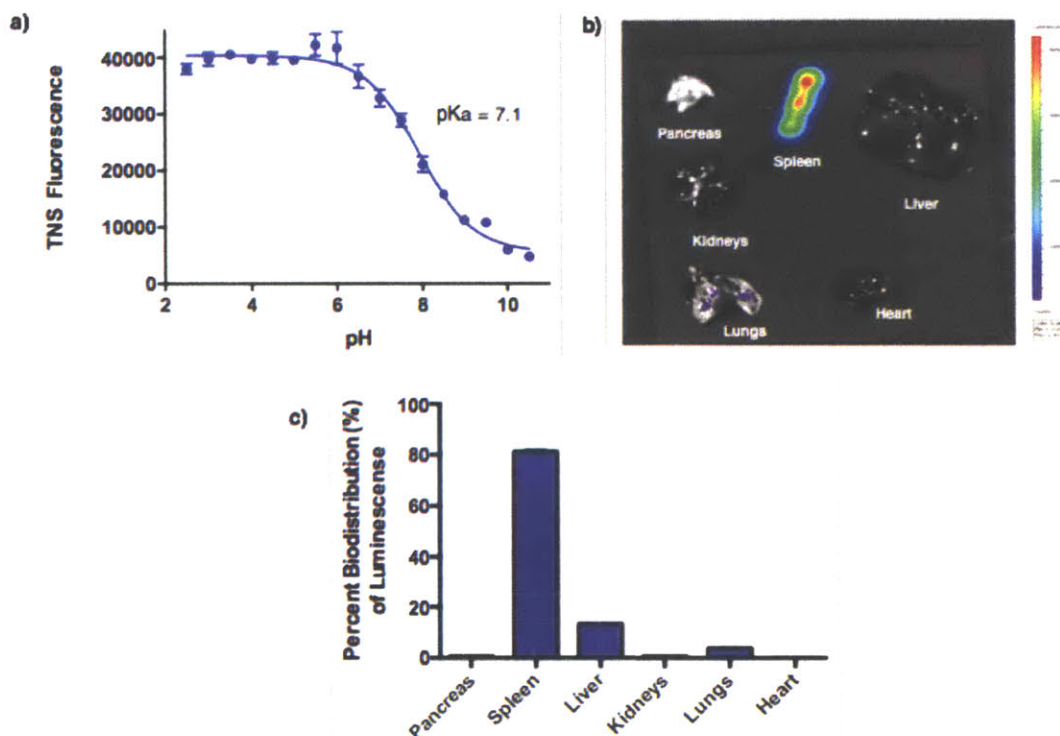


**Figure 4-8.** a) TNS assay for **OF-C4-77** LNPs. b) Representative luminescence biodistribution for **OF-C4-77** Luc LNPs. c) Associated quantification of representative luminescence biodistribution for **OF-C4-77** LNPs.

In summary, we have synthesized, characterized, and formulated a new series of ionizable lipids into both siRNA and mRNA LNPs. We have established several key findings detailing structure-function parameters within this series, and have observed an increased dependence on ApoE incorporation at higher doses. Notably, these particles appear to be completely non-toxic both *in vitro* and *in vivo*, a distinguishing characteristic that is not observed for all LNPs. Preliminary data also suggests that **OF-77** OVA LNPs may be able to activate CD4 T cells or CD8 T cells. In total, this study highlights the importance of utilizing synthetic chemistry in tandem with biological evaluation to promote a better understanding of nucleic acid delivery in cells and in mice.



## **B. Experimental**

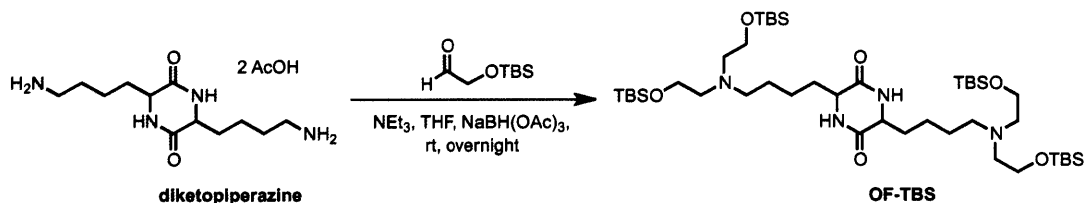
### ***1. Instrumentation and Materials***

Reactions were performed in round bottom flasks. Proton nuclear magnetic resonance ( $^1\text{H}$  NMR) spectra were recorded with a Varian inverse probe INOVA-500 spectrometer (with a Magnex Scientific superconducting actively-shielded magnet), are reported in parts per million on the  $\delta$  scale, and are referenced from the residual protium in the NMR solvent ( $\text{CDCl}_3$ :  $\delta$  7.24). Data are reported as follows: chemical shift [multiplicity (br = broad, s = singlet, d = doublet, t = triplet, sp = septet, m = multiplet), integration, assignment. All commercial reagents and solvents were used as received.

All animal studies were approved by the M.I.T. Institutional Animal Care and Use Committee and were consistent with local, state and federal regulations as applicable. LNPs were intravenously injected in female C57BL/6 mice (Charles River Labs, 18-22 grams) via the tail vein. After six or 24 hours, blood was collected via the tail vein and serum was isolated by centrifugation in serum separation tubes. Serum EPO levels were quantified with an ELISA assay (Human Erythropoietin Quantikine IVD ELISA Kit, R&D Systems, Minneapolis, MD). 24 hours after injection of Luc-mRNA LNPs, mice were injected intraperitoneally with 130  $\mu\text{L}$  of D-luciferin (30 mg/mL in PBS). After fifteen minutes, mice were sacrificed and the organs were isolated (pancreas, spleen, liver, kidneys, lungs, heart, uterus and ovaries) and imaged with an IVIS imaging system (Perkin Elmer, Waltham, MA). Luminescence was quantified using LivingImage software (Perkin Elmer).

## 2. Synthesis of OF-70 Series and All Related Compounds

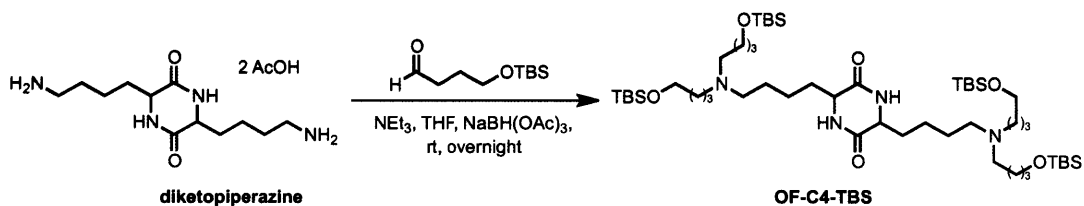
### OF-TBS



To **diketopiperazine** (1.000 g, 2.66 mmol, 1 eq) in THF (88 ml) was added NEt<sub>3</sub> (823  $\mu$ l, 5.90 mmol, 2.2 eq). The reaction mixture was stirred for 1.5 h, until the solid was nearly fully dissolved, and then to it was added the protected aldehyde (3.49 ml, 18.3 mmol, 6.9 eq), followed by NaB(OAc)<sub>3</sub>H (2.814 g, 13.3 mmol, 5 eq). The solution was stirred overnight. It was then diluted in EtOAc, washed with brine, filtered over Na<sub>2</sub>SO<sub>4</sub>, and concentrated in vacuo. The crude product mixture was purified using silica gel chromatography eluting with a 0 $\rightarrow$ 100% gradient of dichloromethane/methanol/ammonium hydroxide (75%/22%/3% v/v/v):dichloromethane. Fractions were concentrated under reduced pressure to afford the desired products in 58% yield.

<sup>1</sup>H NMR (500 MHz, CDCl<sub>3</sub>, ppm): 6.15 (br, 2H, NH), 3.99 (br, 2H, COCHN), 3.8 (t, 8H, NCH<sub>2</sub>CH<sub>2</sub>OSi), 2.65 (t, 8H, NCH<sub>2</sub>CH<sub>2</sub>OSi), 2.55 (t, 4 H, NCH<sub>2</sub>), 1.99 (m, 2H, COCHCH<sub>2</sub>), 1.8 (m, 2H, COCHCH<sub>2</sub>), 1.45 (m, 4H, NCH<sub>2</sub>CH<sub>2</sub>CH<sub>2</sub>CH<sub>2</sub>), 1.40 (m, 4H, NCH<sub>2</sub>CH<sub>2</sub>CH<sub>2</sub>CH<sub>2</sub>), 0.89 (s, 36H, OSi(CH<sub>3</sub>)<sub>2</sub>C(CH<sub>3</sub>)<sub>3</sub>), 0.04 (s, 36H, OSi(CH<sub>3</sub>)<sub>2</sub>C(CH<sub>3</sub>)<sub>3</sub>)

## OF-C4-TBS



To diketopiperazine (373 mg, 0.99 mmol, 1 eq) in THF (33 ml) was added NEt<sub>3</sub> (307  $\mu$ l, 2.18 mmol, 2.2 eq). The reaction mixture was stirred for 30 min, until the solid was nearly fully dissolved, and then to it was added the protected aldehyde (1.382 g, 6.83 mmol, 6.9 eq), followed by NaB(OAc)<sub>3</sub>H (1.05 g, 4.95 mmol, 5 eq). The solution was stirred overnight. It was then diluted in EtOAc, washed with brine, filtered over Na<sub>2</sub>SO<sub>4</sub>, and concentrated in vacuo. The crude product mixture was purified using silica gel chromatography eluting with a 0 $\rightarrow$ 100% gradient of dichloromethane/methanol/ammonium hydroxide (75%/22%/3% v/v/v):dichloromethane. Fractions were concentrated under reduced pressure to afford the desired products in 41% yield.

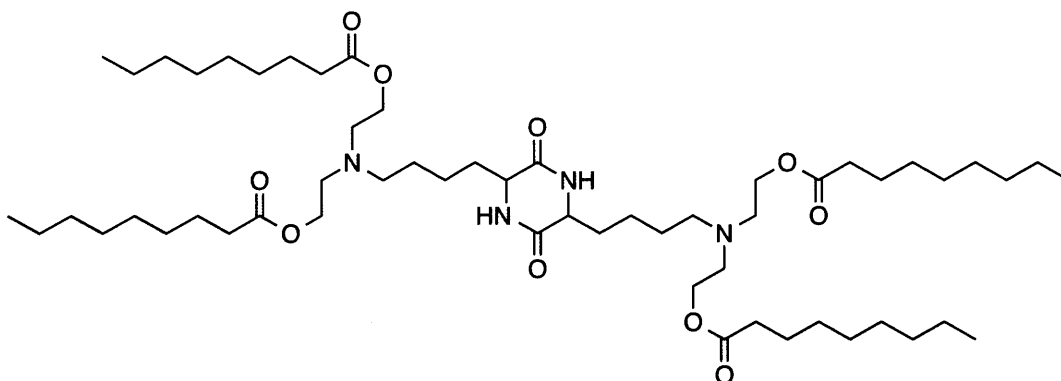
<sup>1</sup>H NMR (500 MHz, CDCl<sub>3</sub>, ppm): 6.4 (br, 2H, NH), 3.95 (br, 2H, COCHN), 3.62 (t, 8H, CH<sub>2</sub>OSi), 2.40 (m, 12H, NCH<sub>2</sub>), 1.98 (m, 4H, COCHCH<sub>2</sub>), 1.33-1.84 (m, 24H, CH<sub>2</sub>), 0.89 (s, 36H, OSi(CH<sub>3</sub>)<sub>2</sub>C(CH<sub>3</sub>)<sub>3</sub>), 0.04 (s, 24H, OSi(CH<sub>3</sub>)<sub>2</sub>C(CH<sub>3</sub>)<sub>3</sub>)

### **Desilylation-Esterification Protocol**

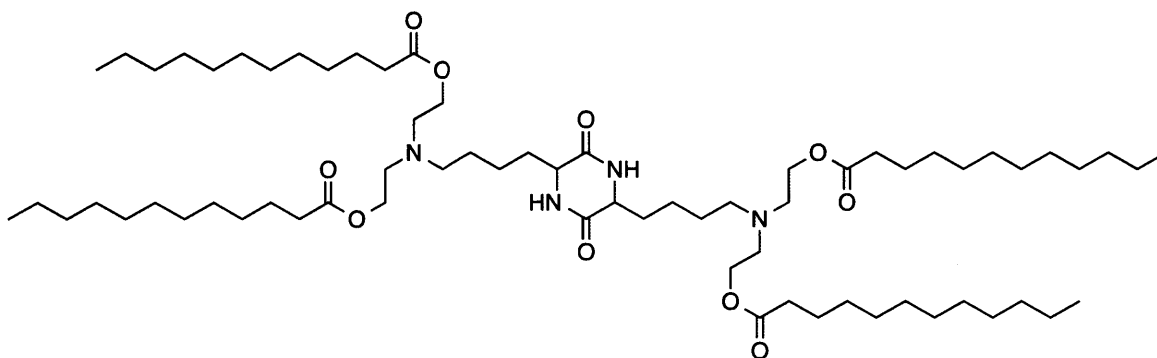
General – all OF-70 series compounds (including OF-C4-77) were synthesized following the following general procedure:

To **OF-TBS** (or **OF-C4-TBS**) (0.088 mmol, 1 eq) in THF (6 ml) was added TBAF (1.75 ml, 1M in THF, 1.75 mmol, 12 equiv). The solution was stirred for one hour and the reaction was then quenched with 1 drop of H<sub>2</sub>O.

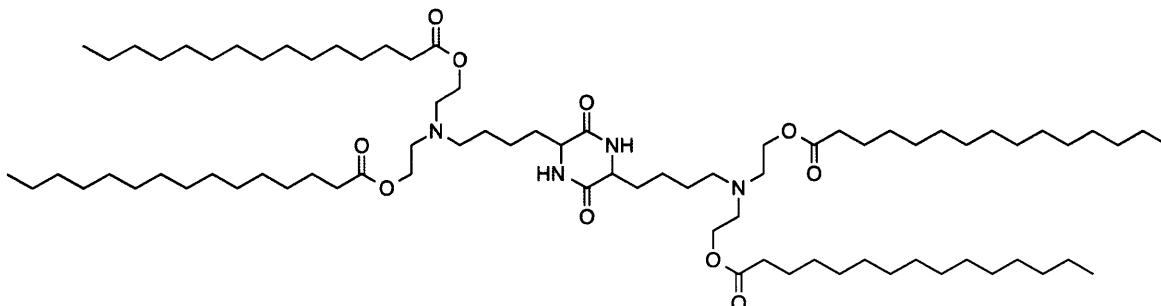
To a solution of the deprotected **OF-TBS** (or **OF-C4-TBS**) in CH<sub>2</sub>Cl<sub>2</sub> (6 ml) was added HOBt (120.7 mg, 0.88 mmol, 10 eq), EDC (168.7 mg, 0.88 mmol, 10 eq), the requisite carboxylic acid (0.88 mmol, 10 eq), and then NEt<sub>3</sub> (178 μl, 2.2 mmol, 25 eq). The reaction was stirred overnight, and was then diluted with ethyl acetate. The organic phase was washed 1 X 1 N HCl, 1 X saturated sodium bicarbonate, and then 1 X brine. The organic phase was dried over sodium sulfate, was filtered through cotton, and was concentrated under reduced pressure. The crude product mixture was purified using silica gel chromatography eluting with a 0→100% gradient of dichloromethane/methanol/ammonium hydroxide (75%/22%/3% v/v/v):dichloromethane. Fractions were concentrated under reduced pressure to afford the desired products in moderate yield.

**OF-71**

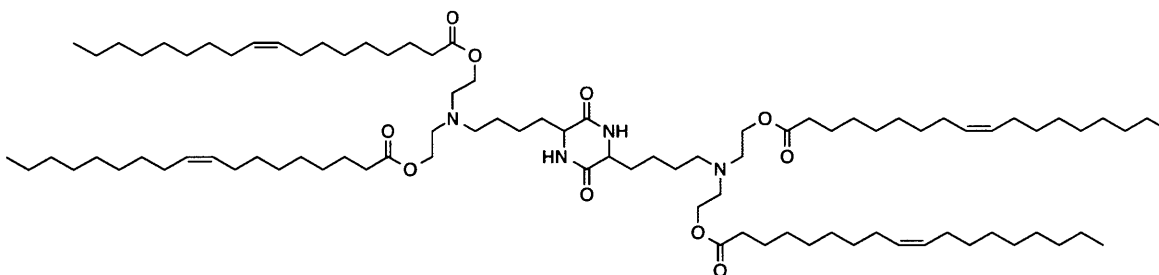
$^1\text{H}$  NMR (500 MHz,  $\text{CDCl}_3$ , ppm): 6.15 (br, 2H, NH), 4.1 (m, 8H,  $\text{NCH}_2\text{CH}_2\text{OCO}$ ), 3.99 (br, 2H,  $\text{COCHN}$ ), 2.73 (t, 8H,  $\text{OCOCH}_2$ ), 2.53 (t, 4 H,  $\text{NCH}_2$ ), 2.29 (t, 8H,  $\text{NCH}_2\text{CH}_2\text{OCO}$ ), 1.96 (m, 2H,  $\text{COCHCH}_2$ ), 1.78 (m, 2H,  $\text{COCHCH}_2$ ), 1.61 (m, 4H,  $\text{NCH}_2\text{CH}_2\text{CH}_2\text{CH}_2$ ), 1.77 (m, 4H,  $\text{NCH}_2\text{CH}_2\text{CH}_2\text{CH}_2$ ), 1.1-1.35 (m, 48H,  $\text{CH}_2$ ), 0.88 (t, 12H,  $\text{CH}_3$ )

**OF-72**

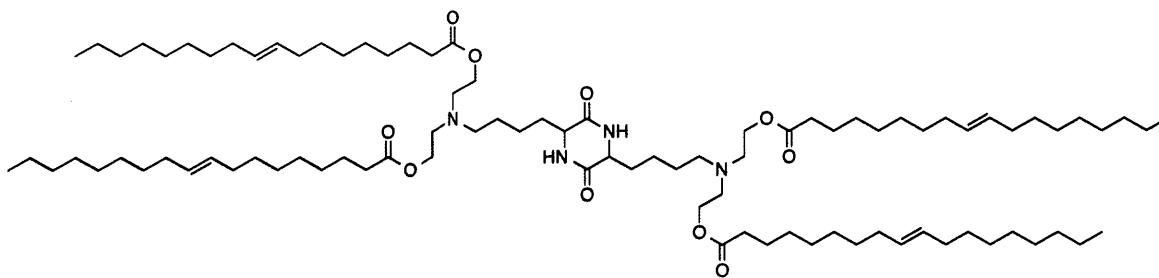
$^1\text{H}$  NMR (500 MHz,  $\text{CDCl}_3$ , ppm): 6.12 (br, 2H, NH), 4.11 (m, 8H,  $\text{NCH}_2\text{CH}_2\text{OCO}$ ), 3.97 (br, 2H,  $\text{COCHN}$ ), 2.75 (t, 8H,  $\text{OCOCH}_2$ ), 2.54 (t, 4 H,  $\text{NCH}_2$ ), 2.29 (t, 8H,  $\text{NCH}_2\text{CH}_2\text{OCO}$ ), 1.97 (m, 2H,  $\text{COCHCH}_2$ ), 1.77 (m, 2H,  $\text{COCHCH}_2$ ), 1.61 (m, 4H,  $\text{NCH}_2\text{CH}_2\text{CH}_2\text{CH}_2$ ), 1.45 (m, 4H,  $\text{NCH}_2\text{CH}_2\text{CH}_2\text{CH}_2$ ), 1.1-1.17 (m, 72H,  $\text{CH}_2$ ), 0.9 (t, 12H,  $\text{CH}_3$ )

**OF-73**

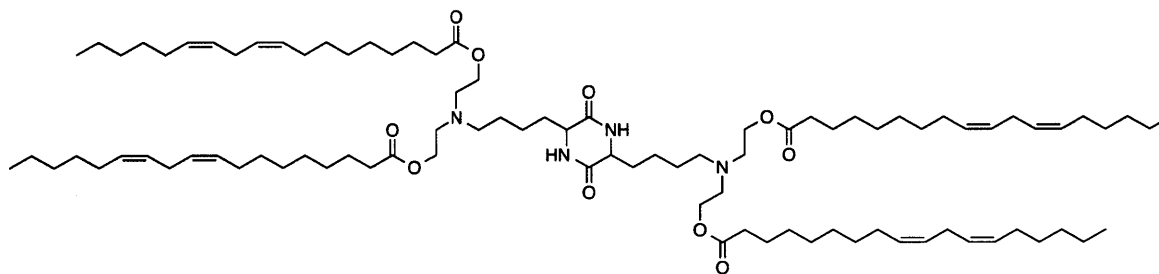
$^1\text{H NMR}$  (500 MHz,  $\text{CDCl}_3$ , ppm): 6.17 (br, 2H, *NH*), 4.11 (m, 8H,  $\text{NCH}_2\text{CH}_2\text{OCO}$ ), 3.97 (br, 2H,  $\text{COCHN}$ ), 2.74 (t, 8H,  $\text{OCOCH}_2$ ), 2.53 (t, 4 H,  $\text{NCH}_2$ ), 2.29 (t, 8H,  $\text{NCH}_2\text{CH}_2\text{OCO}$ ), 1.97 (m, 2H,  $\text{COCHCH}_2$ ), 1.76 (m, 2H,  $\text{COCHCH}_2$ ), 1.59 (m, 4H,  $\text{NCH}_2\text{CH}_2\text{CH}_2\text{CH}_2$ ), 1.45 (m, 4H,  $\text{NCH}_2\text{CH}_2\text{CH}_2\text{CH}_2$ ), 1.17-1.34 (m, 96H,  $\text{CH}_2$ ), 0.9 (t, 12H,  $\text{CH}_3$ )

**OF-75**

$^1\text{H NMR}$  (500 MHz,  $\text{CDCl}_3$ , ppm): 6.13 (br, 2H, *NH*), 5.34 (m, 8H,  $\text{CH}_2\text{CHCHCH}_2$ ), 4.11 (m, 8H,  $\text{NCH}_2\text{CH}_2\text{OCO}$ ), 3.98 (br, 2H,  $\text{COCHN}$ ), 2.74 (t, 8H,  $\text{OCOCH}_2$ ), 2.53 (t, 4H,  $\text{NCH}_2$ ), 2.29 (t, 8H,  $\text{NCH}_2\text{CH}_2\text{OCO}$ ), 2.00 (m, 16H,  $\text{CH}_2\text{CHCHCH}_2$ ), 1.94 (m, 2H,  $\text{COCHCH}_2$ ), 1.77 (m, 2H,  $\text{COCHCH}_2$ ), 1.61 (m, 4H,  $\text{NCH}_2\text{CH}_2\text{CH}_2\text{CH}_2$ ), 1.45 (m, 4H,  $\text{NCH}_2\text{CH}_2\text{CH}_2\text{CH}_2$ ), 1.21-1.36 (m, 88H,  $\text{CH}_2$ ), 0.9 (t, 12H,  $\text{CH}_3$ )

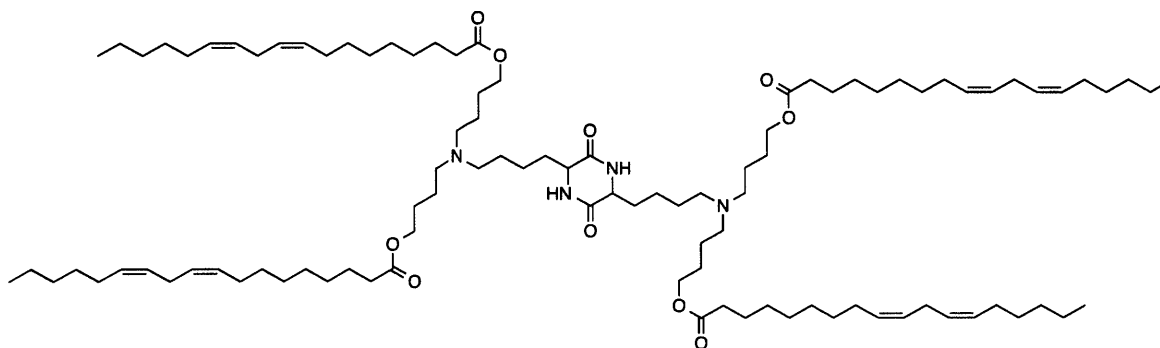
**OF-76**

$^1\text{H}$  NMR (500 MHz,  $\text{CDCl}_3$ , ppm): 6.13 (br, 2H, *NH*), 5.39 (m, 8H,  $\text{CH}_2\text{CHCHCH}_2$ ), 4.10 (m, 8H,  $\text{NCH}_2\text{CH}_2\text{OCO}$ ), 3.97 (br, 2H,  $\text{COCHN}$ ), 2.74 (t, 8H,  $\text{OCOCH}_2$ ), 2.52 (t, 4H,  $\text{NCH}_2$ ), 2.27 (t, 8H,  $\text{NCH}_2\text{CH}_2\text{OCO}$ ), 1.95 (m, 16H,  $\text{CH}_2\text{CHCHCH}_2$ ), 1.78 (m, 2H,  $\text{COCHCH}_2$ ), 1.69 (m, 2H,  $\text{COCHCH}_2$ ), 1.60 (m, 4H,  $\text{NCH}_2\text{CH}_2\text{CH}_2\text{CH}_2$ ), 1.45 (m, 4H,  $\text{NCH}_2\text{CH}_2\text{CH}_2\text{CH}_2$ ), 1.20-1.37 (m, 88H,  $\text{CH}_2$ ), 0.87 (t, 12H,  $\text{CH}_3$ )

**OF-77**

$^1\text{H}$  NMR (500 MHz,  $\text{DMSO-d}_6$ , ppm): 6.13 (br, 2H, *NH*), 5.34 (m, 16H,  $\text{CH}_2\text{CHCHCH}_2$ ), 4.11 (m, 8H,  $\text{NCH}_2\text{CH}_2\text{OCO}$ ), 3.98 (br, 2H,  $\text{COCHN}$ ), 2.74 (t, 8H,  $\text{OCOCH}_2$ ), 2.53 (t, 8H,  $\text{NCH}_2\text{CH}_2\text{OCO}$ ), 2.29 (t, 4H,  $\text{NCH}_2$ ), 2.00 (m, 16H,  $\text{CH}_2\text{CHCHCH}_2\text{CHCHCH}_2$ ), 1.94 (m, 2H,  $\text{COCHCH}_2$ ), 1.77 (m, 2H,  $\text{COCHCH}_2$ ), 1.61 (m, 4H,  $\text{NCH}_2\text{CH}_2\text{CH}_2\text{CH}_2$ ), 1.45 (m, 4H,  $\text{NCH}_2\text{CH}_2\text{CH}_2\text{CH}_2$ ), 1.21-1.36 (m, 88H,  $\text{CH}_2$ ), 0.9 (t, 12H,  $\text{CH}_3$ )

## OF-C4-77



$^1\text{H}$  NMR (500 MHz,  $\text{CDCl}_3$ , ppm): 6.29 (br, 2H, NH), 5.35 (m, 16H,  $\text{CH}_2\text{CHCHCH}_2$ ), 4.07 (m, 8H,  $\text{CH}_2\text{CH}_2\text{OCO}$ ), 3.96 (br, 2H,  $\text{COCHN}$ ), 2.77 (t, 8H,  $\text{OCOCH}_2$ ), 2.44 (br, 12H,  $\text{NCH}_2$ ), 2.29 (t, 8H,  $\text{CHCH}_2\text{CH}$ ), 2.04 (m, 16H,  $\text{CH}_2\text{CHCHCH}_2\text{CHCHCH}_2$ ), 1.96 (m, 2H,  $\text{COCHCH}_2$ ), 1.77 (m, 2H,  $\text{COCHCH}_2$ ), 1.22-1.68 (m, 88H,  $\text{CH}_2$ ), 0.88 (t, 12H,  $\text{CH}_3$ )

### **3. General Lipid Nanoparticle Synthesis**

An organic phase was prepared by solubilizing with ethanol a mixture of **OF-77**, 1,2-dioleoyl-*sn*-glycero-3-phosphoethanolamine (DOPE, Avanti), cholesterol (Sigma), and 1,2-dimyristoyl-*sn*-glycero-3-phosphoethanolamine-N-[methoxy-(polyethyleneglycol)-2000] (ammonium salt) (C14-PEG 2000, Avanti) at a molar ratio of 35:16:46.5:2.5 and an OF-70series:nucleic acid weight ratio of 10:1. All ethanolic stock solutions were prepared at a concentration of 10 mg/mL. The aqueous phase was prepared in 10 mM citrate buffer (pH 3) with either Luc mRNA (Firefly luciferase mRNA, Shire) or anti-FLuc siRNA (Shire). All nucleic acids were stored at  $-80\text{ }^\circ\text{C}$ , and were allowed to thaw on ice prior to use. The ethanol and aqueous phases were mixed at a 3:1 ratio in a microfluidic chip device using syringe pumps as previously described at a



final mRNA concentration of 0.1 mg/mL. Resultant LNPs were dialyzed against 1X PBS in a 20,000 MWCO cassette at 4°C for 2 hours and were stored at 4°C prior to injection.

#### ***4. General Lipid Nanoparticle Characterization***

To calculate the mRNA encapsulation efficiency, a modified Quant-iT RiboGreen RNA assay (Invitrogen) was used as previously described. Briefly, RiboGreen fluorescence was compared in the presence and absence of 2% Triton X-100 in TE buffer. The fluorescence was quantified using a Tecan infinite M200 Pro. The diameter and polydispersity (PDI) of the LNPs were measured using dynamic light scattering (ZetaPALS, Brookhaven Instruments). LNP diameters are reported as the largest intensity mean peak average, which constituted >95% of the nanoparticles present in the sample.

#### ***5. In Vitro Screen and Dose Response With Luciferase siRNA***

HeLa cells (American Type Culture Collection, Manassas, VA) expressing both Firefly and Renilla Luciferase were maintained at 37 °C in high glucose Dulbecco's Modified Eagles Medium with phenol red (Invitrogen) supplemented with 10% fetal bovine serum (Invitrogen). 12–24 h before transfection, cells were seeded in white 96-well plates at a density of 20,000 cells per well. Cells were transfected with a relevant dose anti-Luc siRNA (Firefly luciferase mRNA, Shire) that had been formulated with OF-70series ionizable lipids into lipid nanoparticles as described above. After 24 hours, both the firefly and renilla luciferase levels were quantified using a Bright-Glo Luciferase Assay kit (Promega, Madison, WI) using a Tecan multiplate reader. Firefly luciferase levels were normalized to their renilla counterparts.

## ***6. In Vitro Screen and Dose Response With Luciferase mRNA***

HeLa cells (American Type Culture Collection, Manassas, VA) were maintained at 37 °C in high glucose Dulbecco's Modified Eagles Medium with phenol red (Invitrogen) supplemented with 10% fetal bovine serum (Invitrogen). 12–24 h before transfection, cells were seeded in white 96-well plates at a density of 20,000 cells per well. Cells were transfected with a relevant dose Luc mRNA (Firefly luciferase mRNA, Shire) that had been formulated with **OF-77** into lipid nanoparticles as described above. After 24 hours, cell viability was first assessed using a MultiTox-Fluor multiplex cytotoxicity assay (Promega, Madison, WI). Then luciferase expression was quantified using a Bright-Glo Luciferase Assay kit (Promega, Madison, WI) using a Tecan multiplate reader. Expression levels were normalized to live cell signal.

## ***7. CD4 and CD8 T Cell Activation with OF-77 OVA LNPs***

**OF-77** was formulated with mRNA coding for OVA in the previously described method. The resultant LNPs were then injected via the tail vein of C57BL/6 mice at a 0.5 mg/kg dose. After 72 hours, a second 0.5 mg/kg dose was administered via the tail vein. The mice were bled ten days post first injection, the red blood cells were lysed with RBC buffer, and the monocytes were stained using a tetramer conjugate for either the OVA-epitope ISQAVHAAHAEINEAGR (CD4 T cells) or the OVA-epitope SIINFEKL (CD8 T cells) for both the control (Luc) and test (OVA) groups. Flow cytometry was used to quantify the percent of monocytes positive for each of the specific epitopes.

## ***8. In Vivo Luciferase Expression/IVIS Imaging with OF-C4-77***

All animal studies were approved by the M.I.T. Institutional Animal Care and use Committee and were consistent with local, state, and federal regulations as applicable.

**OF-C4-77** Luc mRNA LNPs were injected via the tail vein of female C57BL/6 mice (Charles Riber Labs, 18-22 g) at a dose of 0.75 mg/kg. After 6 hours, the mice were injected intraperitoneally with 130  $\mu$ L of D-Luciferin (30 mg/mL in PBS). After 15 minutes, mice were sacrificed and the organs were isolated (pancreas, spleen, liver, kidneys, lungs, heart, uterus, and ovaries) and imaged with an IVIS imaging system (Perkin Elmer, Waltham, MA). Luminescence was quantified using LivingImage software (Perkin Elmer).

### C. References

- [1] R. W. Herzog, O. Cao, A. Srivastava, *Discov Med* **2010**, *45*, 105-111.
- [2] a) H. Yin, R. L. Kanasty, A. A. Eltoukhy, A. J. Vegas, J. R. Dorkin, D. G. Anderson, *Nat Rev Genet* **2014**, *15*, 541-555; b) U. Sahin, K. Kariko, O. Tureci, *Nat Rev Drug Discov* **2014**, *13*, 759-780.
- [3] K. A. Whitehead, R. Langer, D. G. Anderson, *Nat Rev Drug Discov* **2009**, *8*, 129-138.
- [4] R. L. Kanasty, K. A. Whitehead, A. J. Vegas, D. G. Anderson, *Mol Ther* **2012**, *20*, 513-524.
- [5] M. Giacca, S. Zacchigna, *J Control Release* **2012**, *161*, 377-388.
- [6] a) I. E. Palama, B. Cortese, S. D'Amone, G. Gigli, *Biomater Sci-Uk* **2015**, *3*, 144-151; b) U. Lungwitz, M. Breunig, T. Blunk, A. Gopferich, *Eur J Pharm Biopharm* **2005**, *60*, 247-266.
- [7] S. Hacein-Bey-Abina, C. von Kalle, M. Schmidt, F. Le Deist, N. Wulffraat, E. McIntyre, I. Radford, J. L. Villeval, C. C. Fraser, M. Cavazzana-Calvo, A. Fischer, *New Engl J Med* **2003**, *348*, 255-256.

- [8] R. S. McIvor, *Mol Ther* **2011**, *19*, 822-823.
- [9] a) K. T. Love, K. P. Mahon, C. G. Levins, K. A. Whitehead, W. Querbes, J. R. Dorkin, J. Qin, W. Cantley, L. L. Qin, T. Racie, M. Frank-Kamenetsky, K. N. Yip, R. Alvarez, D. W. Y. Sah, A. de Fougères, K. Fitzgerald, V. Koteliansky, A. Akinc, R. Langer, D. G. Anderson, *P Natl Acad Sci USA* **2010**, *107*, 9915-9915; b) K. A. Whitehead, J. R. Dorkin, A. J. Vegas, P. H. Chang, O. Veiseh, J. Matthews, O. S. Fenton, Y. L. Zhang, K. T. Olejnik, V. Yesilyurt, D. L. Chen, S. Barros, B. Klebanov, T. Novobrantseva, R. Langer, D. G. Anderson, *Nat Commun* **2014**, *5*; c) Y. Z. Dong, K. T. Love, J. R. Dorkin, S. Sirirungruang, Y. L. Zhang, D. L. Chen, R. L. Bogorad, H. Yin, Y. Chen, A. J. Vegas, C. A. Alabi, G. Sahay, K. T. Olejnik, W. H. Wang, A. Schroeder, A. K. R. Lytton-Jean, D. J. Siegwart, A. Akinc, C. Barnes, S. A. Barros, M. Carioto, K. Fitzgerald, J. Hettinger, V. Kumar, T. I. Novobrantseva, J. N. Qin, W. Querbes, V. Koteliansky, R. Langer, D. G. Anderson, *P Natl Acad Sci USA* **2014**, *111*, 5753-5753.
- [10] H. T. Lv, S. B. Zhang, B. Wang, S. H. Cui, J. Yan, *J Control Release* **2006**, *114*, 100-109.
- [11] K. J. Kauffman, J. R. Dorkin, J. H. Yang, M. W. Heartlein, F. DeRosa, F. F. Mir, O. S. Fenton, D. G. Anderson, *Nano Lett* **2015**, *15*, 7300-7306.
- [12] a) J. J. Lu, R. Langer, J. Z. Chen, *Mol Pharmaceut* **2009**, *6*, 763-771; b) T. M. Allen, P. R. Cullis, *Adv Drug Deliver Rev* **2013**, *65*, 36-48.
- [13] I. S. Zuhorn, U. Bakowsky, E. Polushkin, W. H. Visser, M. C. A. Stuart, J. B. F. N. Engberts, D. Hoekstra, *Mol Ther* **2005**, *11*, 801-810.

- [14] B. L. Mui, Y. K. Tam, M. Jayaraman, S. M. Ansell, X. Y. Du, Y. Y. C. Tam, P. J. C. Lin, S. Chen, J. K. Narayanannair, K. G. Rajeev, M. Manoharan, A. Akinc, M. A. Maier, P. Cullis, T. D. Madden, M. J. Hope, *Mol Ther-Nucl Acids* **2013**, *2*.
- [15] G. Sahay, W. Querbes, C. Alabi, A. Eltoukhy, S. Sarkar, C. Zurenko, E. Karagiannis, K. Love, D. L. Chen, R. Zoncu, Y. Buganim, A. Schroeder, R. Langer, D. G. Anderson, *Nat Biotechnol* **2013**, *31*, 653-U119.
- [16] a) A. Staubli, E. Ron, R. Langer, *J Am Chem Soc* **1990**, *112*, 4419-4424; b) R. van Dijkhuizen-Radersma, S. C. Hesselink, P. E. Kaim, K. de Groot, J. M. Bezemer, *Biomaterials* **2002**, *23*, 4719-4729; c) Y. Geng, D. E. Discher, *J Am Chem Soc* **2005**, *127*, 12780-12781.
- [17] a) J. W. Gillard, R. Fortin, H. E. Morton, C. Yoakim, C. A. Quesnelle, S. Daignault, Y. Guindon, *J Org Chem* **1988**, *53*, 2602-2608; b) B. Neises, W. Steglich, *Angew Chem Int Edit* **1978**, *17*, 522-524.
- [18] D. L. Chen, K. T. Love, Y. Chen, A. A. Eltoukhy, C. Kastrup, G. Sahay, A. Jeon, Y. Z. Dong, K. A. Whitehead, D. G. Anderson, *J Am Chem Soc* **2012**, *134*, 6948-6951.

*Curriculum Vitae*  
**OWEN SHEA FENTON**

**Work Address**

Koch Institute for Integrative Cancer Research  
Massachusetts Institute of Technology  
Cambridge, MA 02139, USA

**Home Address**

49 Montrose Street #1  
Somerville, MA 02142, USA  
E-mail: osfenton@mit.edu

**EDUCATION**

---

**PhD, Chemistry**

**June 2016 (Expected)**

*Massachusetts Institute of Technology*

"Design, Synthesis, and Biological Evaluation of Diketopiperazine Based Ionizable Lipids for the In Vivo Delivery of mRNA"

**MSc, Organic Chemistry**

**September 2012**

*Massachusetts Institute of Technology*

"A General Entry to C7-Borono Indole Derivatives"

**BS, Chemistry**

**May 2010**

*College of the Holy Cross*

"Development of Lewis and Bronsted Acid Catalyzed Reactions for the Phosphorylation of Alcohols: Applications Towards Chemical Synthesis and Undergraduate Chemical Education"

GPA: 3.98/4.00

Class Rank: 1/730

**PROFESSIONAL EXPERIENCE**

---

**David H. Koch Institute for Integrative Cancer Research, MIT**

**July 2012 - present**

Research Advisor: *Prof. Daniel G. Anderson*

Synthesis and characterization of ionizable lipids for highly potent and non-toxic nucleic acid delivery *in vivo*

**Department of Chemistry, MIT**

**September 2010 - July 2012**

Research Advisor: *Prof. Mohammad Movassaghi*

Concise Total Synthesis of (+)-Asperazine, (+)-Pestalazine A, and (+)-*iso*-Pestalazine A.

**Department of Chemistry, University of California, Berkeley**

**May 2009 - August 2010**

Research Advisor: *Prof. F. Dean Toste*

Asymmetric gold catalyzed [4+2] cycloadditions of allene-dienes; biaryl ligand synthesis and evaluation

**Department of Chemistry, College of the Holy Cross**

**June 2008 - May 2010**

Research Advisor: *Prof. Bianca R. Sculimbrene*

Titanium(IV) catalyzed phosphorylation of alcohols using pyrophosphates; novel reagents and methodologies

**Department of Chemistry, College of the Holy Cross**

**March 2007 - June 2008**

Research Advisor: *Prof. Kimberley A. Frederick*

Qualitative and quantitative analysis of simulated illicit street drug samples using Raman spectroscopy

**HONORS, AWARDS and SCHOLARSHIPS**

---

National Science Foundation Graduate Research Fellowship

2012 - 2015

Phi Beta Kappa

2010

American Institute of Chemists Award, *College of the Holy Cross*

2010

Fenwick Scholarship, *College of the Holy Cross*

2009 - 2010

Goldwater Scholar, *Barry Goldwater Scholarship and Excellence in Education Program*

2009 - 2010

Amgen Scholar, *University of California, Berkeley*

2009

Goldwater Scholar Honorable Mention, <i>Barry Goldwater Scholarship and Excellence in Education Program</i>	2008
Mrs. Kate C. Power Medal, <i>College of the Holy Cross</i>	2008
Jean Dreyfus Boissevain Undergraduate Scholarship, <i>College of the Holy Cross</i>	2008
PolyEd Achievement in Organic Chemistry Award	2008
Poster and Presentation Award, <i>College of the Holy Cross Annual Research Symposium</i>	2008
CRC Press Freshman Chemistry Award	2007

## PUBLICATIONS

---

13. Fenton, O.S.; Kauffman, K.J.; Kaczmarek, J.C.; McClellan, R.L.; Jhunjhunwala, S.; Zeng, M.D.; Appel, E.A.; Dorkin, J.R.; Mir, F.; Yang, J.; Tibbitt, M.W.; Heartlein, M.W.; DeRosa, F.; Langer, R.; Anderson, D.G.\* "Fatty Acid Derived Lipid Nanoparticles Deliver mRNA to B Lymphocytes In Vivo," *in preparation*.
12. Fenton, O.S.; Kauffman, K.J.; McClellan, R.L.; Appel, E.A.; Dorkin, J.R.; Tibbitt, M.W.; Heartlein, M.W.; DeRosa, F.; Langer, R.; Anderson, D.G.\* "Bioinspired Alkenyl Amino Alcohol Ionizable Lipid Materials for Highly Potent In Vivo mRNA Delivery," *Advanced Materials*, **2016**, *in press*.
11. Fischer, K.M.; Morgan, K.Y.; Hearon, K.; Sklaviadis, D.; Tochka, Z.L.; Fenton, O.S.; Anderson, D.G.; Langer, R.; Freed, L.E.\* "Poly(limonene thioether) Scaffold for Tissue Engineering," *Adv. Healthcare Mater.*, **2016**, *in press*.
10. Loach, R.P.; Fenton, O.S.; Movassaghi, M.\* "Concise Total Synthesis of (+)-Asperazine, (+)-Pestalazine A, and (+)-iso-Pestalazine A. Structure Revision of (+)-Pestalazine A," *J. Am. Chem. Soc.*, **2016**, *138*, 1057-1064.
9. Kauffman, K.J.; Dorkin, J.R.; Yang, J.H.; Heartlein, M.W.; DeRosa, F.; Mir, F.F.; Fenton, O.S.; Anderson, D.G.\* "Optimization of Lipid Nanoparticle Formulations for mRNA Delivery in Vivo with Fractional Factorial and Definitive Screening Designs," *Nano Lett.*, **2015**, *15*, 7300-7306.
8. Appel, E.A.; Tibbitt, M.W.; Greer, J.M.; Fenton, O.S.; Kreuels, K.; Anderson, D.G.; Langer, R.\* "Exploiting Electrostatic Interactions in Polymer-Nanoparticle Hydrogels," *ACS Macro Lett.*, **2015**, *4*, 848-852.
7. Loach, R.P.; Fenton, O.S.; Amaike, K.; Seigel, D.S.; Ozkal, E.; Movassaghi, M.\* "C7-Derivatization of C3-Alkylindoles Including Tryptophans and Tryptamines," *J. Org. Chem.*, **2014**, *79*, 11254-11263.
6. Whitehead, K.A.; Dorkin, J.R.; Vegas, A.J.; Chang, P.H.; Veiseh, O.; Matthews, J.; Fenton, O.S.; Zhang, Y.L.; Olejnik, K.T.; Yesilyurt, V; Chen, D.L.; Barros, S.; Klevanov, B.; Novobrantseva, T.; Langer, R.; Anderson, D.G.\* "Degradable Lipid Nanoparticles with Predictable in Vivo siRNA Delivery Activity," *Nat. Comm.*, **2014**, *5*, 4277.
5. Fenton, O.S.; Allen, E.E.; Pedretty, K.P.; Till, S.D.; Todaro, J.E.; Sculimbrene, B.R.\* "Catalytic Lewis Acid Phosphorylation with Pyrophosphates," *Tetrahedron*, **2012**, *68*, 9023-9028.
4. Fenton, O.S.; Sculimbrene, B.R.\* "A Wet-Lab Approach to Stereochemistry Using P-31 NMR Spectroscopy," *J. Chem. Ed.*, **2012**, *88*, 662-664.
3. Fenton, O.S.; Tonge, L.A.; Moot, T.H.; Frederick, K.A.\* "Quantitative Analysis of Simulated Illicit Street-Drug Samples Using Raman Spectroscopy and Partial Least Squares Regression," *Spectroscopy Lett.*, **2011**, *44*, 229-234.
2. Noonan, K.Y.; Tonge, L.A.; Fenton, O.S.; Damiano, D.B.; Frederick, K.A.\* "Rapid Classification of Simulated Street Drug Mixtures Using Raman Spectroscopy and Principal Component Analysis," *Applied Spectroscopy*, **2009**, *63*, 742-747.
1. Brady, P.B.; Morris, E.M.; Fenton, O.S.; Sculimbrene, B.R.\* "Efficient Catalyst Turnover in the Phosphitylation of Alcohols with Phosphoramidites," *Tetrahedron Lett.*, **2009**, *50*, 975-978.

## PATENTS

---

2. **Fenton, O.S.**; Dorkin, J.R.; Anderson, D.G.; McClellan, R.M. "Polyamine-Fatty Acid Derived Lipidoids and Uses Thereof". US Patent No.: 20,160,002,178. Filing Date: July 1, 2015.

1. Anderson, D.G.; Dorkin, J.R.; **Fenton, O.S.**; Kauffman, K.J.; McClellan, R.L. "Alkenyl Substituted 2,5-Piperazinediones, Compositions, and Uses Thereof," US Provisional Application No.: 62/182,264. Filing Date: June 19, 2015.

## SELECTED MEETING and CONFERENCE PRESENTATIONS

---

"Exploring stereochemistry in a teaching laboratory using 31P NMR spectroscopy" **Fenton, O.S.**; Sculimbrene, B.R. 239<sup>th</sup> ACS National Meeting, San Francisco, CA, March 2010 (Poster).

"Development of catalytic phosphorylation reactions" **Fenton, O.S.**; Sculimbrene, B.R. 239<sup>th</sup> ACS National Meeting, San Francisco, CA, March 2010 (Poster).

"Asymmetric Gold-Catalyzed [4+2] Cycloadditions of Allene-Dienes" **Fenton, O.S.**; Gonzalez, A.Z.; Toste, F.D. Amgen Scholars Research Symposium, Berkeley, CA, August 2009 (Poster).

"Development of a Catalytic Reaction for the Phosphorylation of Alcohols" **Fenton, O.S.**; Morris, E.M.; Sculimbrene, B.R. 237<sup>th</sup> ACS National Meeting, Salt Lake City, UT, March 2009 (Poster).

"Quantitative Measurements of Illicit Drugs Using Raman Spectroscopy and Chemometrics" **Fenton, O.S.**; Damiano, D.B.; Frederick, K.A. 234<sup>th</sup> ACS National Meeting, Boston, MA, August 2007 (Poster).

## TEACHING and PERSONAL EXPERIENCE

---

### Lecture course teaching assistant:

- **Organic Chemistry II** (September 2011 - December 2011, September 2012 - December 2012 )

Instructor: *Prof. Mohammad Movassaghi*

Material Covered: Synthesis and Reactivity of: Carboxylic Acid Derivatives, Amines, Aromatics, and Alcohols. Carbocation and Radical Chemistries; Enol/Enolate Chemistry (Aldol, Claisen, Mannich).

Responsibilities: Organized two one hour weekly recitations for 20+ students, as well as 3 weekly office hours. Helped design and grade all problem sets and exams.

### Laboratory practical teaching assistant:

- **Organic Chemistry I** (September 2008 - December 2008)

Instructor: *Prof. Bianca R. Sculimbrene*

Experiments Performed: Electrophilic and Nucleophilic Aromatic substitution reactions; Alcohol Oxidation and Carboxylic Acid Derivative Reduction Chemistries

### Leadership experience:

- Mentored two technical assistants in complex multistep organic synthesis and characterization at the MIT, which has resulted in multiple co-authored publications (June 2014-August 2015, June 2015-Present)
- Chair; Chemistry Department Student Advisory Council, College of the Holy Cross. Served as a liaison between the faculty and student body addressing curriculum strategy and course evaluations.
- Innovative Services for Latino Adolescents. Served as bilingual translator for non-native English speaking students in Worcester elementary schools.

### Professional membership:

- ACS (ORGN)

### Hobbies:

- Ice hockey and various outdoor sports including running, hiking, and volleyball.
- International travel as well as modern languages and literature.